Tibet ASγ experiment

Masato TAKITA, ICRR, U. of Tokyo

(For the Tibet ASγ collaboration)

External Review@ICRR 19/Oct/2006

The Tibet ASγ Collaboration (China-Japan joint experiment)

M. Amenomori(a), S. Ayabe(b), X.J. Bi(c), D. Chen(d), S.W. Cui(e), Danzengluobu(f), L.K. Ding(c), X.H. Ding(f), C.F. Feng(g), Zhaoyang Feng(c), Z.Y. Feng(h), X.Y. Gao(i), Q.X. Geng(i), H.W. Guo(f), H.H. He(c), M. He(g), K. Hibino(j), N. Hotta(k), Haibing Hu(f), H.B. Hu(c), J. Huang(l), Q. Huang(h), H.Y. Jia(h), F. Kajino(m), K. Kasahara(n), Y. Katayose(d), C. Kato(o), K. Kawata(l), Labaciren(f), G.M. Le(p), A.F. Li(g), J.Y. Li(g), H. Lu(c), S.L. Lu(c), X.R. Meng(f), K. Mizutani(b,q),J. Mu(i), K. Munakata(o), A. Nagai(r), H. Nanjo(a), M. Nishizawa(s), M. Ohnishi(l), I. Ohta(t), H. Onuma(b), T. Ouchi(j), S. Ozawa(l), J.R. Ren(c), T. Saito(u), T. Y. Saito(l), M. Sakata(m), T. K. Sako(l), T. Sasaki(j), M. Shibata(d), A. Shiomi(l), T. Shirai(j), H. Sugimoto(v), M. Takita(l), Y.H. Tan(c), N. Tateyama(j), S. Torii(q), H. Tsuchiya(w), S. Udo(l), B. Wang(i), H. Wang(c), X. Wang(l), Y.G. Wang(g), H.R. Wu(c), L. Xue(g), Y. Yamamoto(m), C.T. Yan(l), X.C. Yang(i), S. Yasue(x), Z.H. Ye(p), G.C. Yu(h), A.F. Yuan(f), T. Yuda(j), H.M. Zhang(c), J.L. Zhang(c), N.J. Zhang(g), X.Y. Zhang(g), Y. Zhang(c), Yi Zhang(c), Zhaxisangzhu(f) and X.X. Zhou(h)

(a) Department of Physics, Hirosaki University, Hirosaki 036-8561, Japan
(b) Department of Physics, Saitama University, Saitama 338-8570, Japan
(c) Key Laboratory of Particle Astrophysics, Institute of High Energy Physics, Chinese Academy of Sciences, Beijing 100049, China
(d) Faculty of Engineering, Yokohama National University, Yokohama 240-8501, Japan
(e) Department of Physics, Hebei Normal University, Shijiazhuang 050016, China
(f) Department of Mathematics and Physics, Tibet University, Lhasa 850000, China
(g) Department of Physics, Shandong University, Jinan 250100, China
(h) Institute of Modern Physics, South West Jiaotong University, Chengdu 610031, China
(i) Department of Physics, Yunnan University, Kunming 650091, China
(j) Faculty of Engineering, Kanagawa University, Yokohama 221-8686, Japan
(k) Faculty of Education, Utsunomiya University, Utsunomiya 321-8505, Japan
(l) Institute for Cosmic Ray Research, University of Tokyo, Kashiwa 277-8582, Japan
(m) Department of Physics, Konan University, Kobe 658-8501, Japan
(n) Faculty of Systems Engineering, Shibaura Institute of Technology, Saitama 337-8570, Japan
(o) Department of Physics, Shinshu University, Matsumoto 390-8621, Japan
(p) Center of Space Science and Application Research, Chinese Academy of Sciences, Beijing 100080, China
(q) Advanced Research Institute for Science and Engineering, Waseda University, Tokyo 169-8555, Japan
(r) Advanced Media Network Center, Utsunomiya University, Utsunomiya 321-8585, Japan
(s) National Institute for Informatics, Tokyo 101-8430, Japan
(t) Tochigi Study Center, University of the Air, Utsunomiya 321-0943, Japan
(u) Tokyo Metropolitan College of Industrial Technology, Tokyo 116-8523, Japan
(v) Shonan Institute of Technology, Fujisawa 251-8511, Japan
(w) RIKEN, Wako 351-0198, Japan
(x) School of General Education, Shinshu University, Matsumoto 390-8621, Japan

Our site : Tibet

Yangbajing , Tibet, China

90° 53E, 30° 11N, 4,300 m a.s.l. (606g/cm^2)

Photo Gallery

The Potala Palace

Lake Namutso

!

Research Purpose

Complementary to Air Cherenkov Telescopes
Wide-field-of-view (~2sr) high-duty cycle CR telescope

1. 3TeV~100TeV cosmic γ rays
2. 100TeV～100 PeV primary cosmic rays

-> Origin, acceleration of cosmic rays

3. The Sun's shadow in cosmic rays
(Shielding effect on cosmic rays by the Sun)
-> Global structure of solar and interplanetary magnetic fields

Tibet-I to Tibet-II/HD

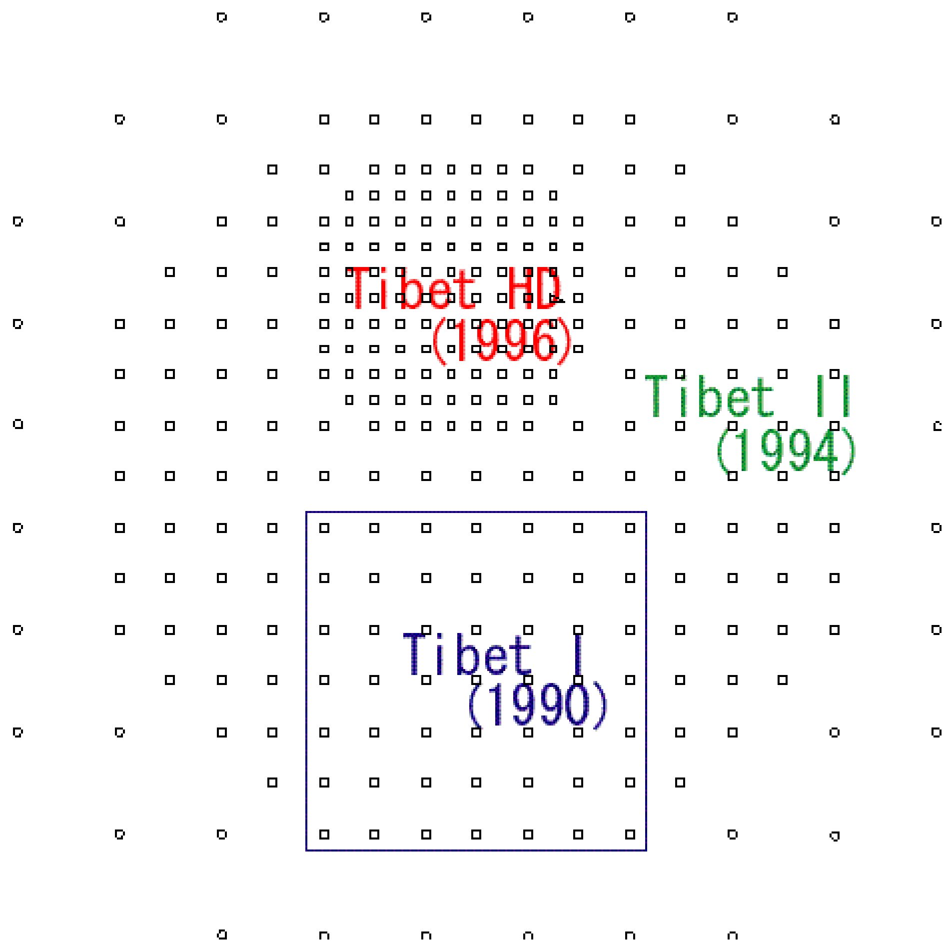

Number of detector
- I : 45
- II : 185
- HD: 109

Mode Energy
- I : 10 TeV
- II : 10 TeV
- HD: 3 TeV

Area
- I : 7 ,650 m^2
- II : 37,000 m^2
- HD: 5,200 m^2

Tibet III (22000m^2)

Yangbajing (4300a.s.l.=606g/cm^2), Tibet, China, as of 1999

Tibet III (22000m^2)

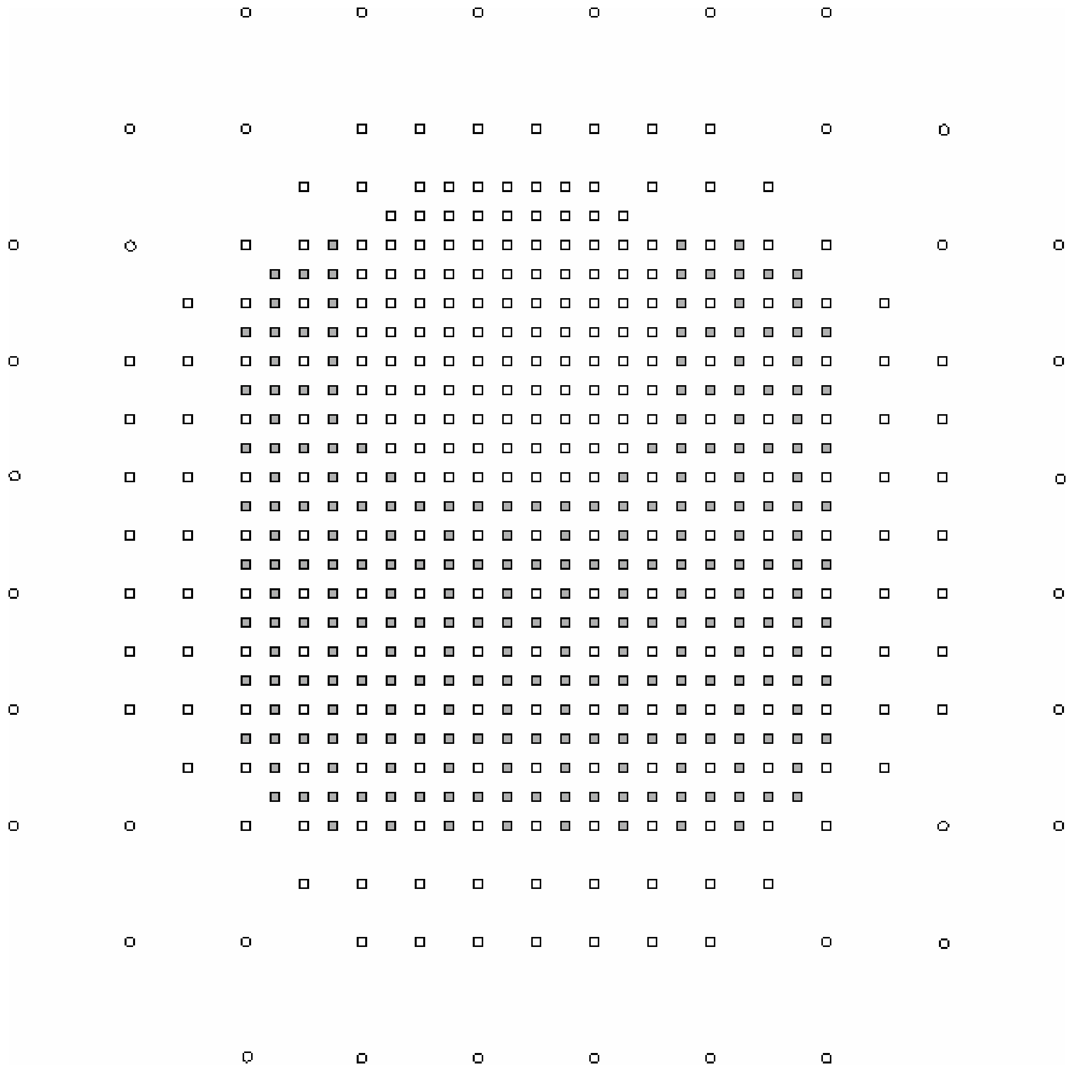

Total 545 detectors
Modal Energy
~ 3 TeV
Angular Resolution
~ 0.9 deg@3TeV
Trigger Rate
~680 Hz
Data size
~20GB/day

Operation
1999 October-
2002 September

Tibet Airshower Array

Tibet III (37000m^2)

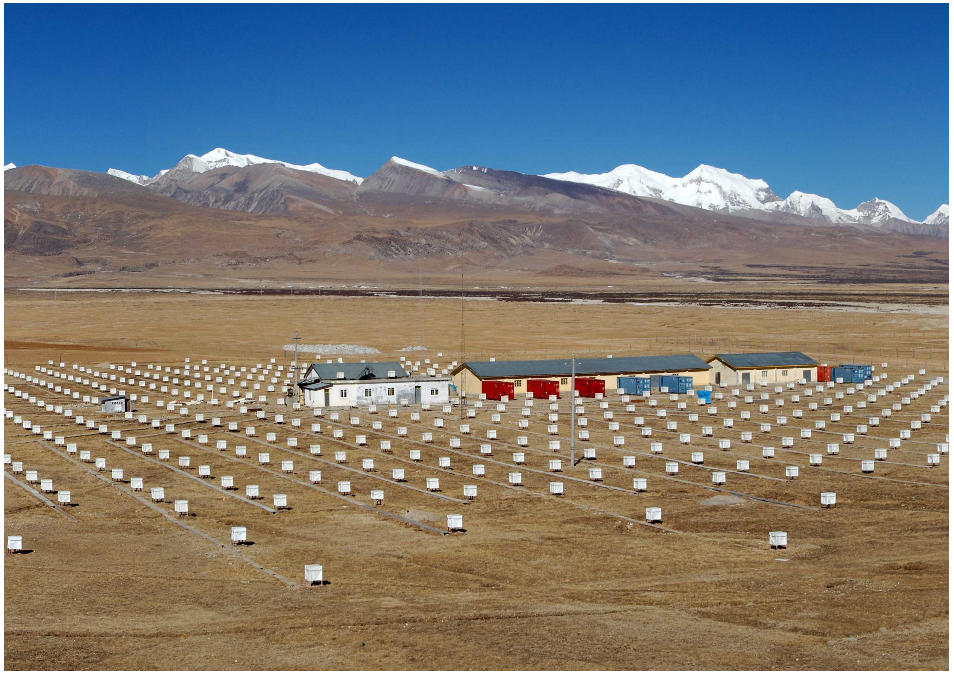

Yangbajing (4,300m a.s.l.=606g/cm^2),
Tibet, China, as of 2003

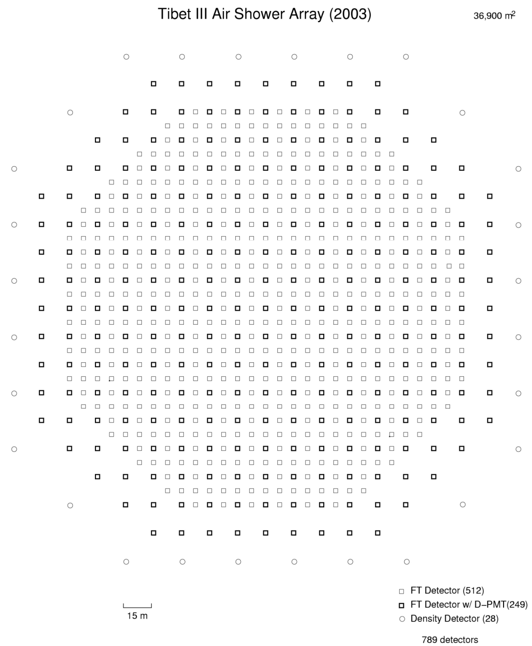

Total 789 detectors

Modal Energy
~3 TeV

Angular Resolution
~0.9 deg @3TeV

Trigger Rate
~1700 Hz

Detection Principle

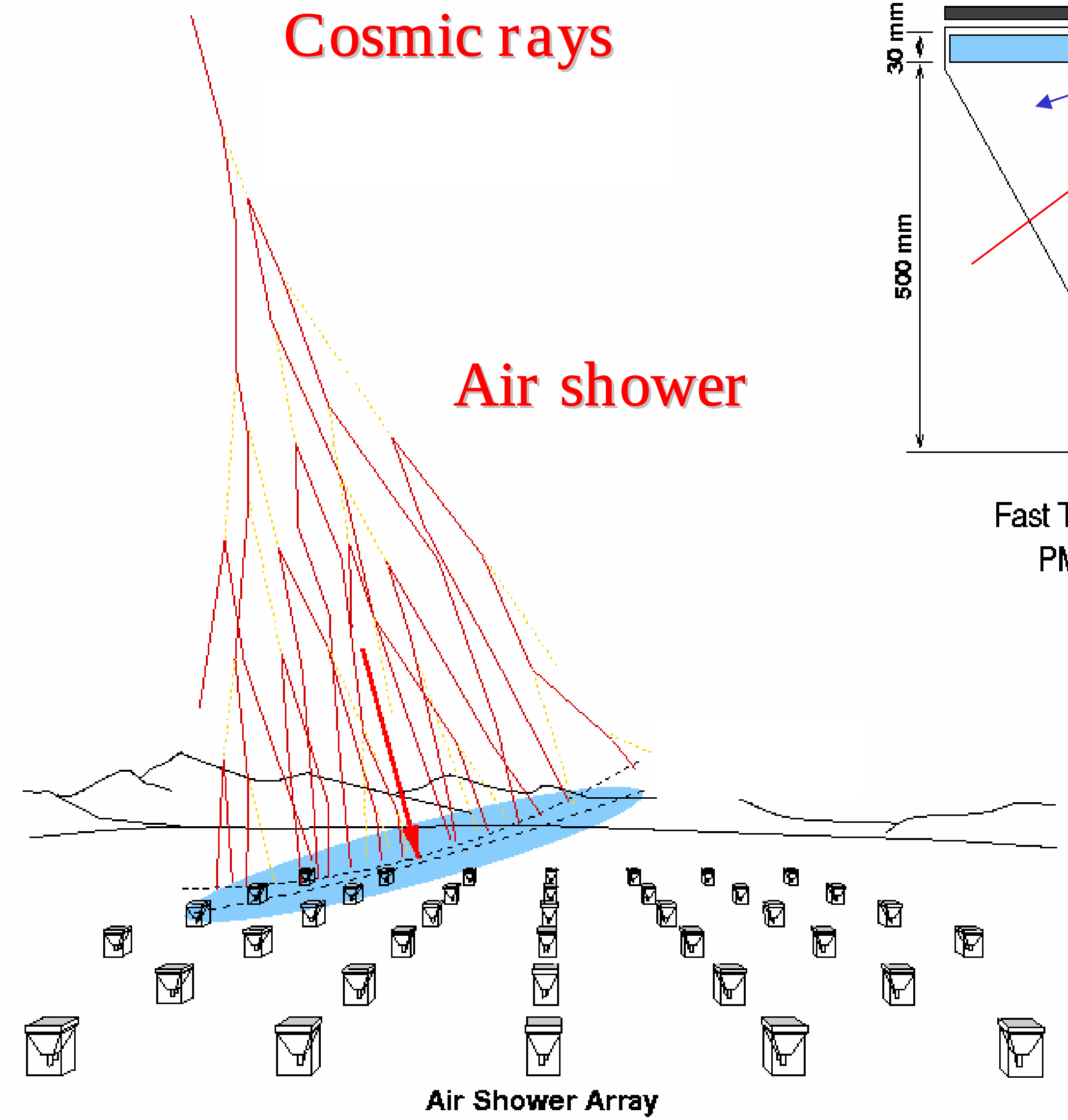

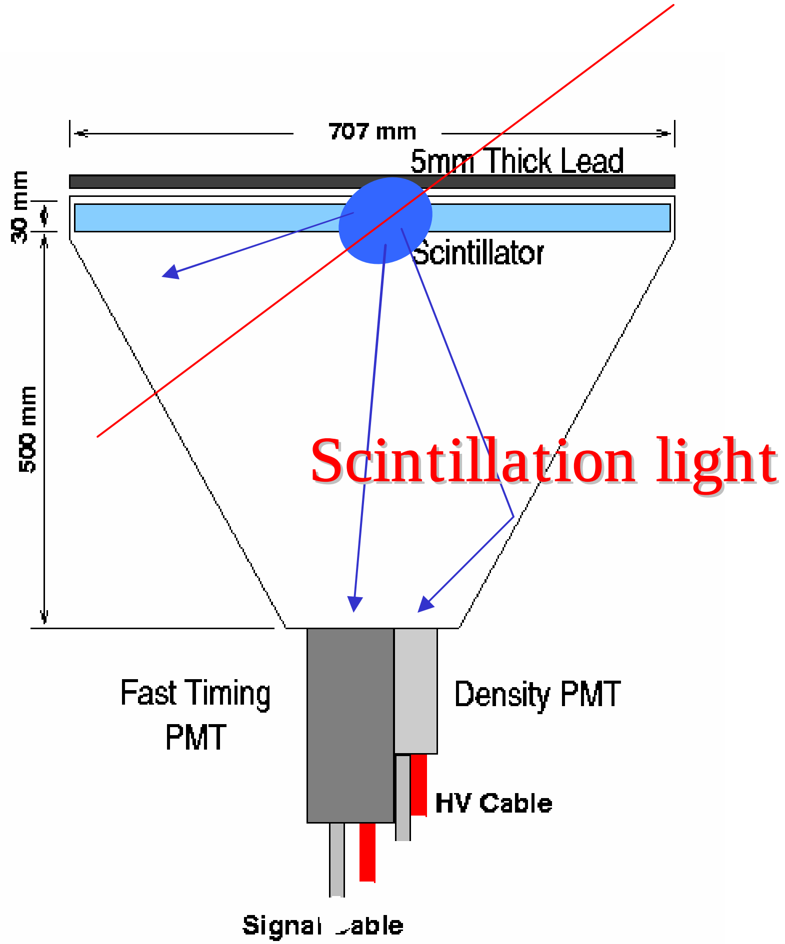

Event Schematics

of particles (charge)

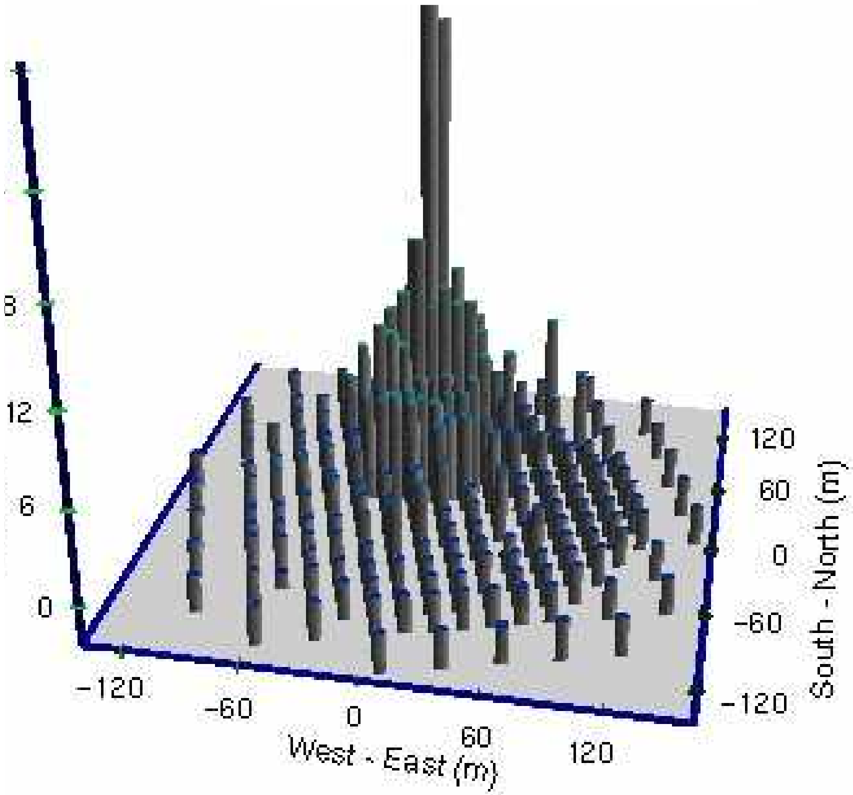

Relative timing (time)

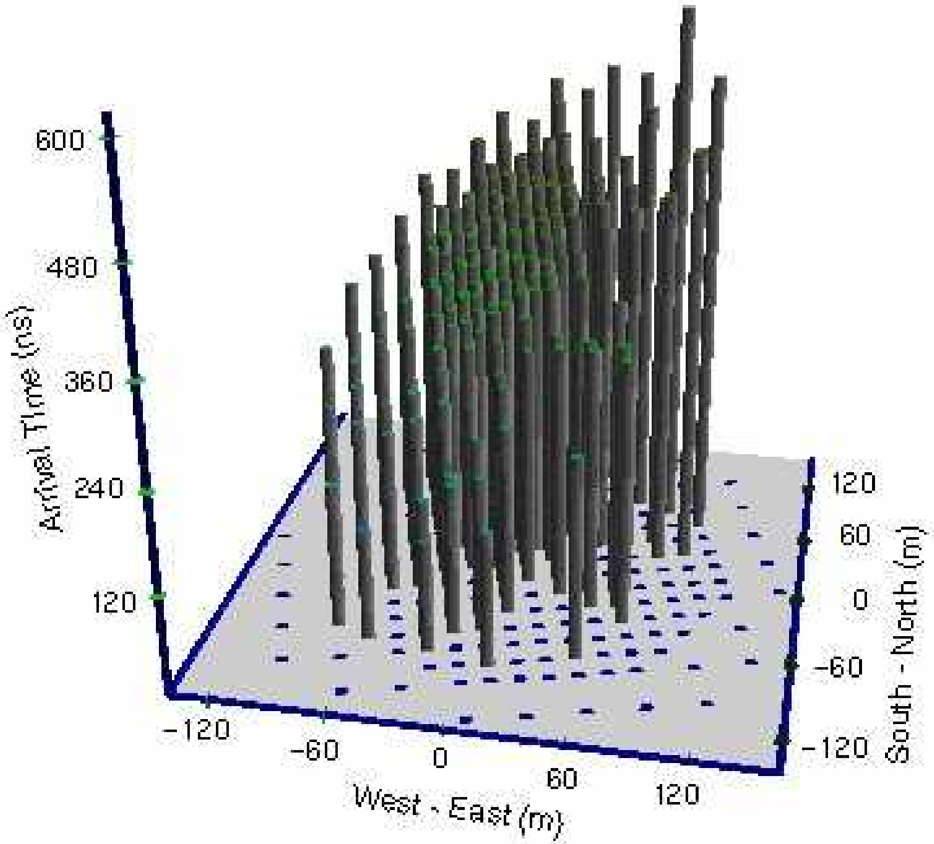

Moon's Shadow and Geomagnetic Field

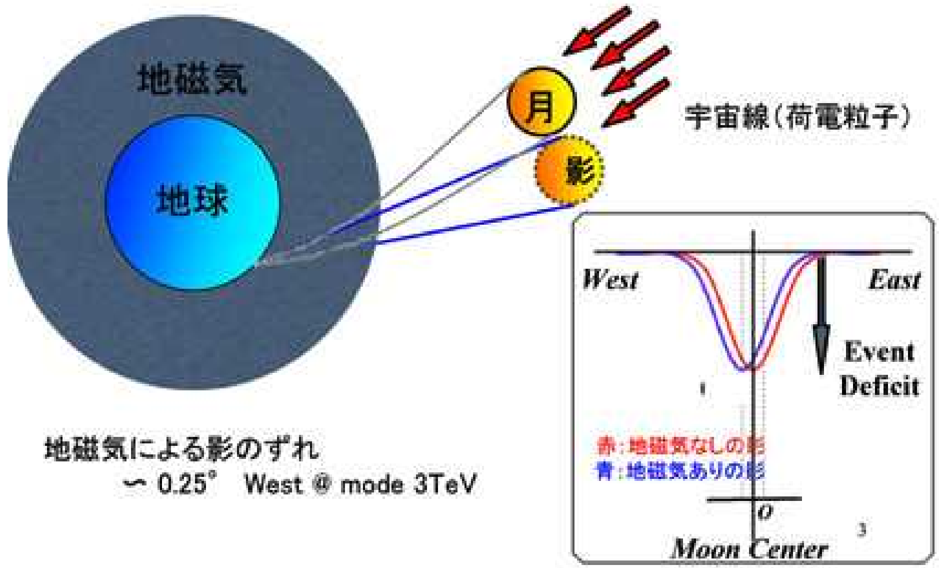

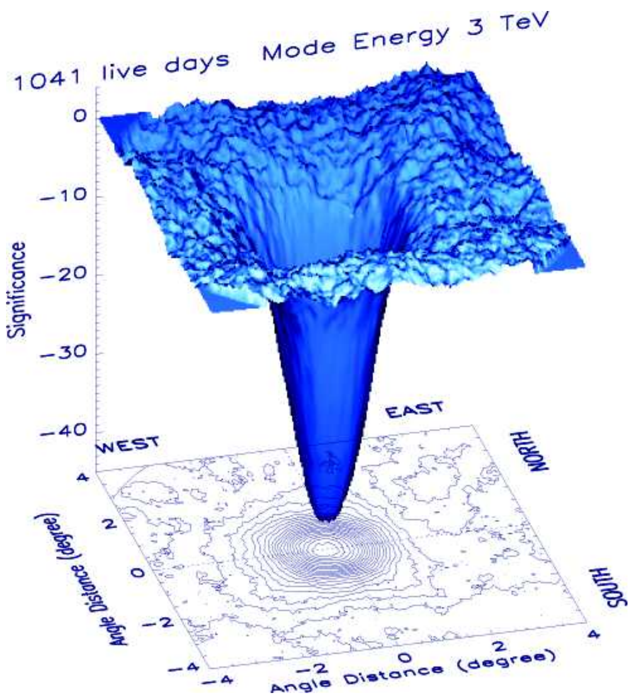

Observed Moon's shadow

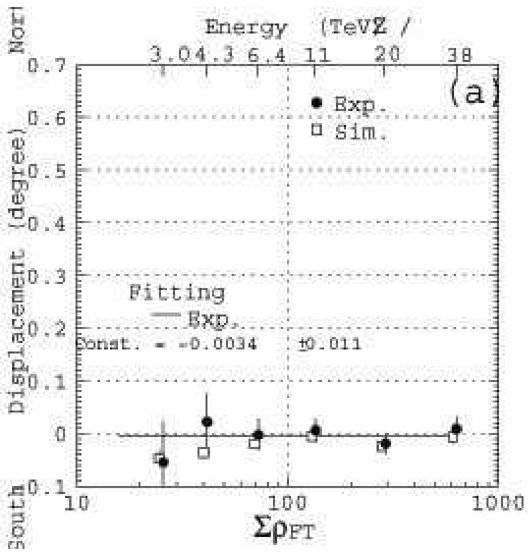

North-south deviation

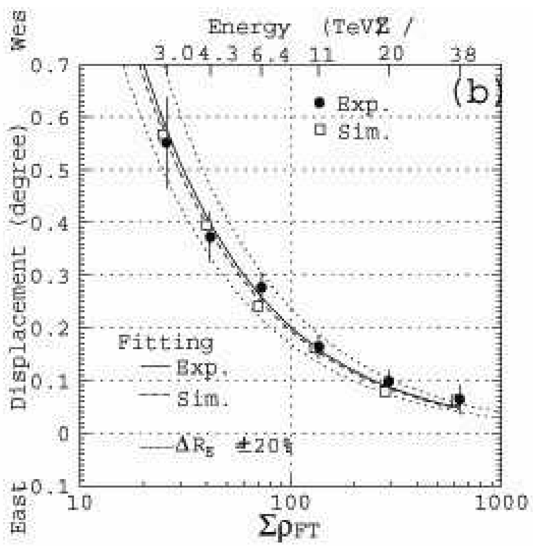

Westward shift

γ from Crab

5.5σ Tibet-HD (5200m^2)

(1996 Nov-1999 May 502days)

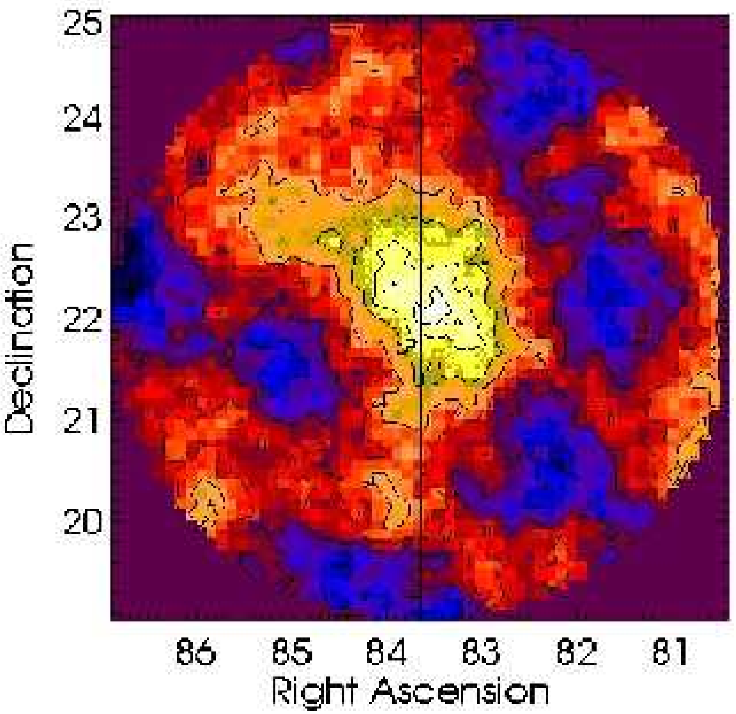

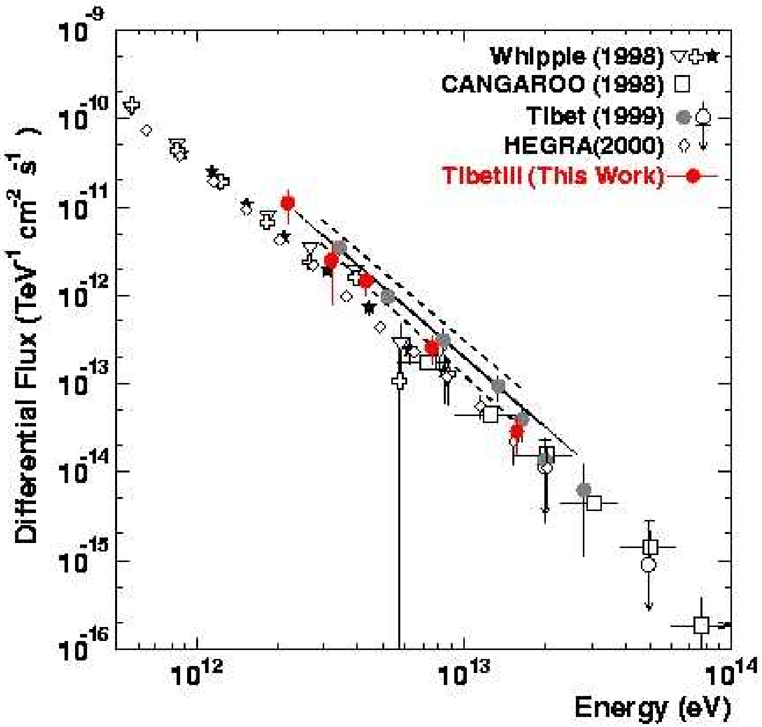

ApJ 525, L93-L96, (1999)

Crab γ unpulsed

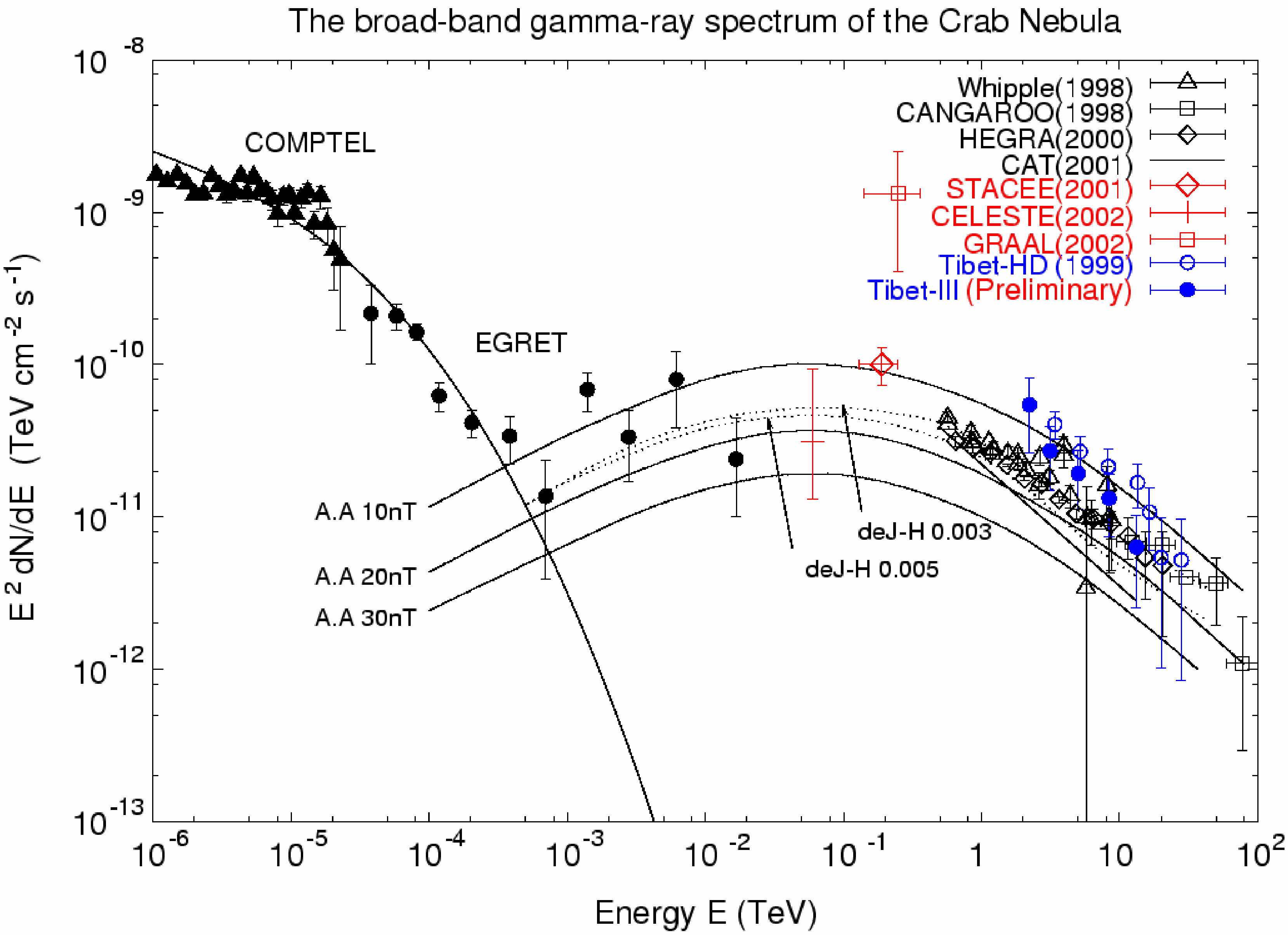

Flare γ from Mrk501 (1997)
3.7σ(Feb-Aug)~4.7σ(Apr-Jun)

Tibet-HD (5200m^2)

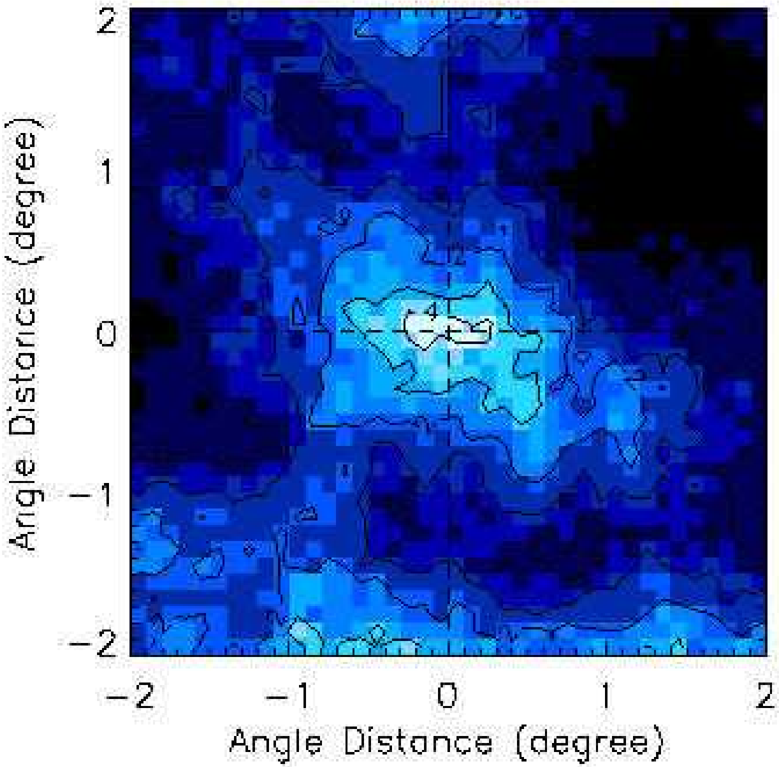

ApJ 532, 302-307, (2000)

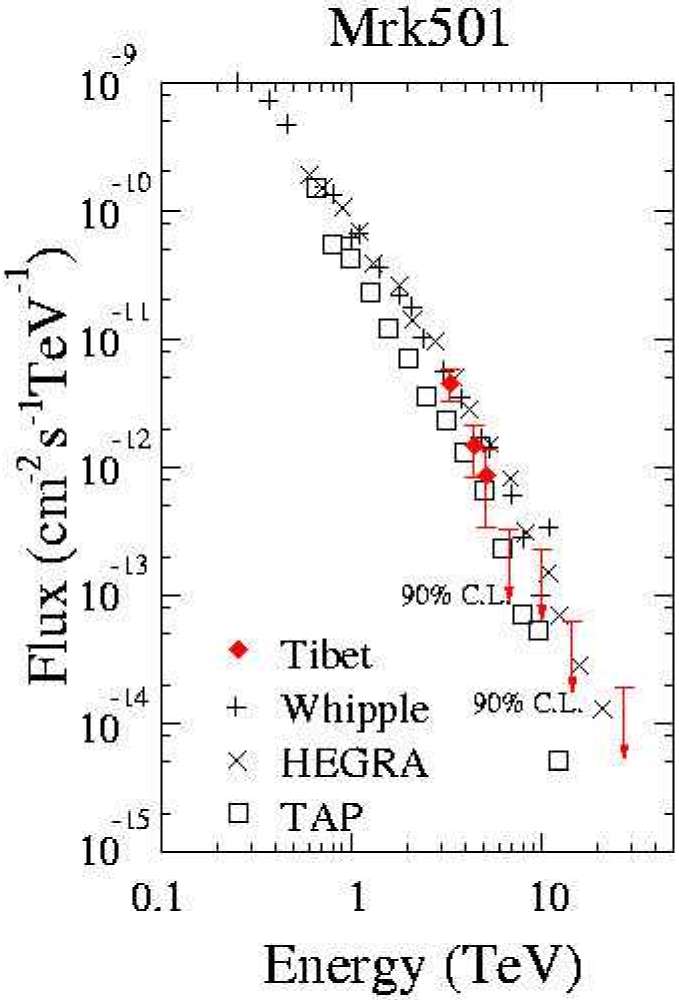

Flare γ from Mrk421 (2000-2001)

5.1σ

Tibet-III (22000m^2) 457days

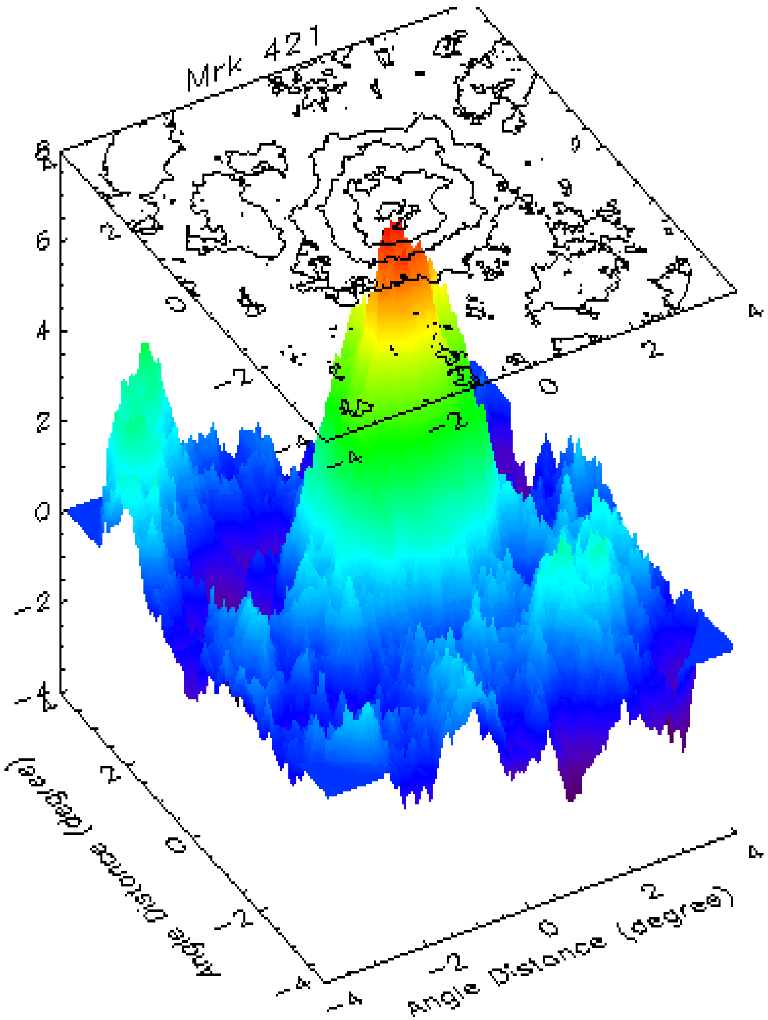

Mrk421 long-term correlation between X-ray and TeV γ-ray data

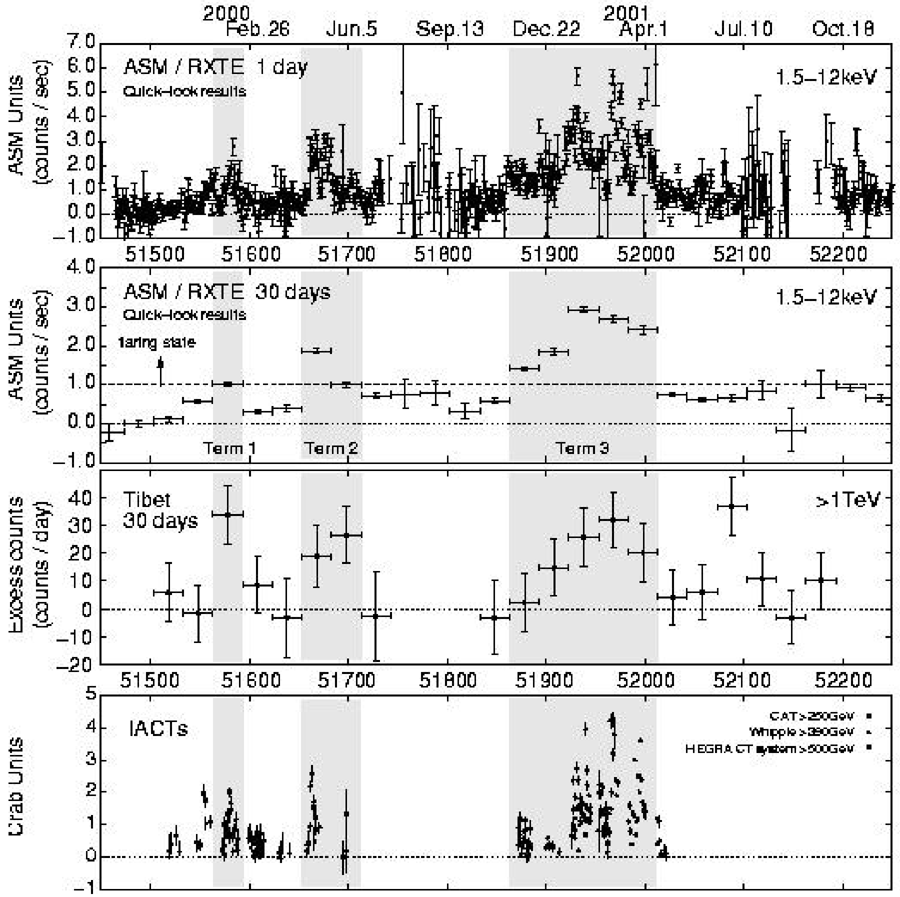

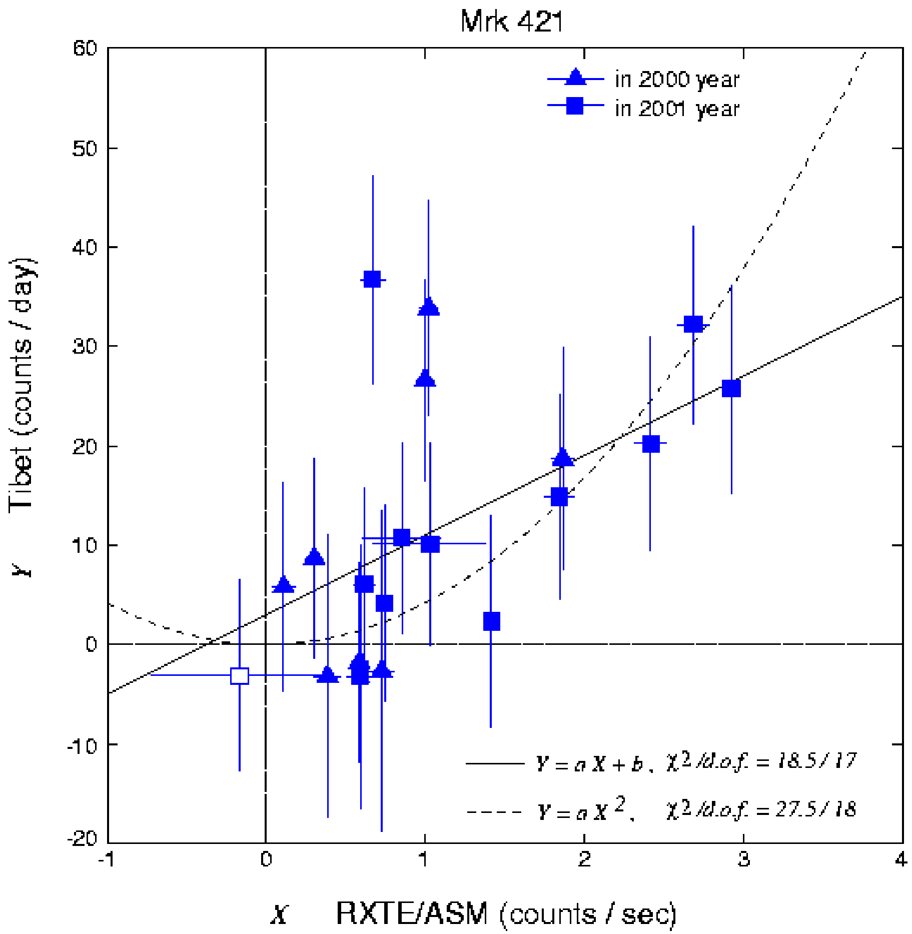

ApJ 598 (2003) 242—249

Upper limits on galactic diffuse γ rays

Inner galaxy (20<l<55deg)

Outer galaxy (140<l<225)

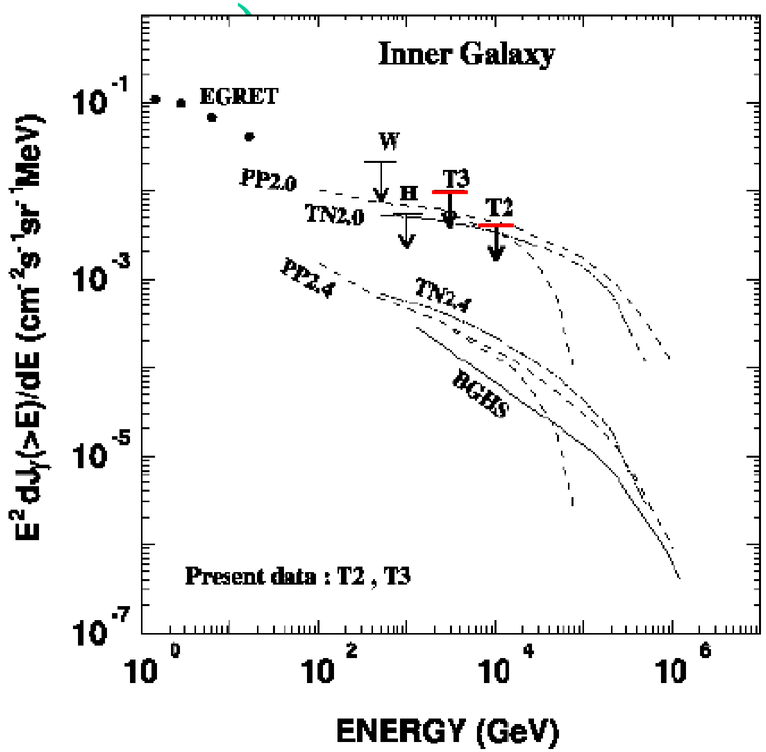

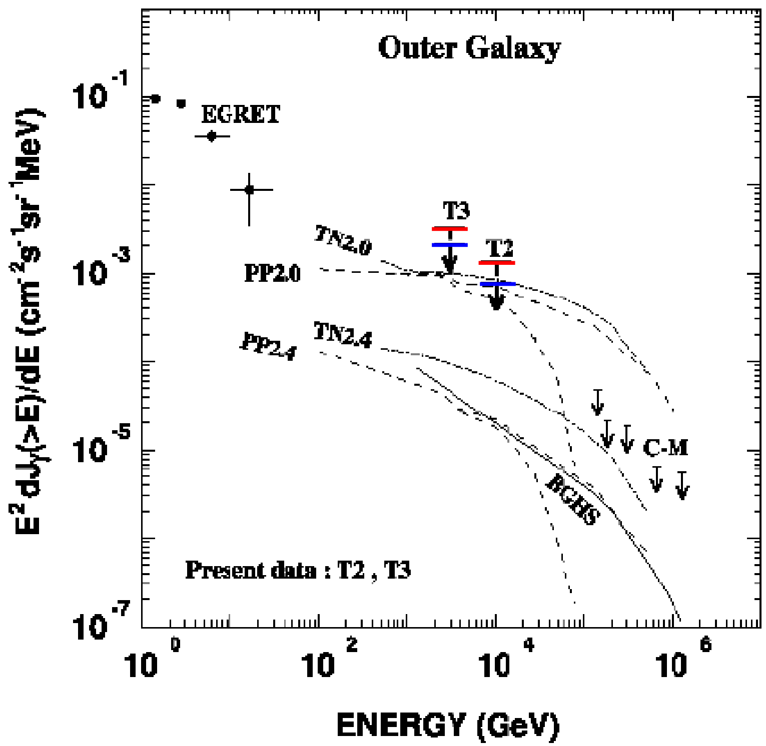

Red:99%CL, Blue:90%CL

ApJ, 580, 887-895,2002

T-II 551days, T-III 517days

Northern Sky TeV γ-ray Source Search

Tibet-HD ($5200m^2$) 556 days +
Tibet-III($22000m^2$) 457 days)

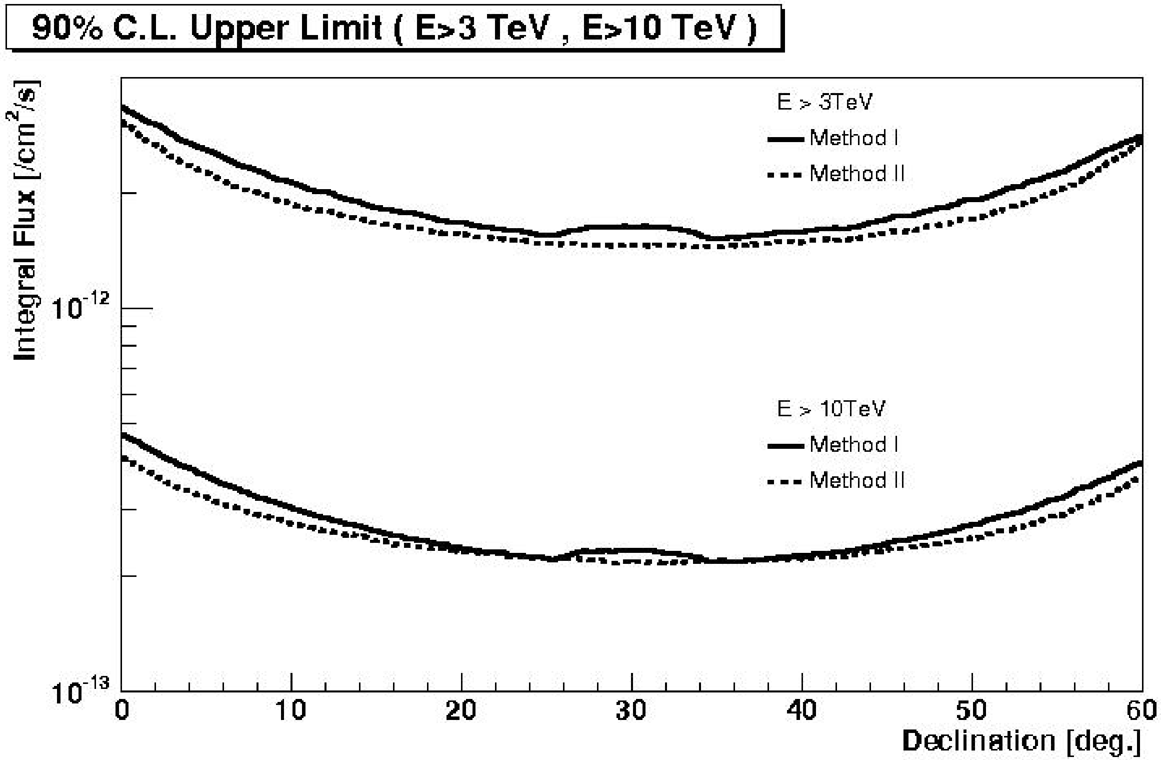

No new steady bright point source (like Crab) found

0.3 to 0.6 Crab

Flux upper limit

@90% CL

ApJ, 633, 1005-1012, (2005)

Search for PeV signal from Monogem Ring

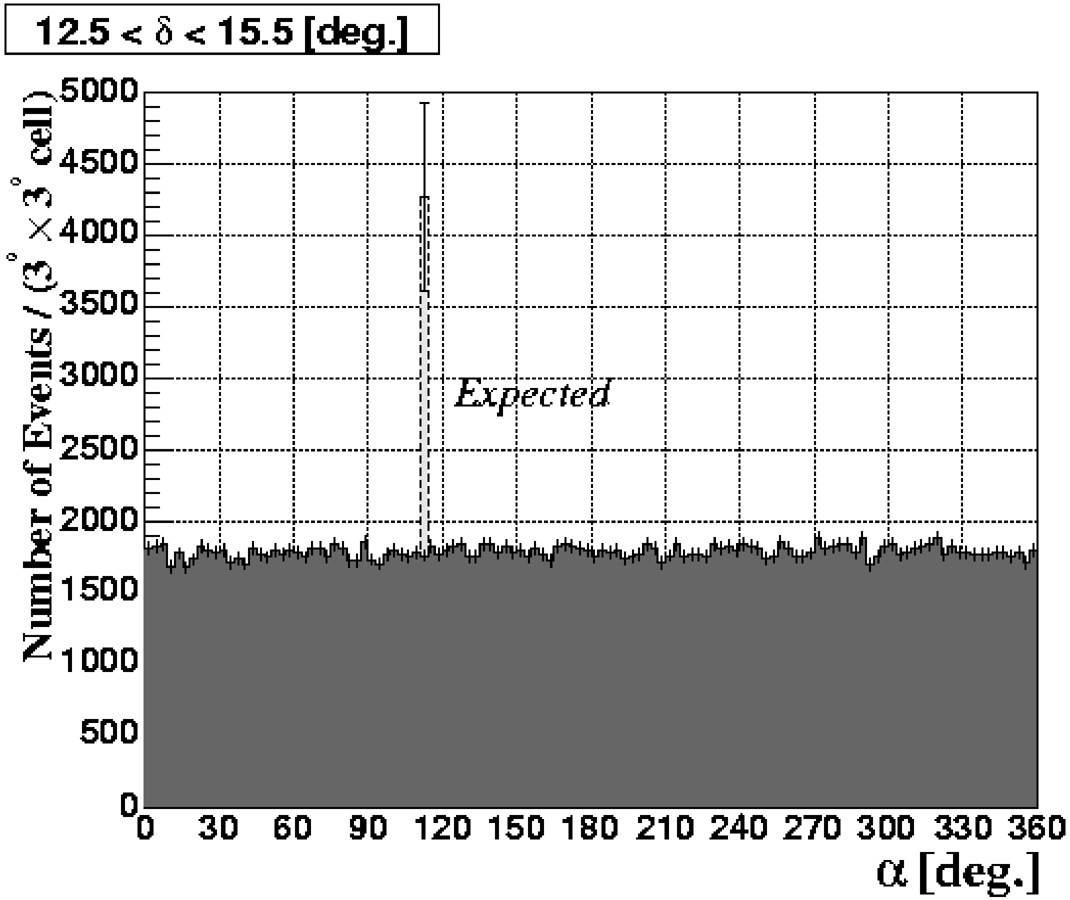

MAKET-ANI

6 σ signal from Monogem

3^Ox3^O bin, 1997-2003

However,

Tibet ~ x 100 statistics

x 10 sensitivity

No significant signal

$<4.0\times10^{-12}$/cm^2/sec/sr

above 1PeV @99%

ApJ, 635, L53-L56, (2005)

TIBET Hybrid Experiment

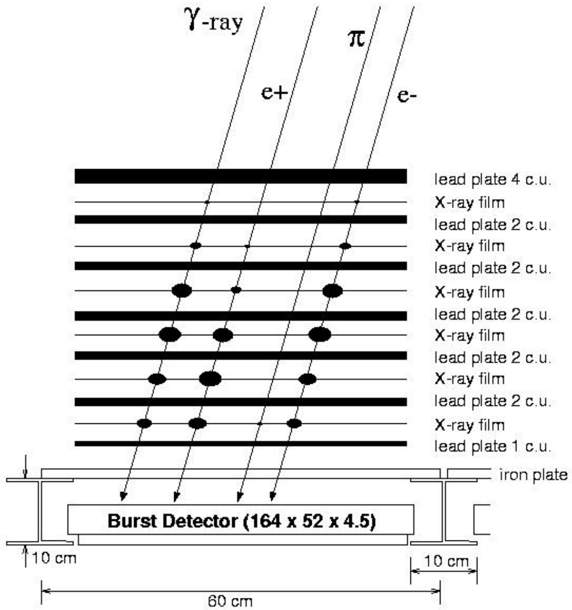

Longitudinal development of AS

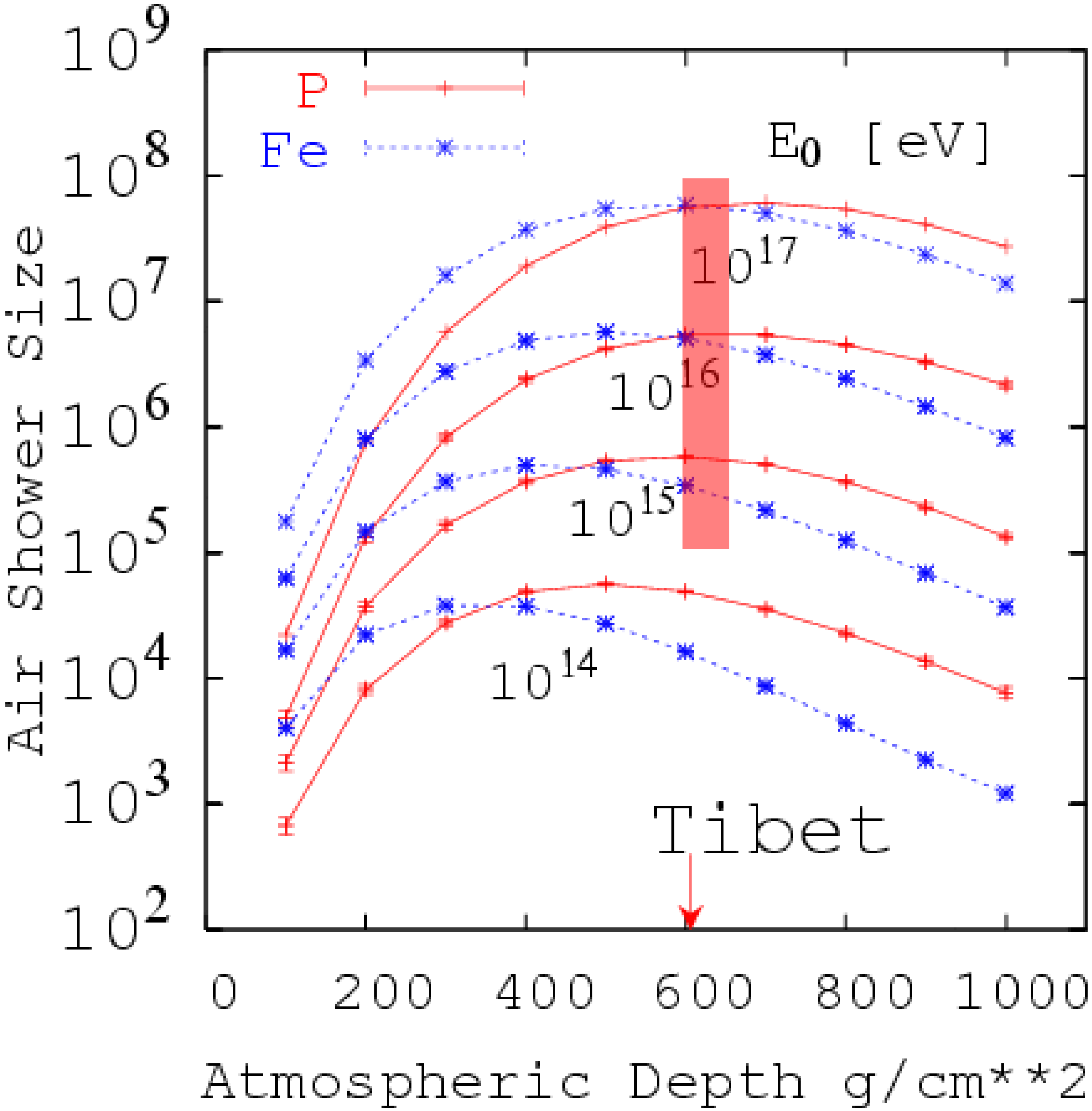

How to obtain proton spectrum?

Hybrid system

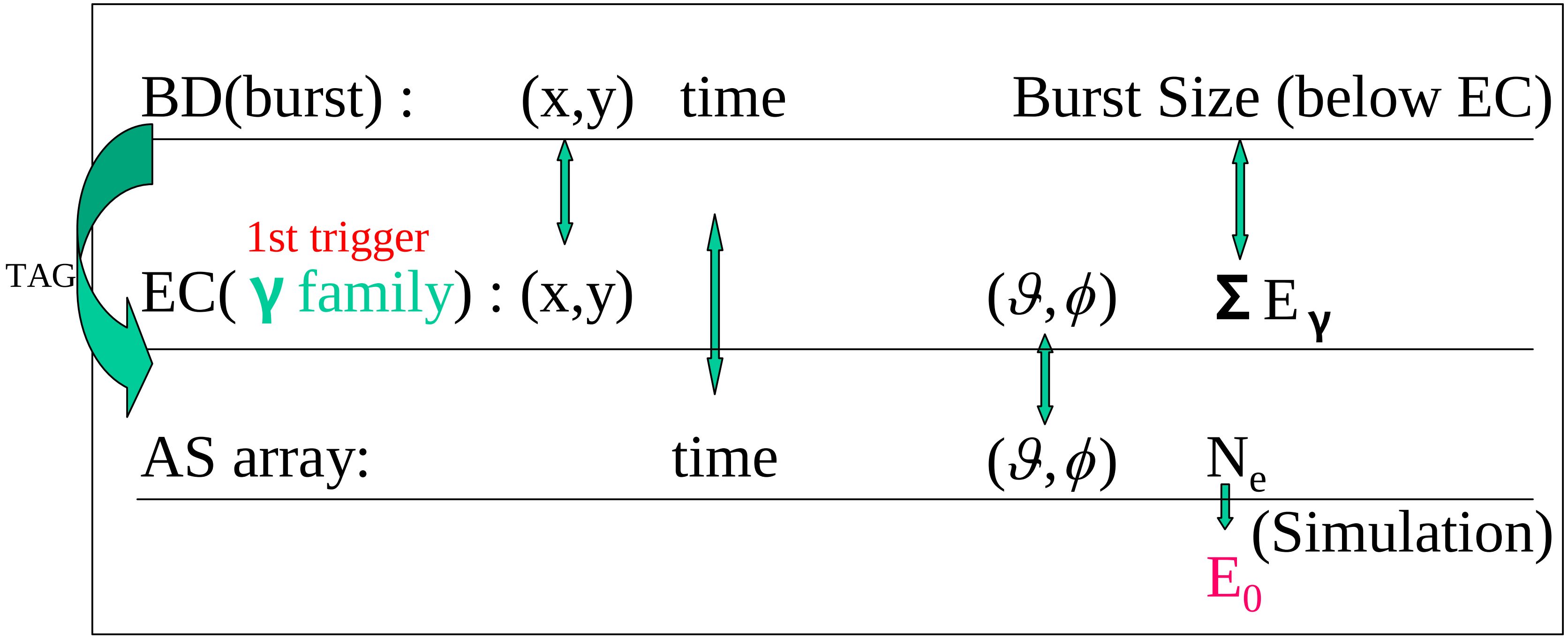

EC-Xray film image → Scanner → (GUI Software) family detection

AS+family matching event → ANN → Proton Identification ~100 eV/699 days

(Correlations)

Artificial Neural Network

JETNET 3.5

Parameters for training: N_γ, ΣE_γ, $\langle R_\gamma \rangle$, $\langle ER_\gamma \rangle$, N_e, θ

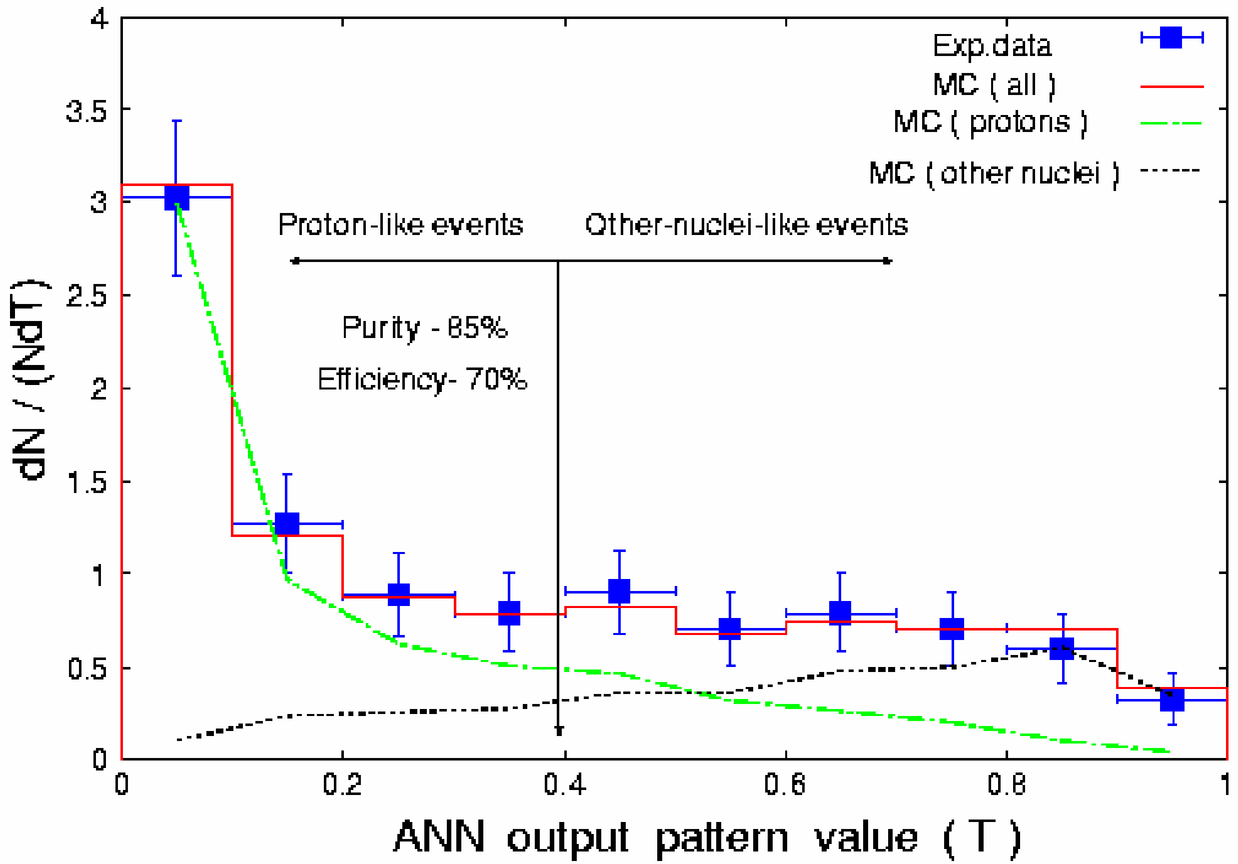

Primary proton spectrum

(a) (by QGSJET model)

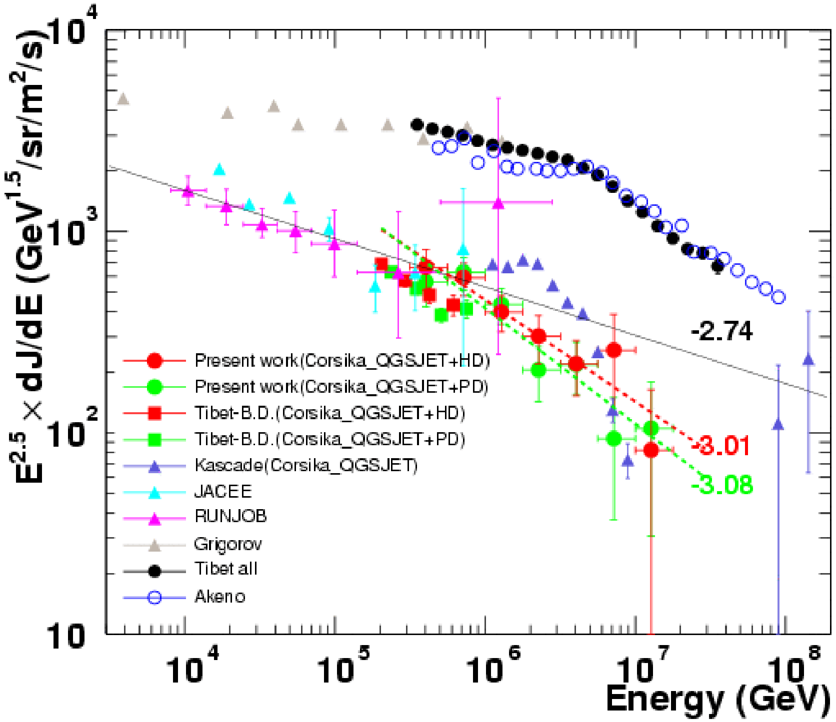

(b) (by SIBYLL model)

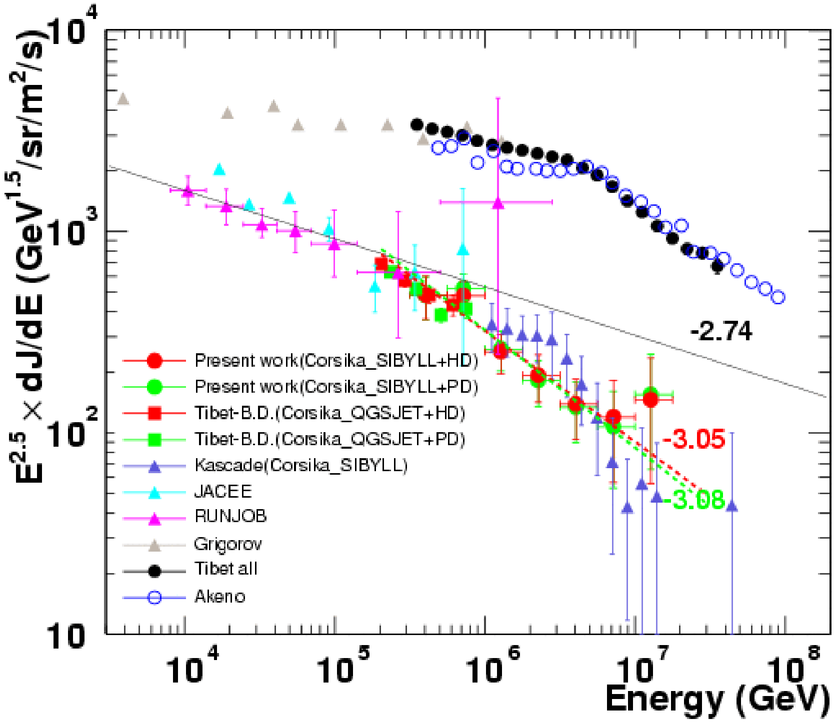

(KASCADE data: astro-ph/0312295)

Primary helium spectrum

(a) (by QGSJET model)

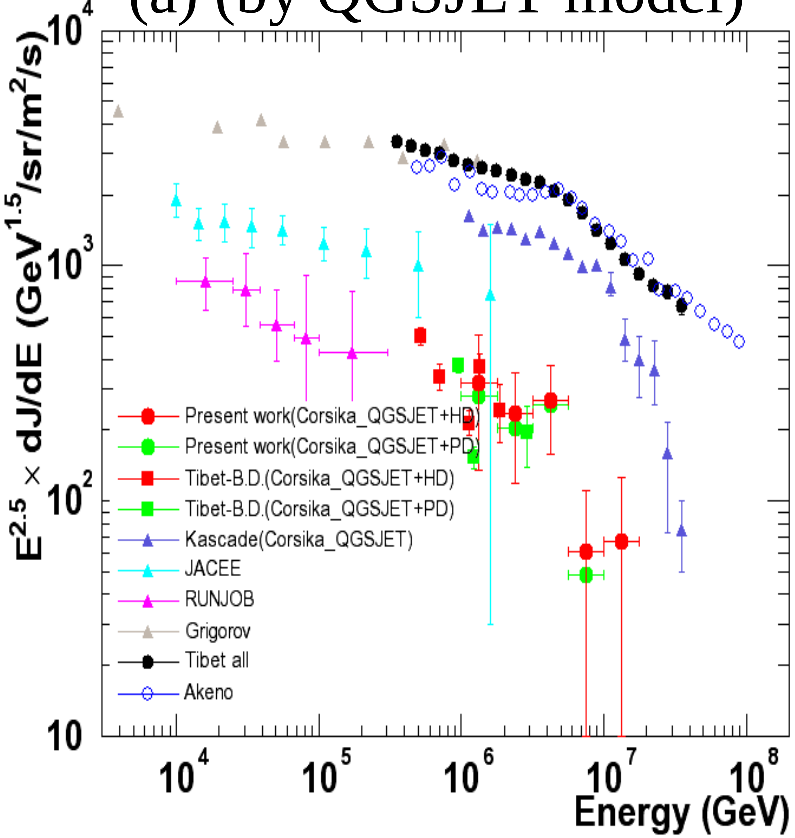

(b) (by SIBYLL model)

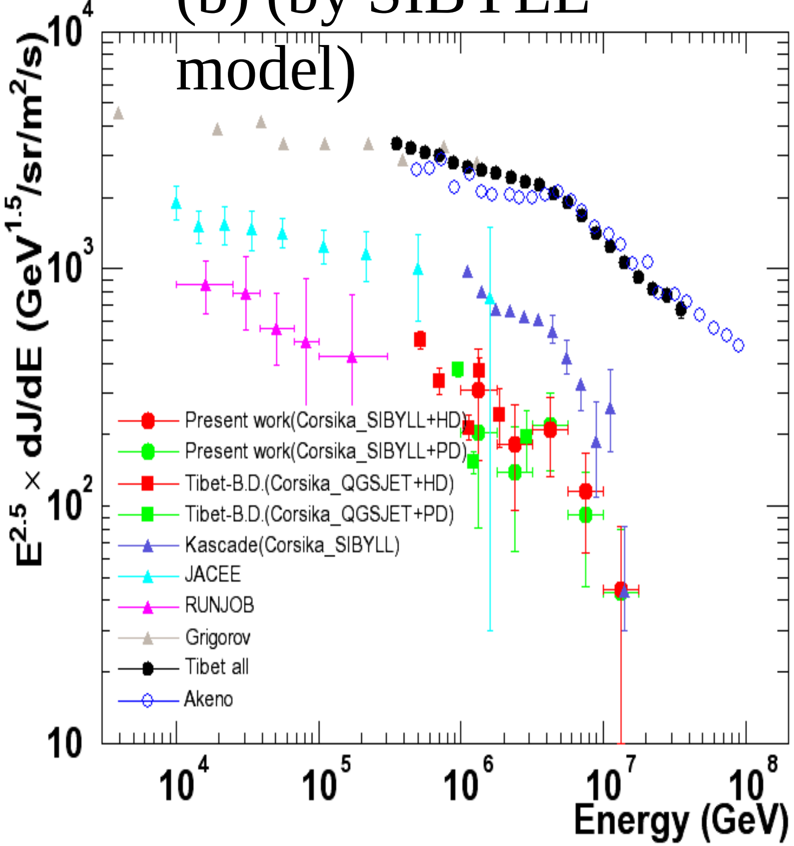

p+helium selection: purity=93%, efficiency=70%

Primary Cosmic Ray Energy Spectrum

CORSIKA_QGSJET

CORSIKA_SIBYLL

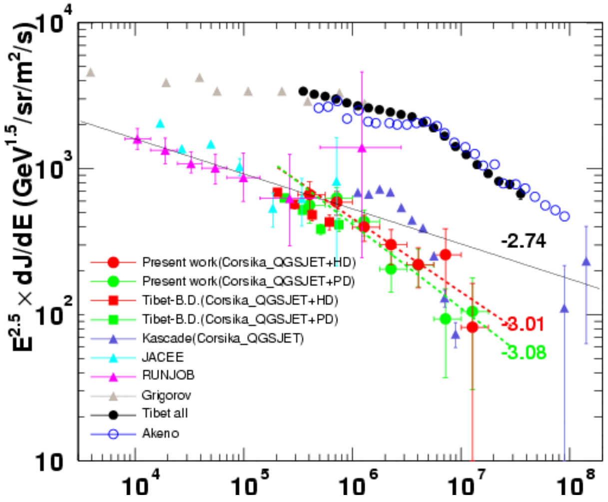

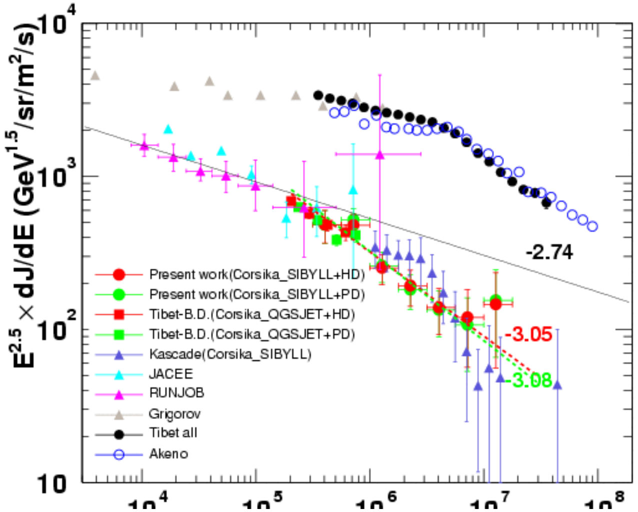

Proton

Small model dependence

(30 %)

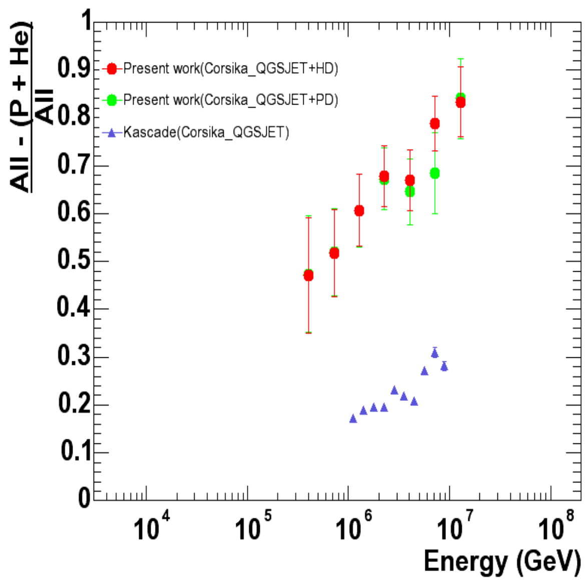

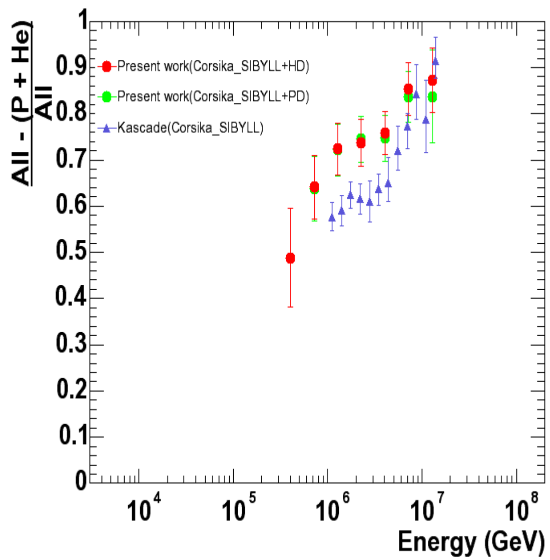

$$\frac{\text{All} - (\text{p+He})}{\text{All}}$$

PL B632 (2006) 58-64

The anisotropy at the solar time frame

- Compton - Getting effect

(Compton, A. H., Getting, I. A. 1935, Phys. Rev. Let. 47, 817-821)

Apparent anisotropy due to terrestrial orbital motion around the Sun

$$CG(t) = (2+\gamma)\frac{v}{c}\cos(t)$$

$$(2+\gamma)\frac{v}{c} \approx 0.05\%$$

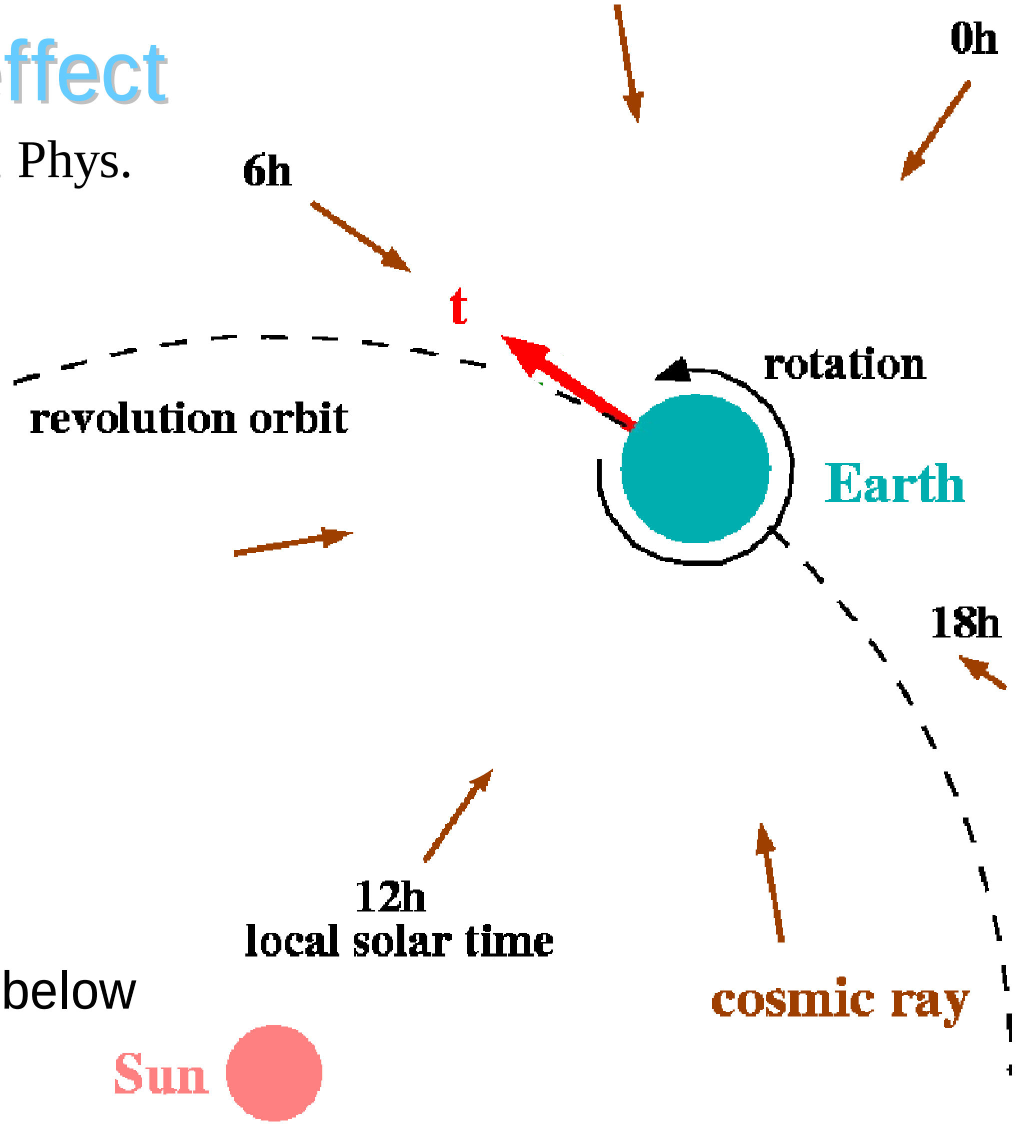

- Energy independent effect
- Afftected by solar acitivities below TeV energies

CG effect (Nov1999 – Nov2003)

PRL 93, 061101,(2004)

~$3x10^{10}$ EV in Total

Some other effects at low energies?

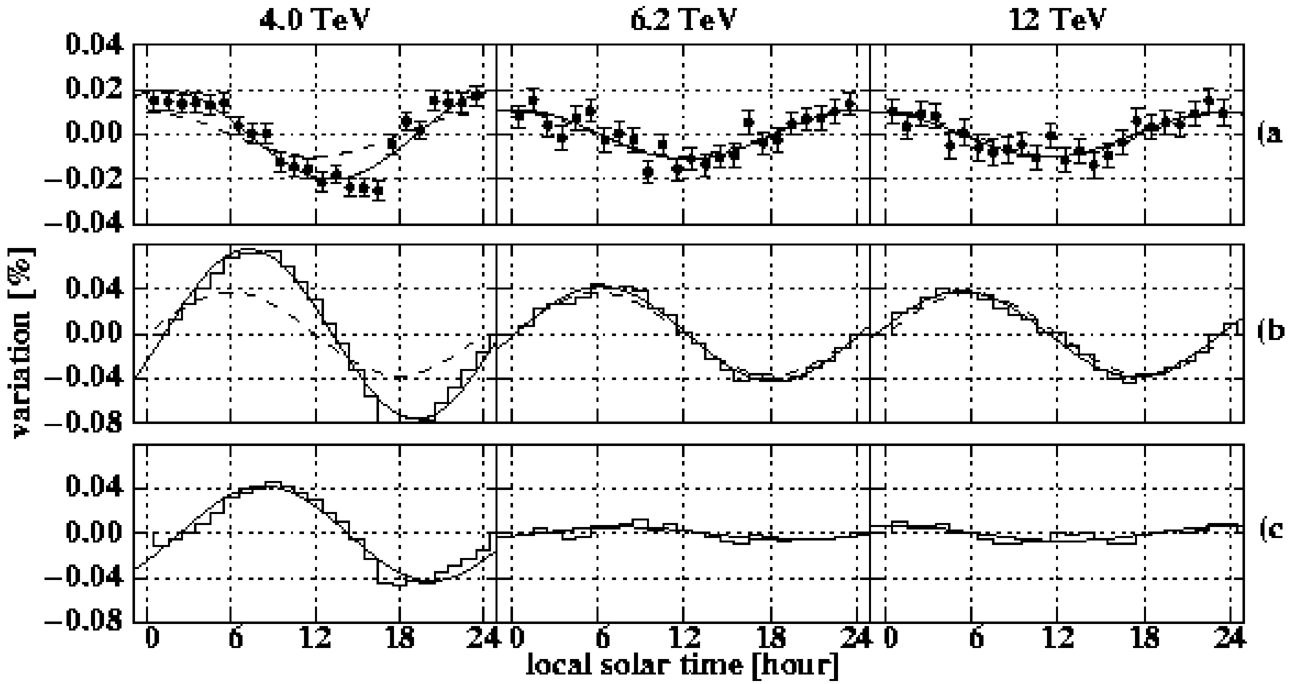

Differential

Integral

Data-CG

CG expected: ---

Cosmic Ray Anisotropy at Sidereal Time (ApJ, 626 (2005) L29-L32)

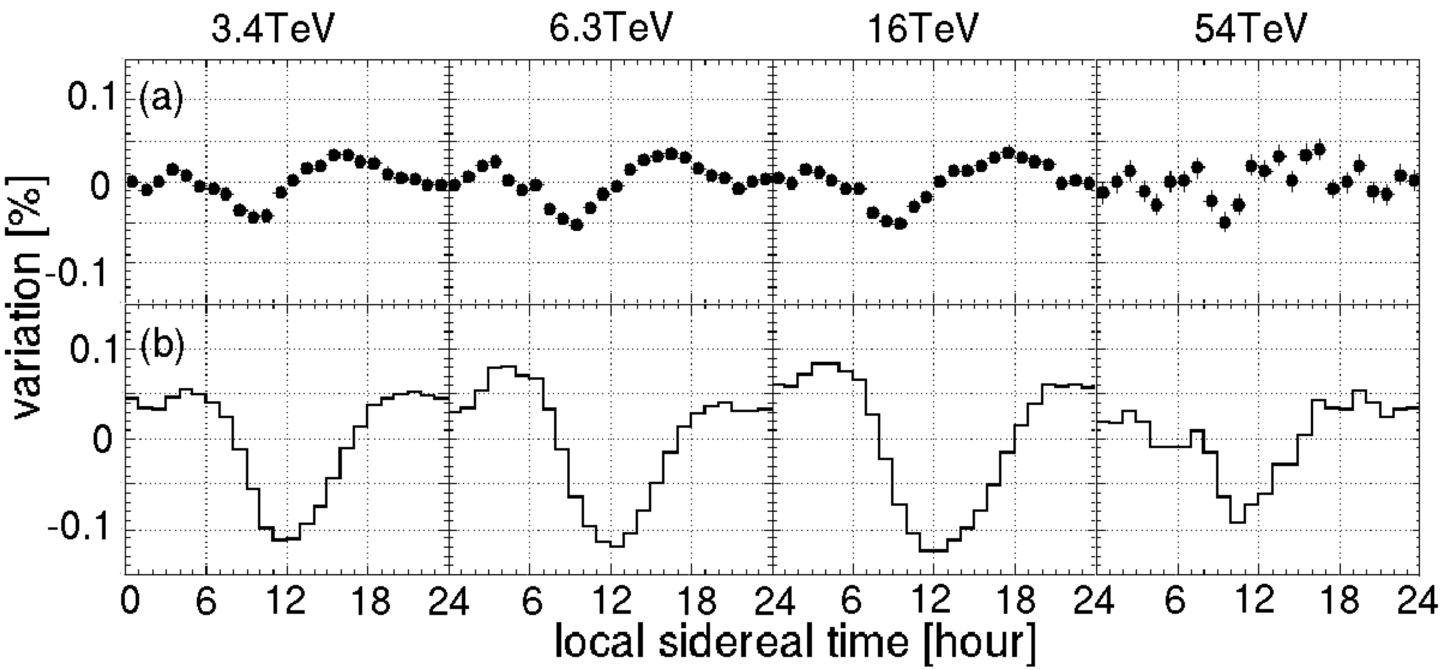

1999Nov-2003Nov 918 live days

~$3x10^{10}$ ev

Differential

Integral=

(Physical

Quantity)

Sidereal Time Anisotropy

Fourier First Harmonics

F

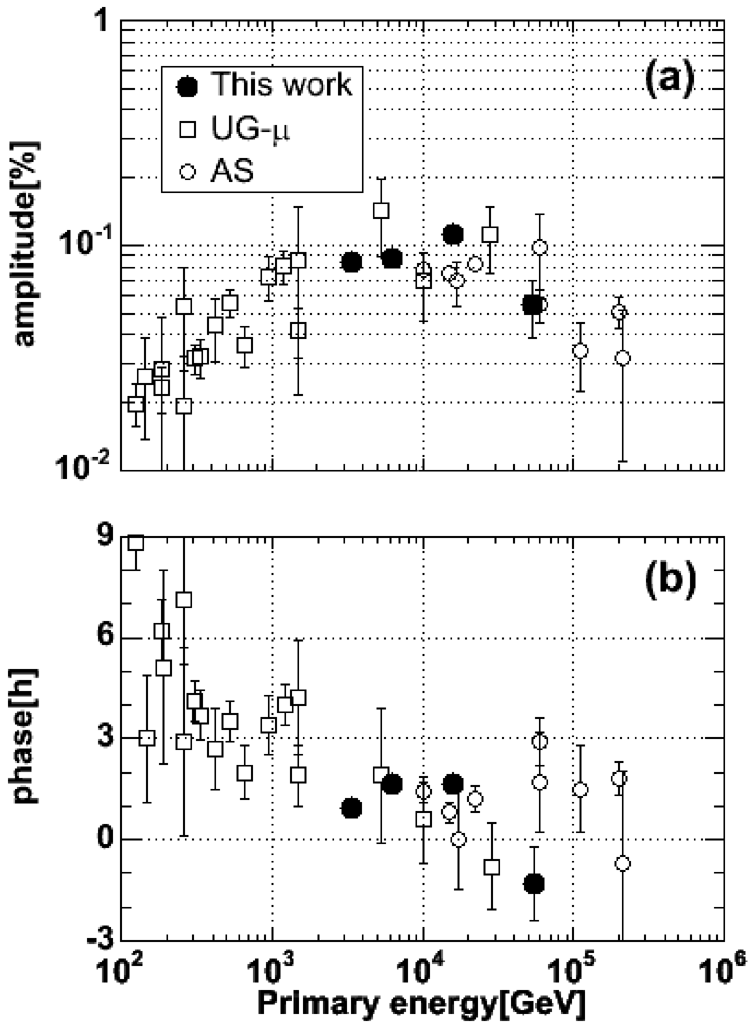

Declination Dependence of Amplitude

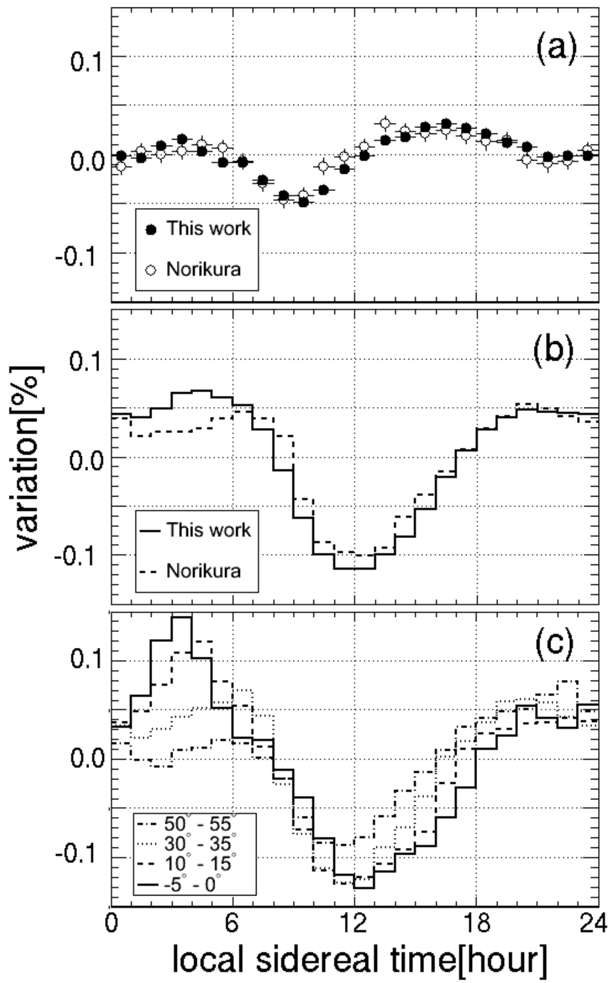

All Dec

Dec Dep

Multi-TeV Cosmic Ray Anisotropy

at Sidereal Time

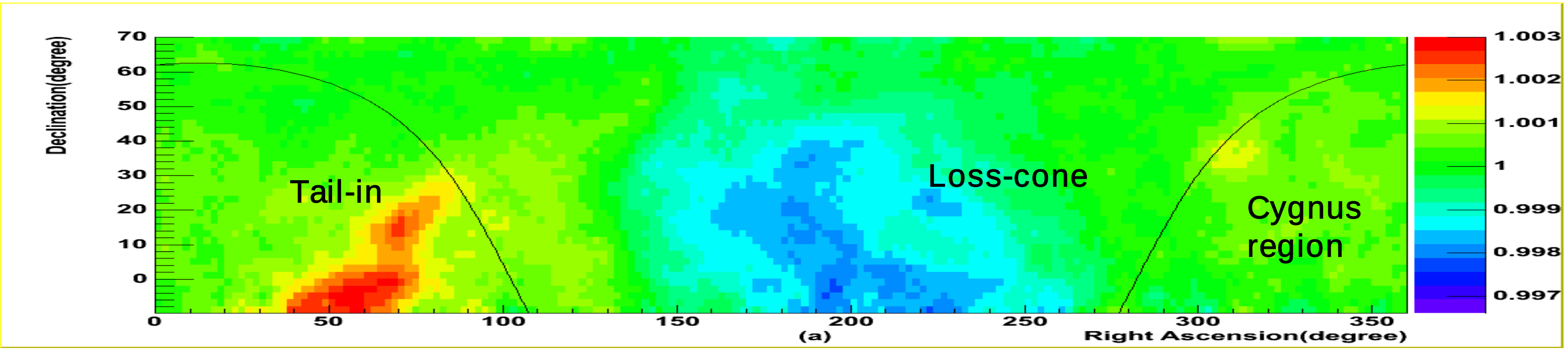

Relative Intensity (%) to CR

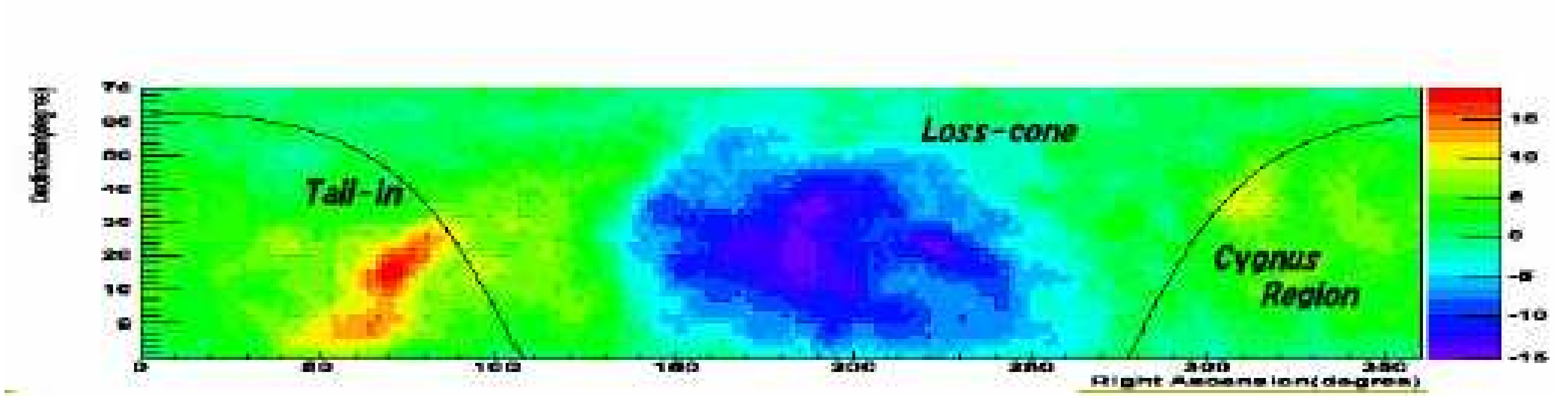

Excess(σ)

(ICRC2005, vol 2, 49-52), to be published in Science on Oct 20, 2006

Three calendar years data starting July 2000

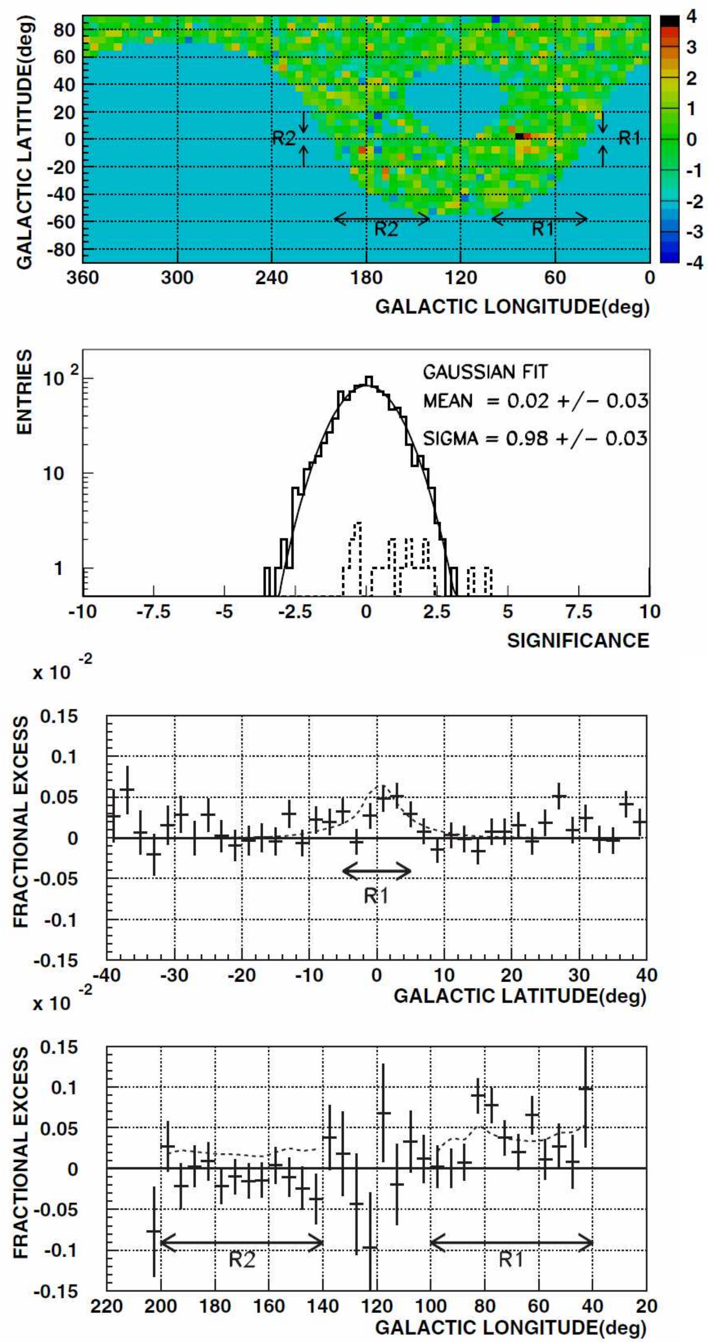

Milagro Paper

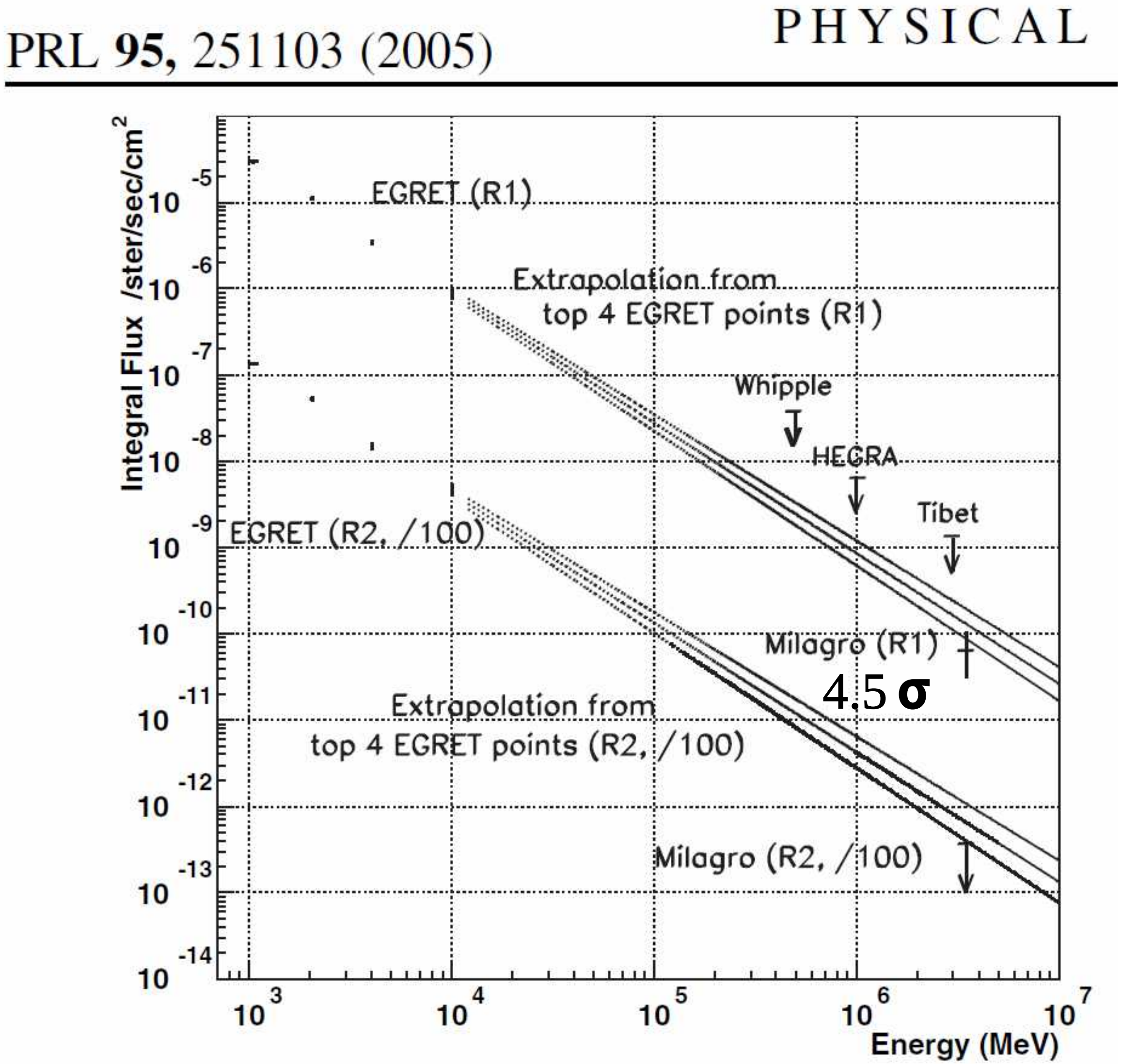

The Sun's shadow in cosmic rays

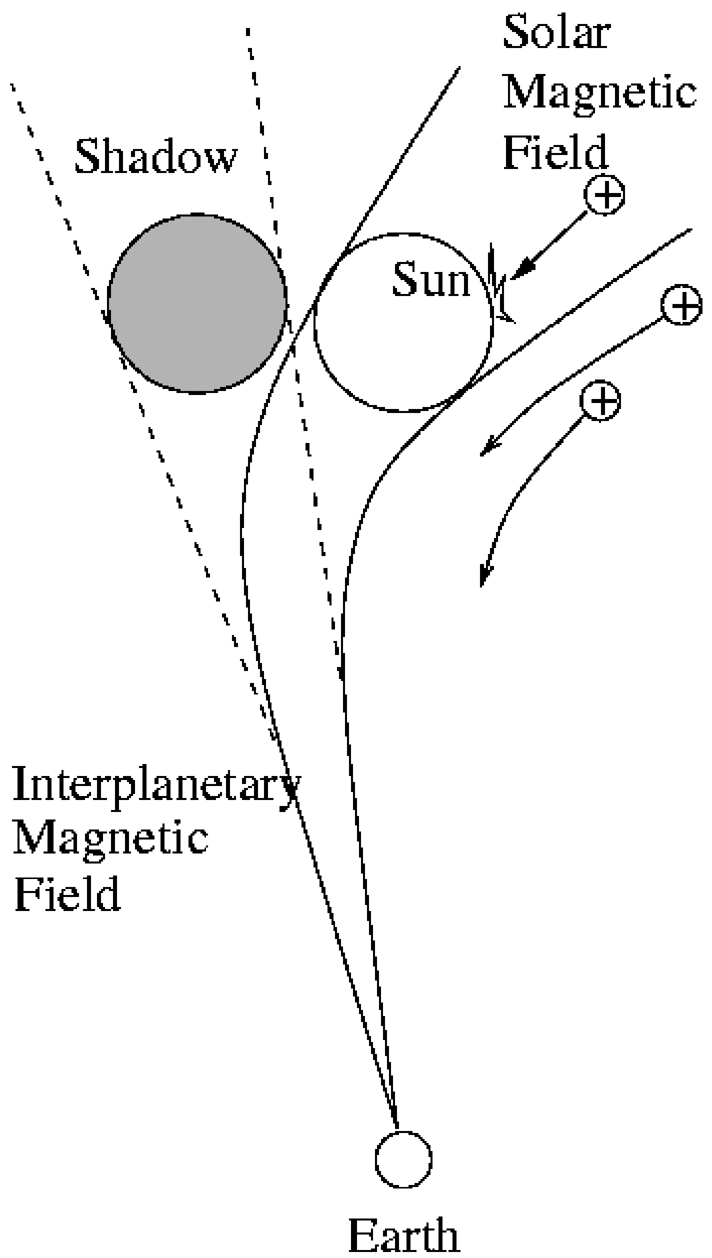

Solar Activity – Sunspots (Monthly)

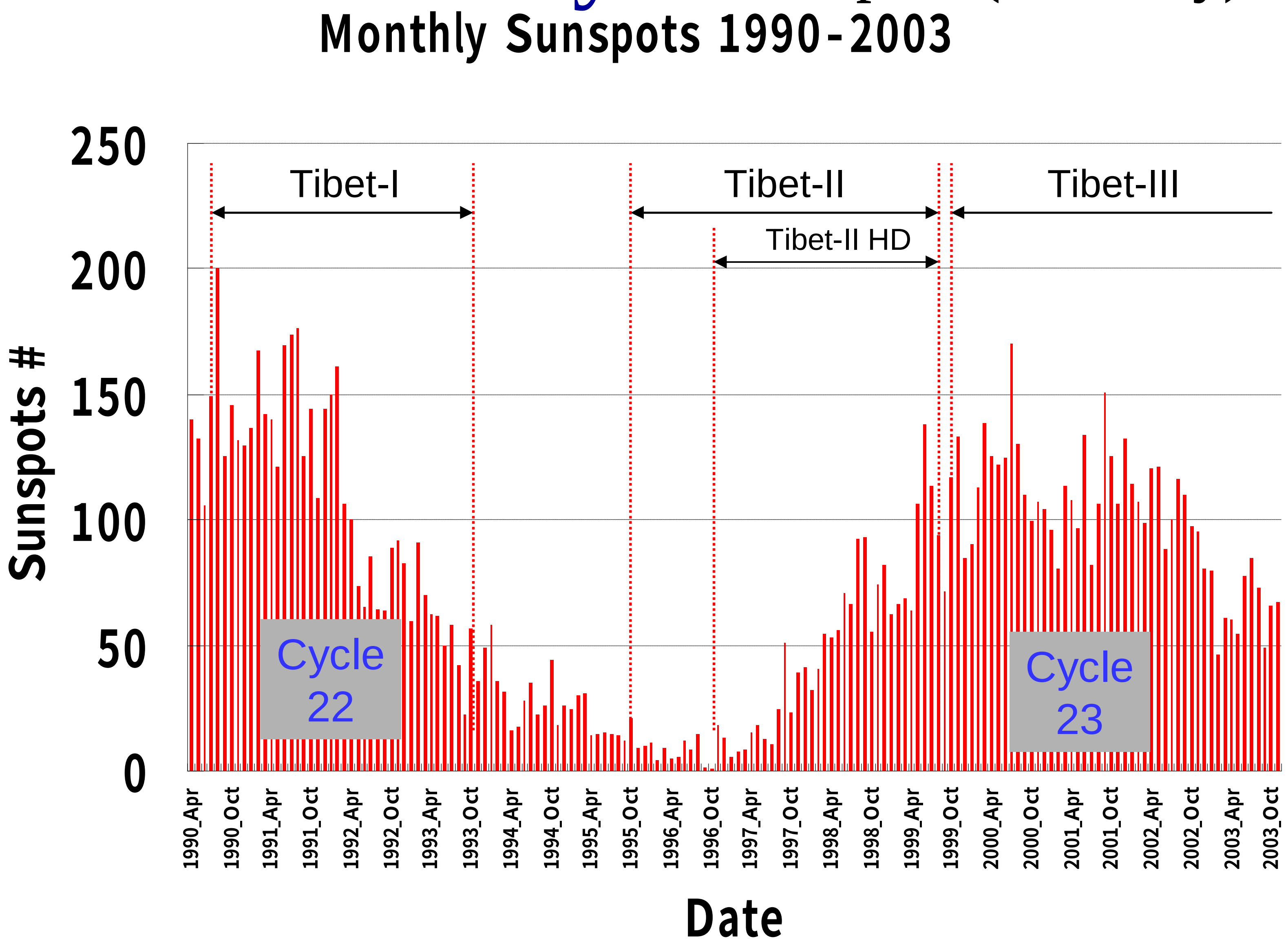

Observation – Sun Shadow

Anti-correlation between Sun shadow and sun spot # @ 10 TeV

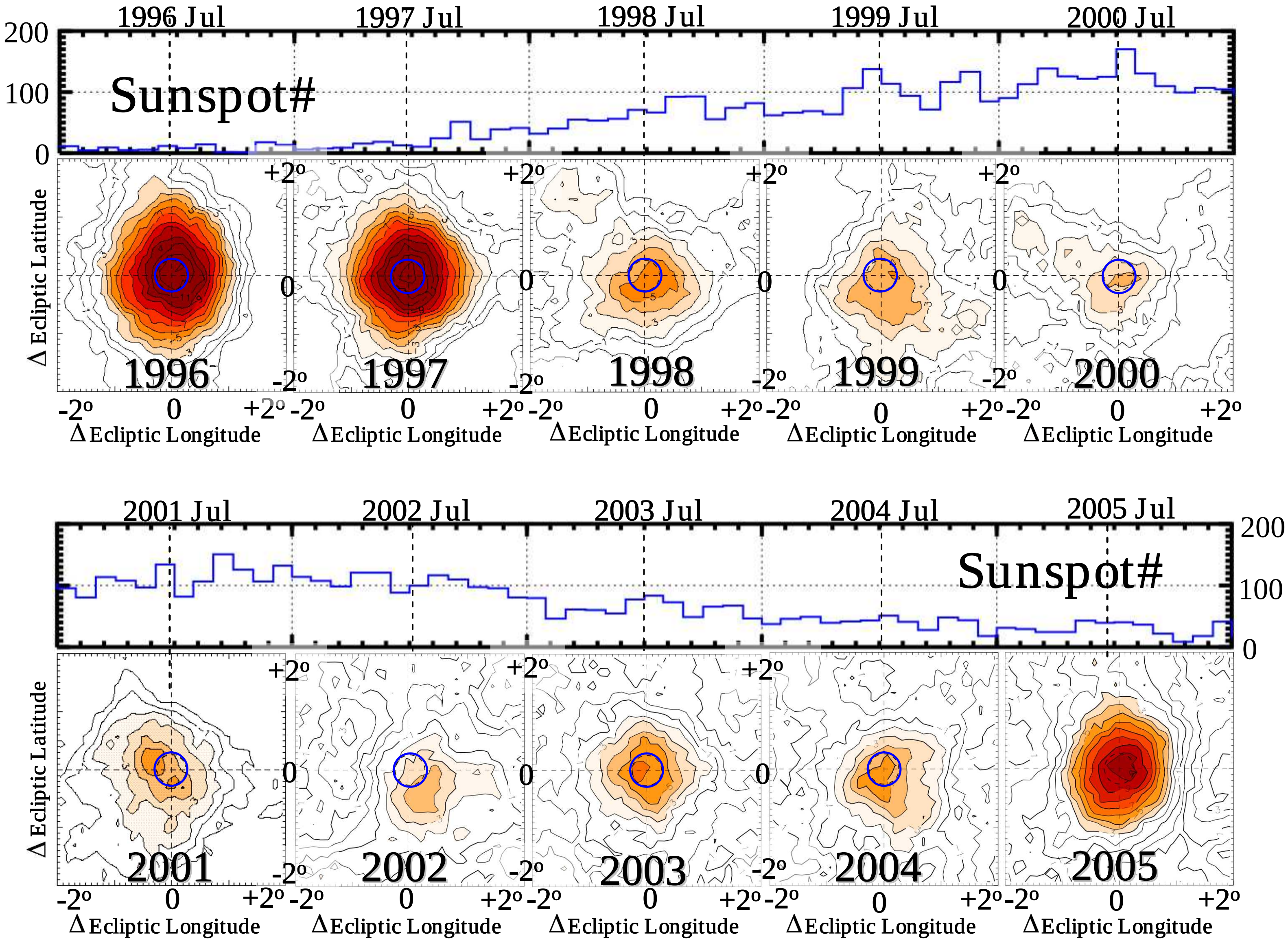

Potential Field Source Surface Model

- Radial Field model by Hakamada, Chubu U.
- scalar potential in the coronal magnetic field
  - expansion by spherical harmonics (order: n)
- Assumption
  - No coronal current (no influence on magnetic field)
  - Scalar potential(@$R_{2.5}$)=0 (to prevent troidal magnetic field)
  - Only radial component at the solar surface

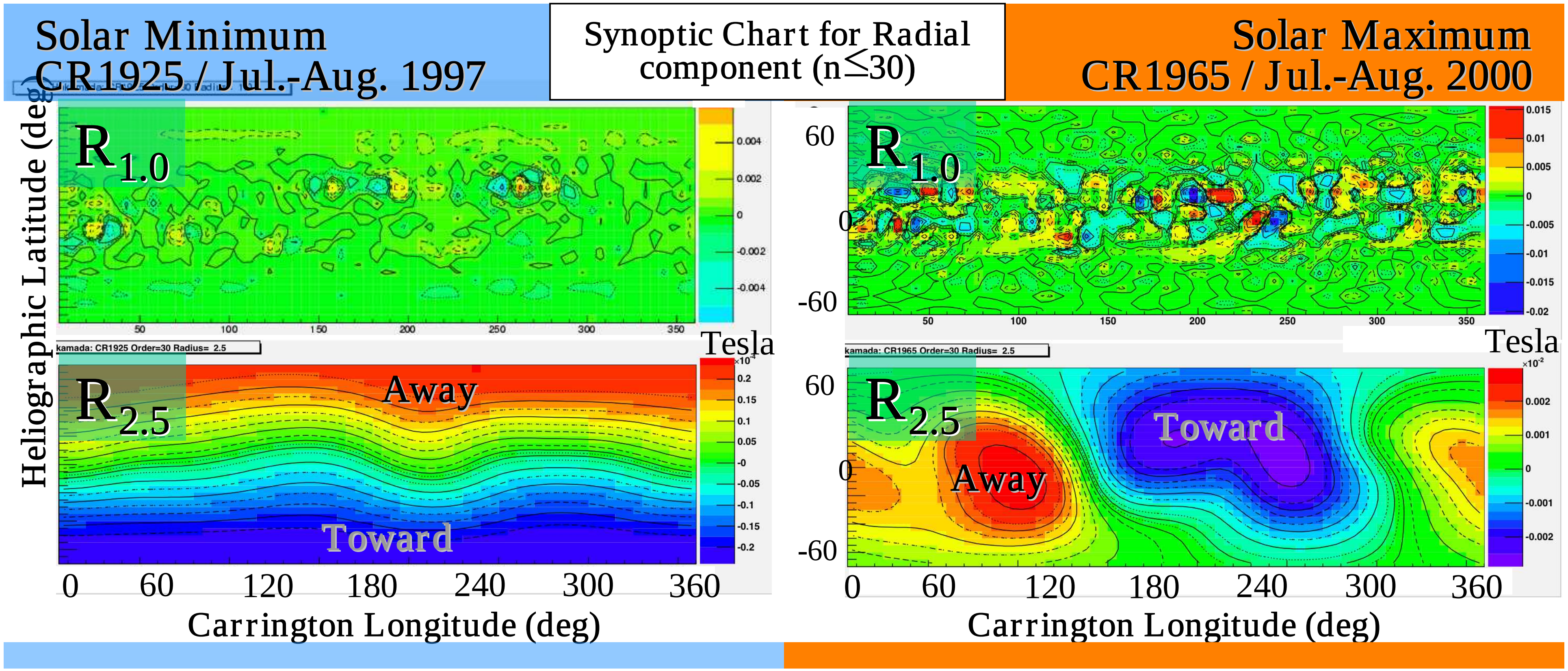

Yearly Variation of Deficit within 3°
around the apparent sun's direction @ 10 TeV

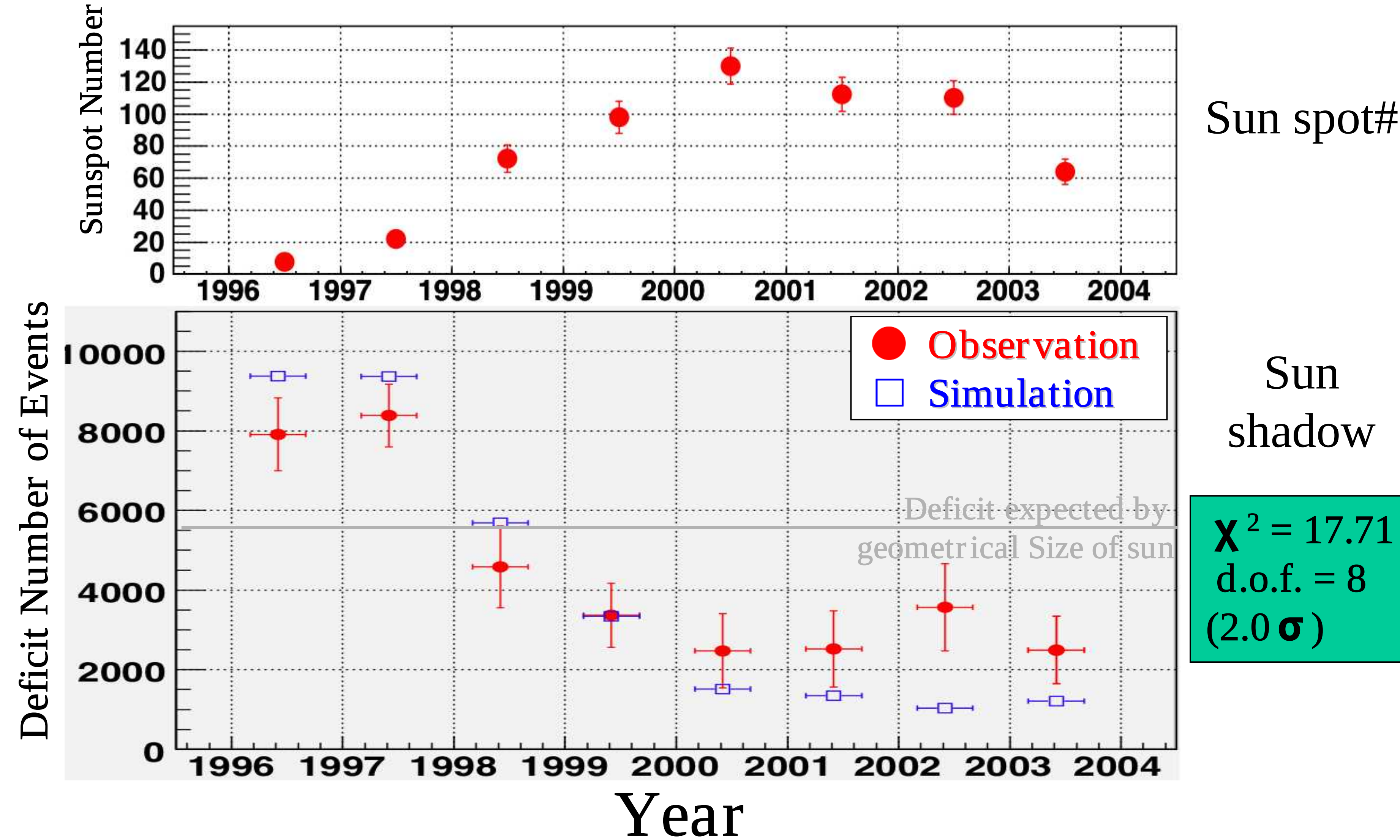

$\chi^2 = 17.71$
d.o.f. = 8
(2.0 σ)

Gnevyshev gap in 2001

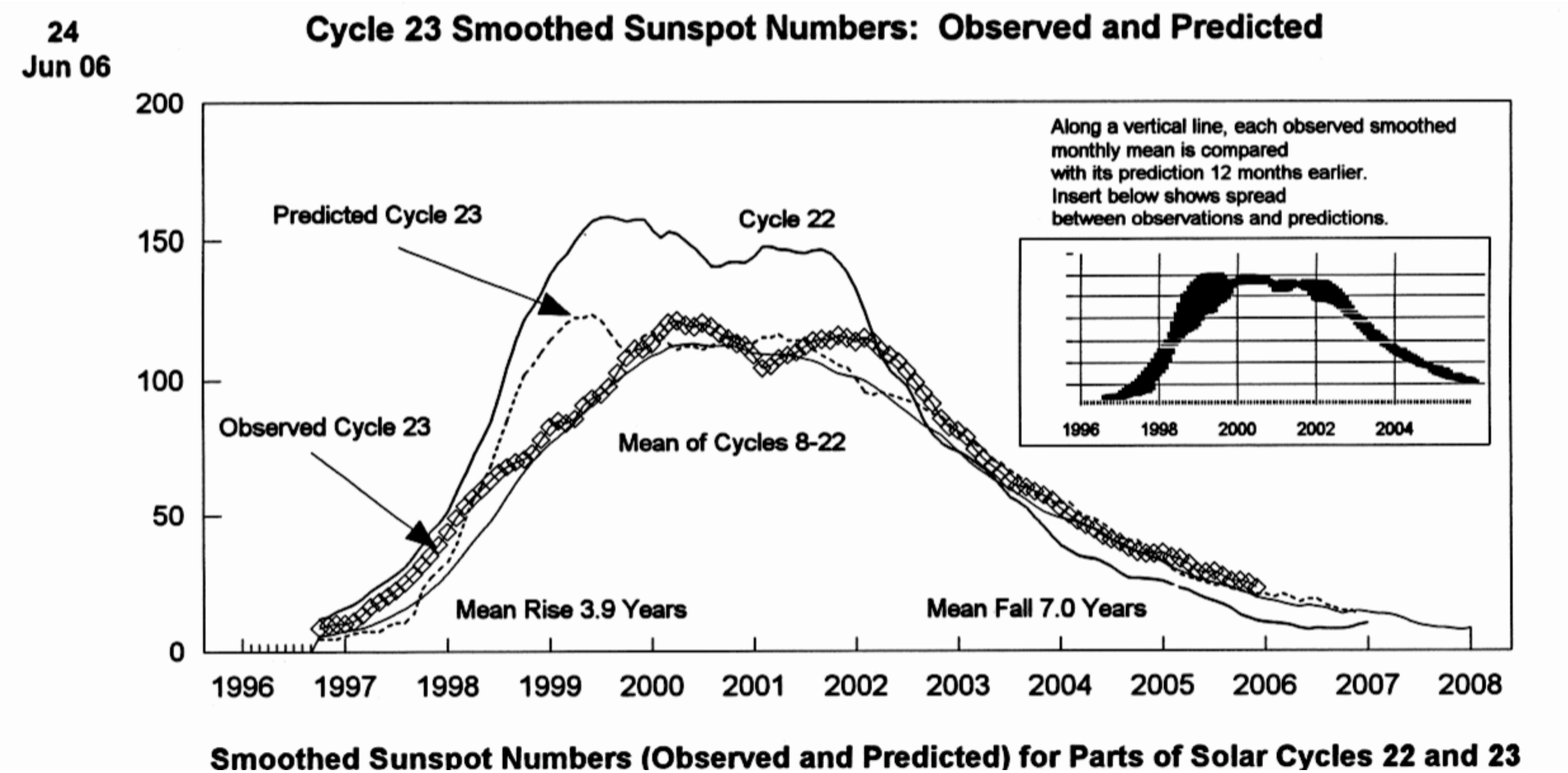

Yearly change of Sun shadow (1996–2005) , 3TeV

Gnevyshev gap

in 2001

2000(Tibet-III) 2001(Tibet-III) 2002(Tibet-III) 2003(Tibet-III)

2004(Tibet-III) 2005(Tibet-III)

What we have found out:

Crab, Mrk501 , Mrk421 observed, but

No new steady bright TeV γ-ray point source found

Possible diffuse γ-ray signal from Cygnus region?

P, He, all-particle E-spectrum (Galactic cosmic rays accelerated to the knee region ~10^{15} eV)

What we should do next:

1. 100 TeV (10 – 1000 TeV) region γ-ray astronomy

   Where do galactic cosmic rays under knee come from?

2. E-spectrum of heavy component around ‘ knee’

   All-particle knee = CNO? Fe knee?

1. 100 TeV γ-ray astronomy

Let's see 100 TeV-region gamma rays by

Tibet-III (AS) + a large underground

muon detector array (MD)

(8640m^2 in total)!

Origin of cosmic rays and acceleration

mechanism and limit at SNRs.

Diffuse gamma rays could be detected.

Design

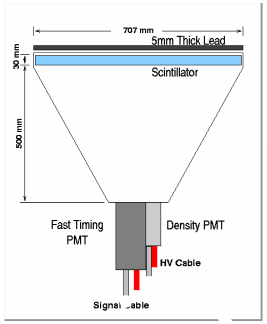

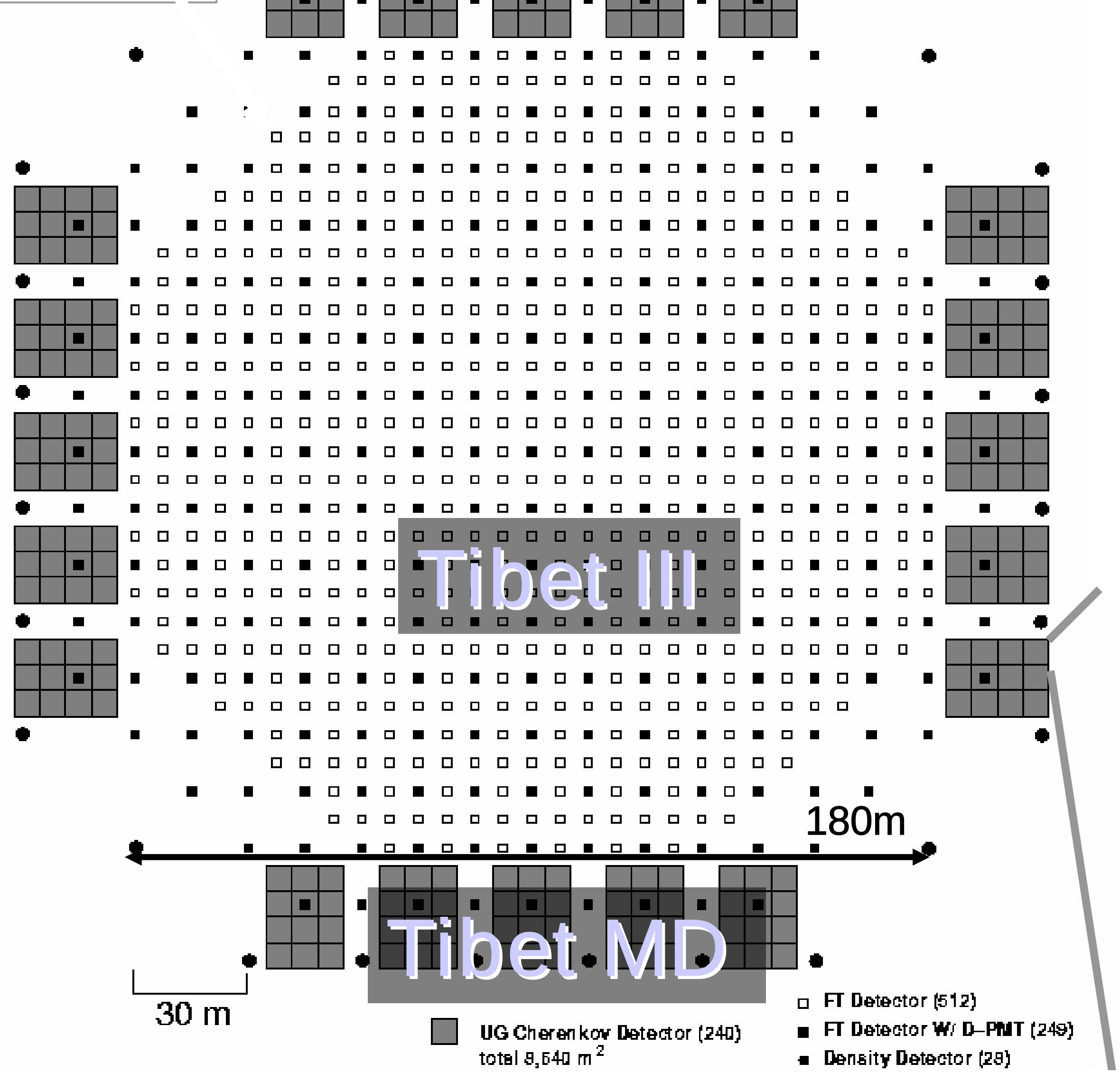

~ Muon detector ~

2.5m underground
(500g/cm^2: ~19 Xo)
waterproof concrete pool
6m x 6 m, 1.5m deep
20 ϕ PMT @ 1 detector

Inside is painted with white epoxy paint to waterproof and to efficiently gather catoptric water Cherenkov lights by a downward facing PMT

240 detectors Total: 8640m^2

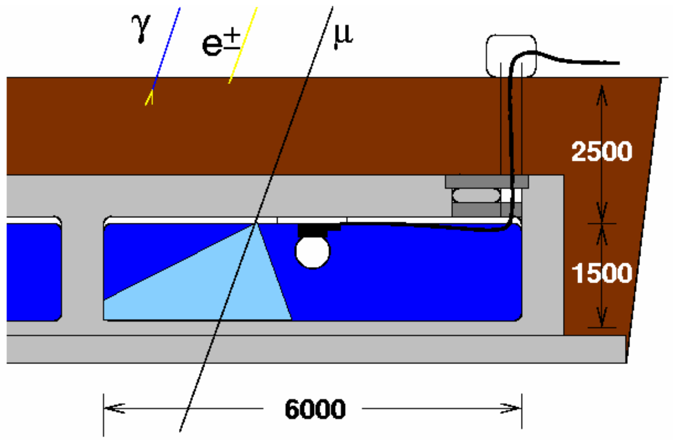

Image

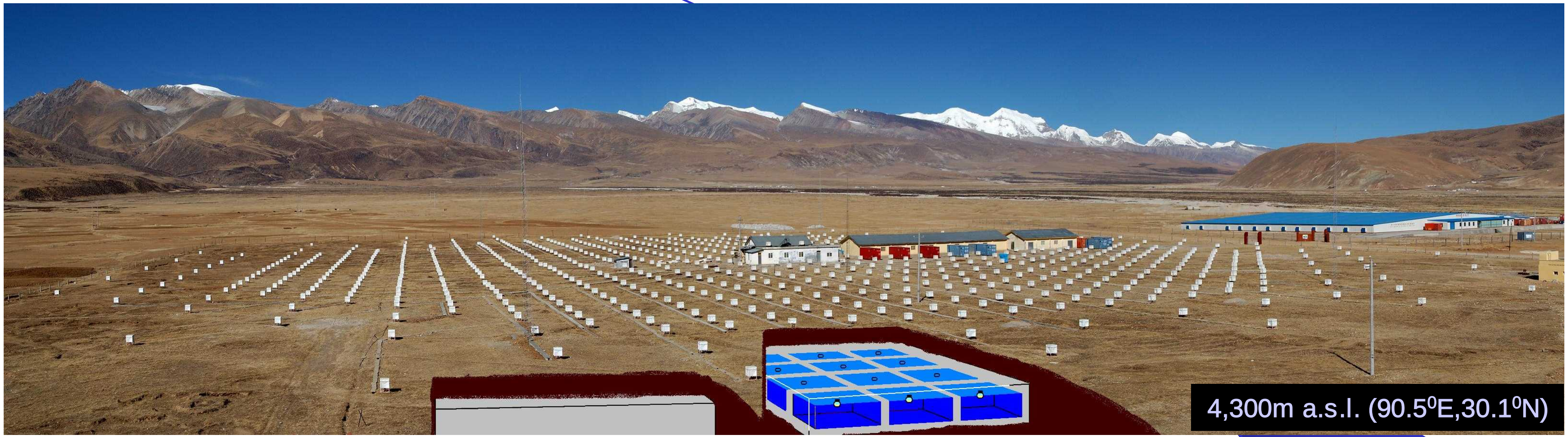
4,300m a.s.l. (90.5^{0}E,30.1^{0}N)

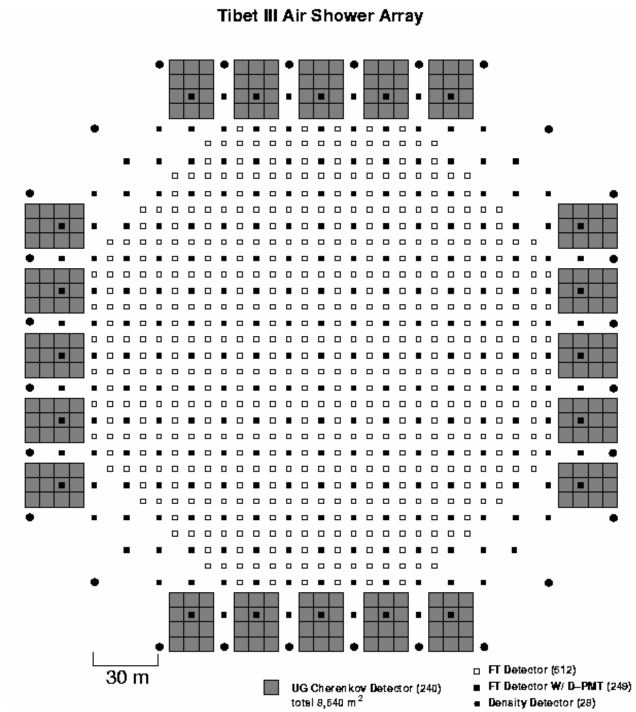
Tibet III Air Shower Array
30 m
UG Cherenkov Detector (240)
total 8,640 m^2
FT Detector (512)
FT Detector W/ D–PMT (249)
Density Detector (28)

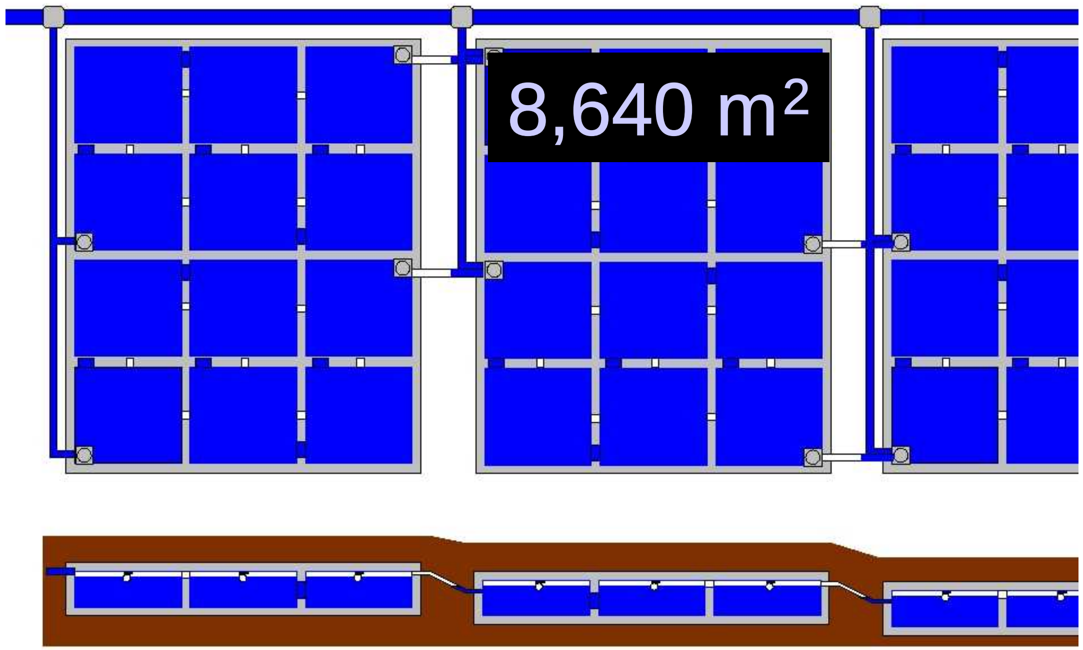
8,640 m^2

Advantages of the Cherenkov type muon detector are

- High cost performance
- High sensitivity to muons rather than electromagnetic component caused by the environmental background radioactivity and the air shower cascade,

because it is easy to design its pool depth (=path length of a muon) deeper, compared with a scintillation detector.

20 inch in diameter PMT (HAMAMASTU R3600)

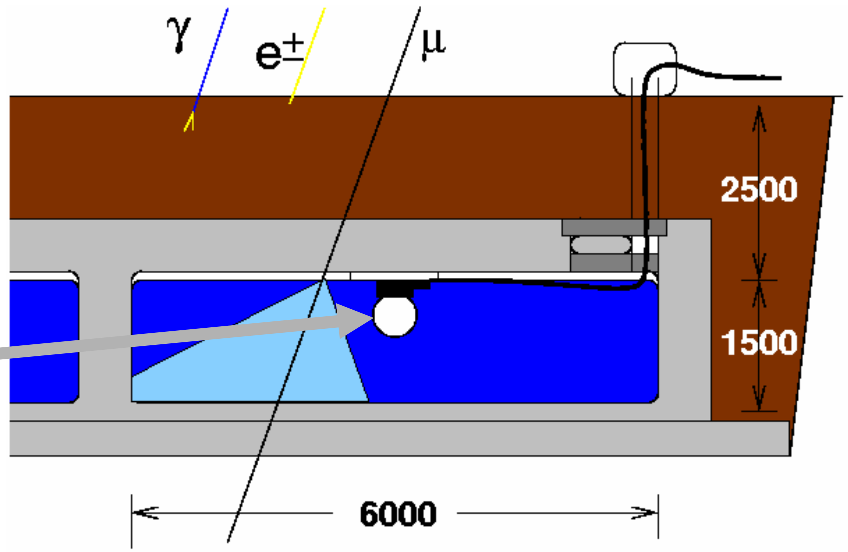

Example of existent Cherenkov detector design

	Milagro	Super-K (anti-D)	Tibet MD
PMT	8-inch PMT	8-inch PMT	20 inch PMT
Detector Size	80m x 60m, D=8m (Top 4800m^2/ Bottom 2000m^2)		ex.) 8640m^2
Grid or 1 Unit	2.8m x 2.8m	2 PMT@6m^2	1 PMT@ 36m^2
Photo-sensitive coverage	0.4%	0.52%	0.54%
Number of PMTs	Top: D=1.4m, 450 PMTs Bot.: D=6.0m, 273 PMTs	1885 PMTs	240 PMTs

Tibet MD detector will be expected enough response for muon detector.

Distribution of ΣN_{PE} as a function of $\Sigma\rho$

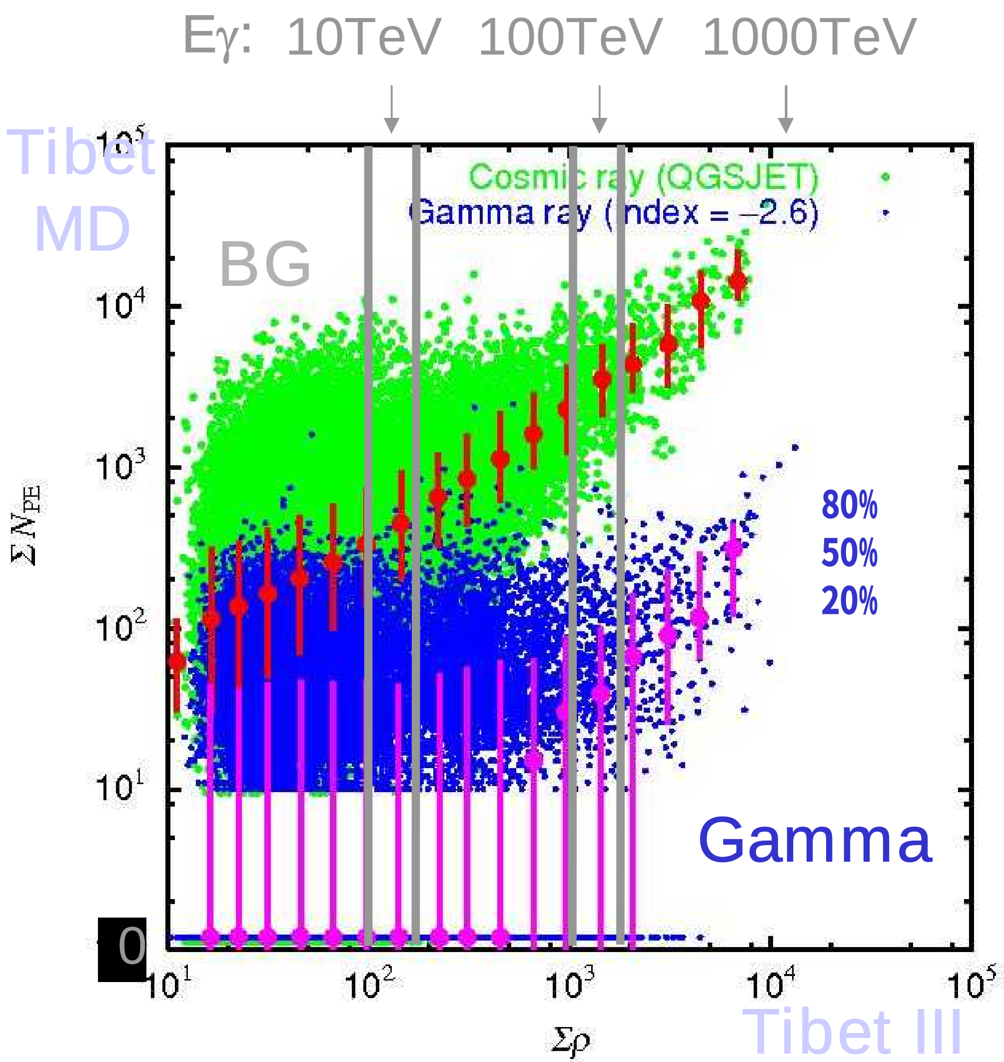

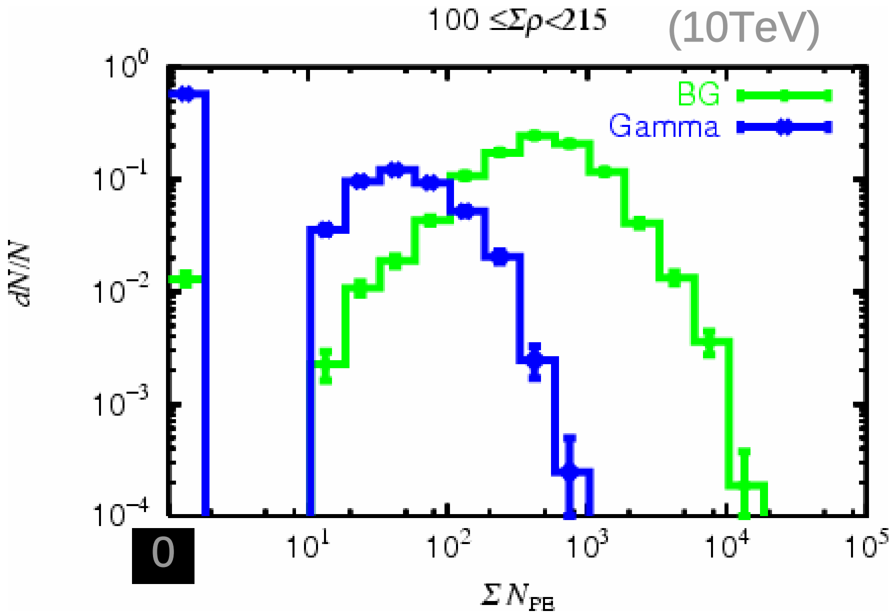

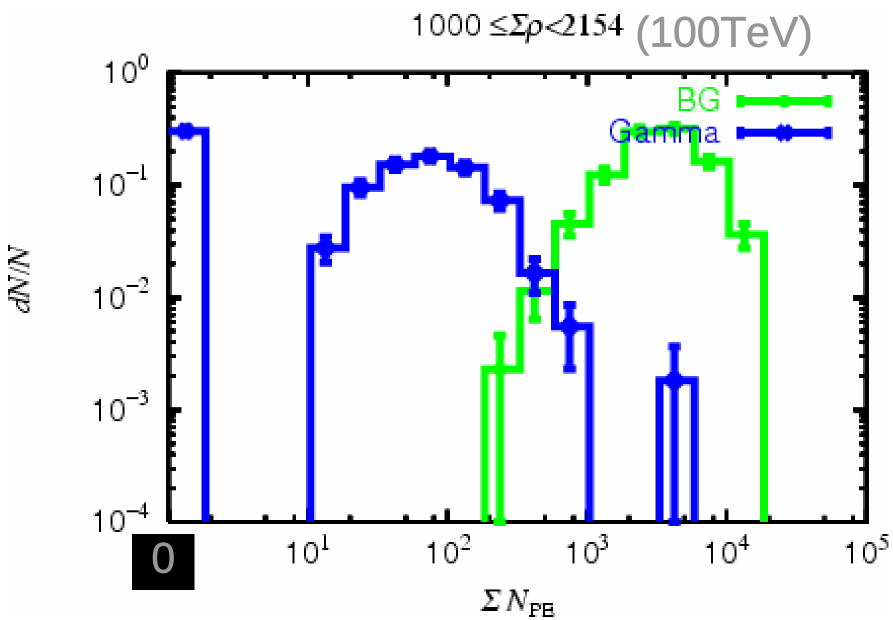

Hadron / Gamma Separation

10TeV:
ΣN_{PE}=~30
BG: ~97% rejection
Gamma: ~35% rejection
~65% survival
Sensitivity:
~4 times better!

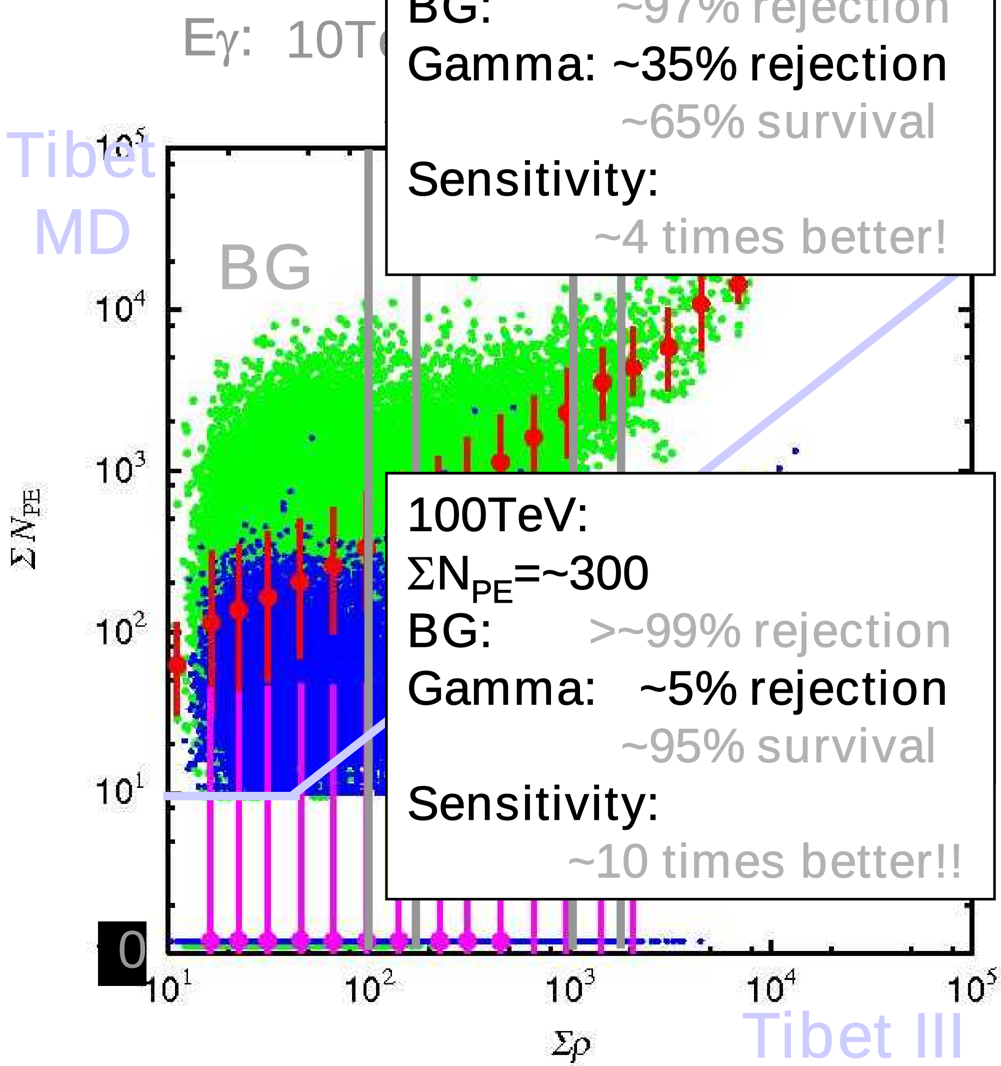

100TeV:
ΣN_{PE}=~300
BG: >~99% rejection
Gamma: ~5% rejection
~95% survival
Sensitivity:
~10 times better!!

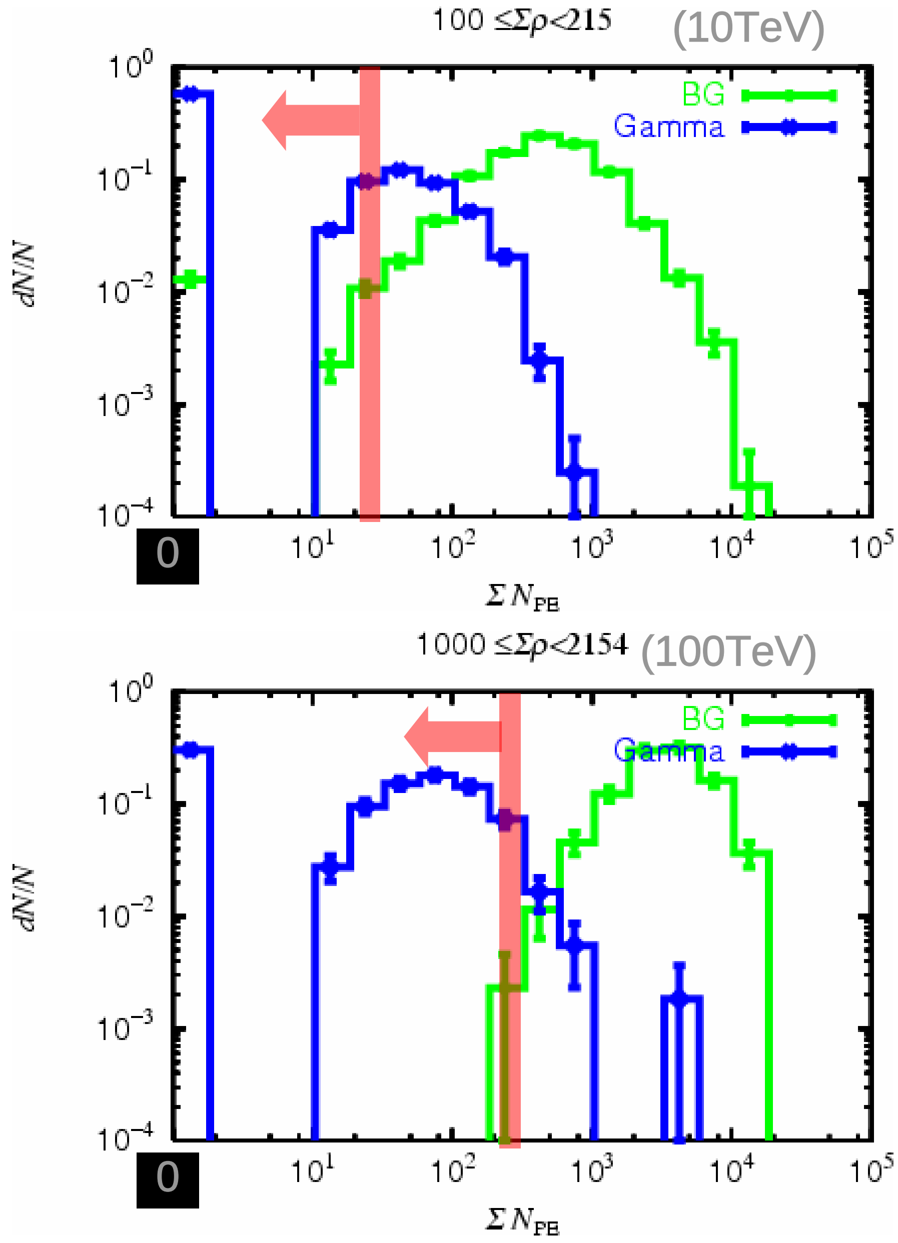

Survival efficiency after the cut

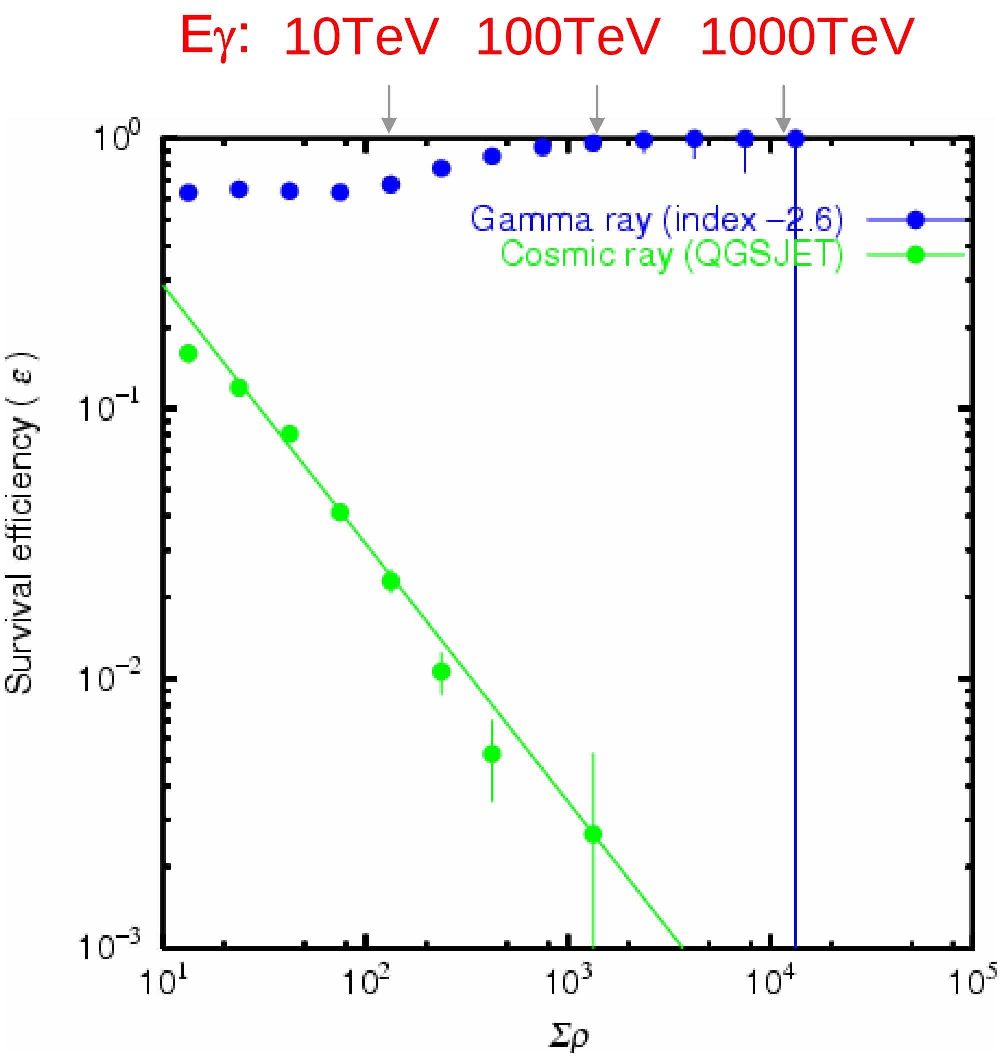

10TeV:
ΣN_{PE} =~30
BG: ~97% rejection
Gamma: ~35% rejection
~65% survival
Sensitivity:
~4 times better!

100TeV:
ΣN_{PE}=~300
BG: >~99% rejection
Gamma: ~5% rejection
~95% survival
Sensitivity:
~10 times better!!

1000TeV: (need more data)
ΣN_{PE}=~3000
BG: > ~99.9% rejection
Gamma: ~1% rejection
~99% survival

Background
FREE!!!

Sensitivity (Tibet AS + MD)

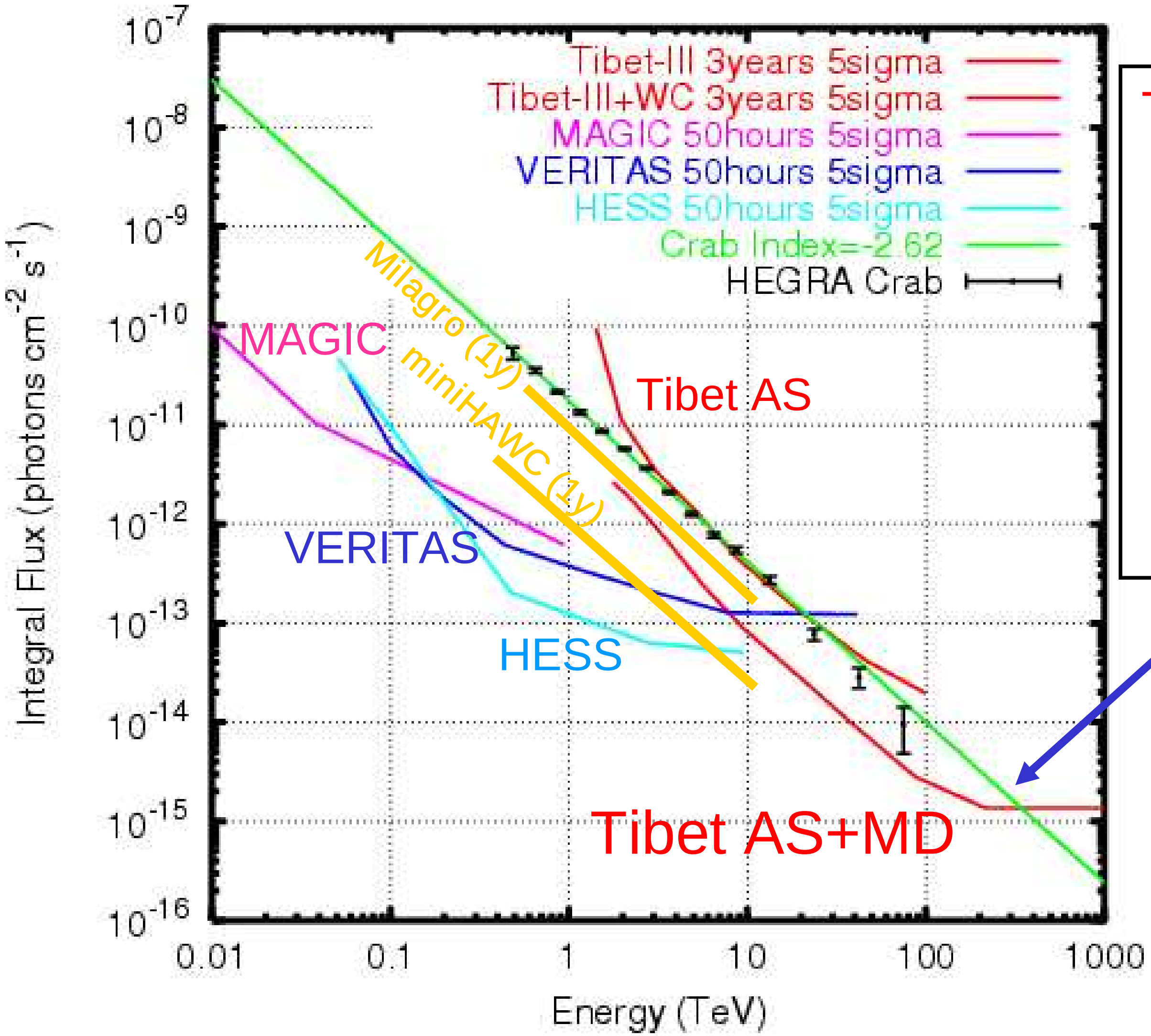

Tibet-III Scintillation Counters
37,000m^2
+
Underground
Water Cherenkov Detector
8,640m^2

Crab orbit

Flat region (> 200TeV)
Background << 1 event
15 photon sensitivity
(Poisson 5 **σ**)

Comparison between Tibet AS + MD and HESS

	Tibet AS+MD ~100 TeV	H.E.S.S. ~200 GeV
Location	30N-90E	23S-16E
F.O.V.	~1.5 sr	~0.02 sr
Duty cycle	~90%	~10%
Angular Resolution	~0.2 °	~0.1 °
Energy Resolution	~40%	~20%
Background Rejection	~99%	~99%
Sensitivity (RX J1713 Unit Index = –2.19)	~5% RXJ1713 (3 year 5 $\boldsymbol{\sigma}$)	~1% RXJ1713 (50 hours 5 $\boldsymbol{\sigma}$)
Detected Sources	?	~20

TeV Source Catalog in the Northern Sky

Object Name	Class	Culmination Zenith at Tibet (deg.)
Crab Nebula	PWN	8
Cas A	SNR	29
TeV J2032+4130	SNR? (vicinity of Cyg X-3)	11
Milagro Region	Diffuse **γ**	10
HESS J1837-069	SNR? (G25.5+0.0?, AX J1838-0655?)	37
HESS J1834-089	SNR? (G23.3-0.3 / W41?)	39
LS I +61 303	XRB	31
M87	AGN (z=0.00436)	18
Mrk 421	AGN (z=0.031)	8
Mrk 501	AGN (z=0.034)	10
1ES 1959+650	AGN (z=0.047)	35
H 1426+428	AGN (z=0.129)	13

Tibet AS+MD can detect in the 100 TeV region?

Diffuse gamma rays from Milagro IG region

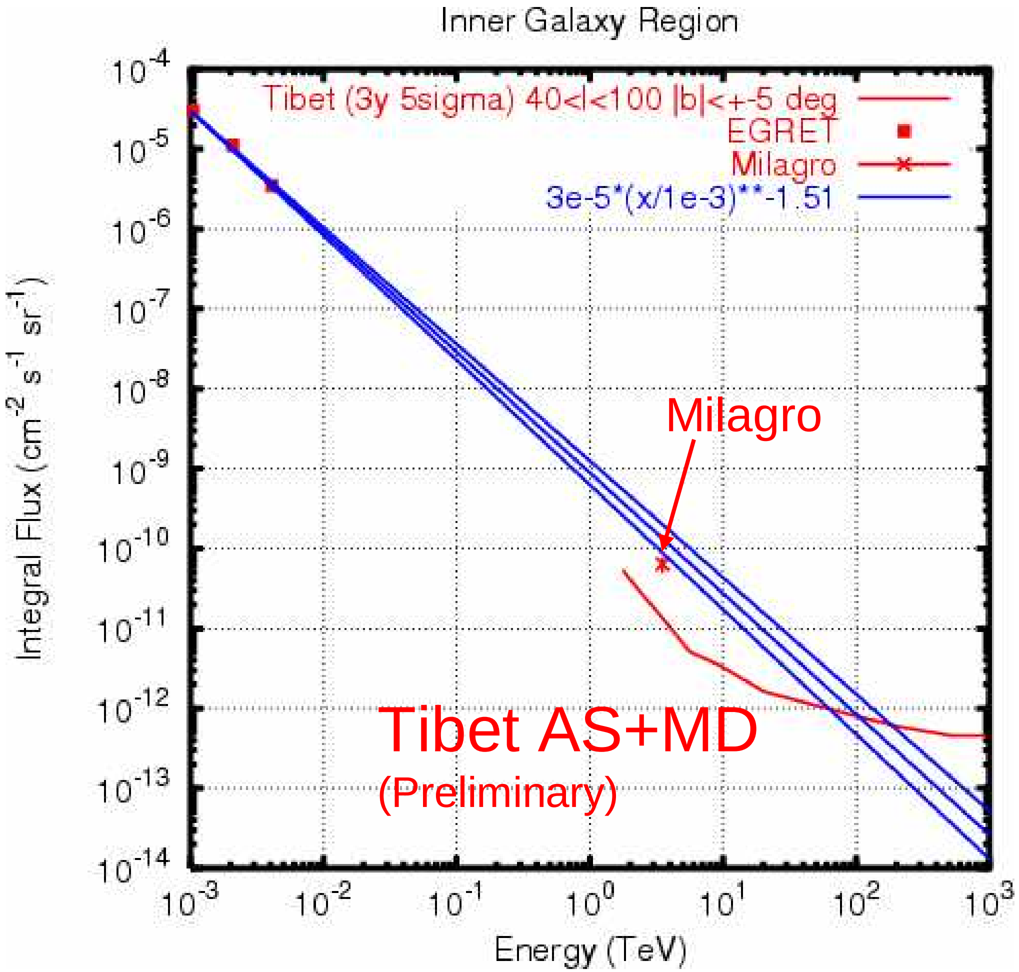

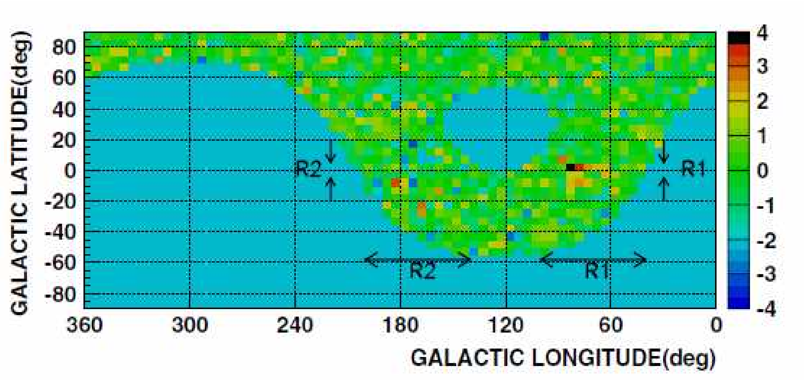

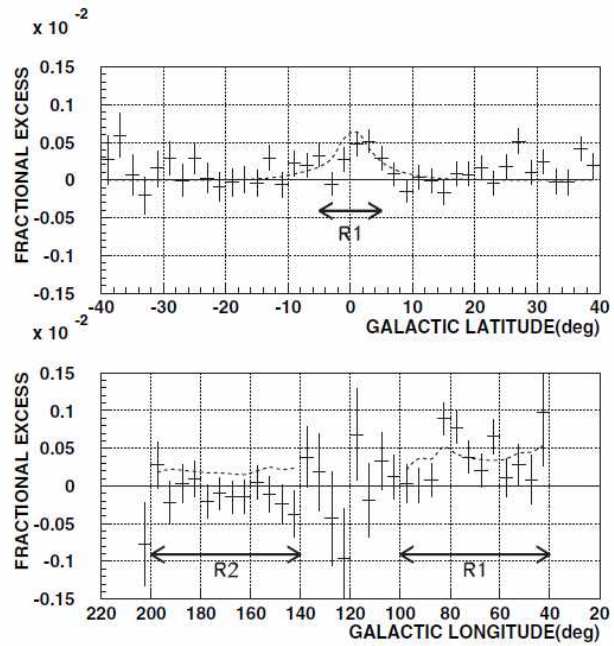

FIG. 3. Profiles of the fractional excess in latitude for the $R1$ longitude band $l \in (40°, 100°)$, and in longitude for the latitude band $|b| < 5°$ of $R1$ and $R2$. The dashed lines show the EGRET source shape.

Atkins et al, Phys. Rev. Let., 95, 251103 (2005)

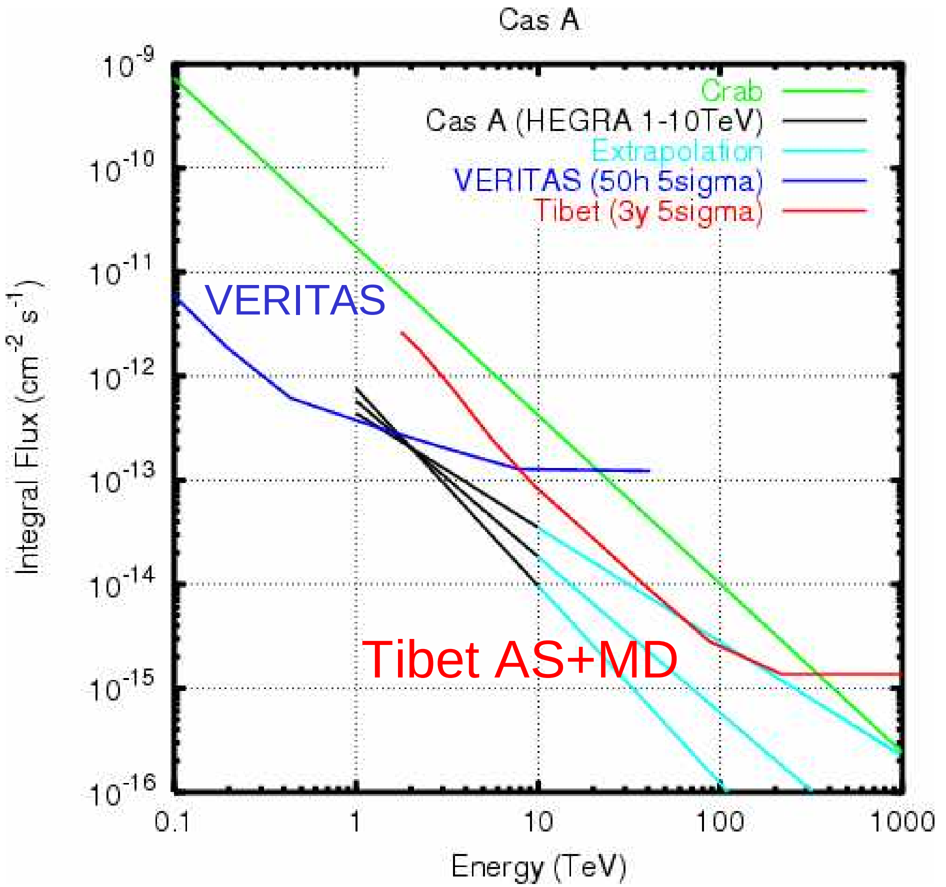

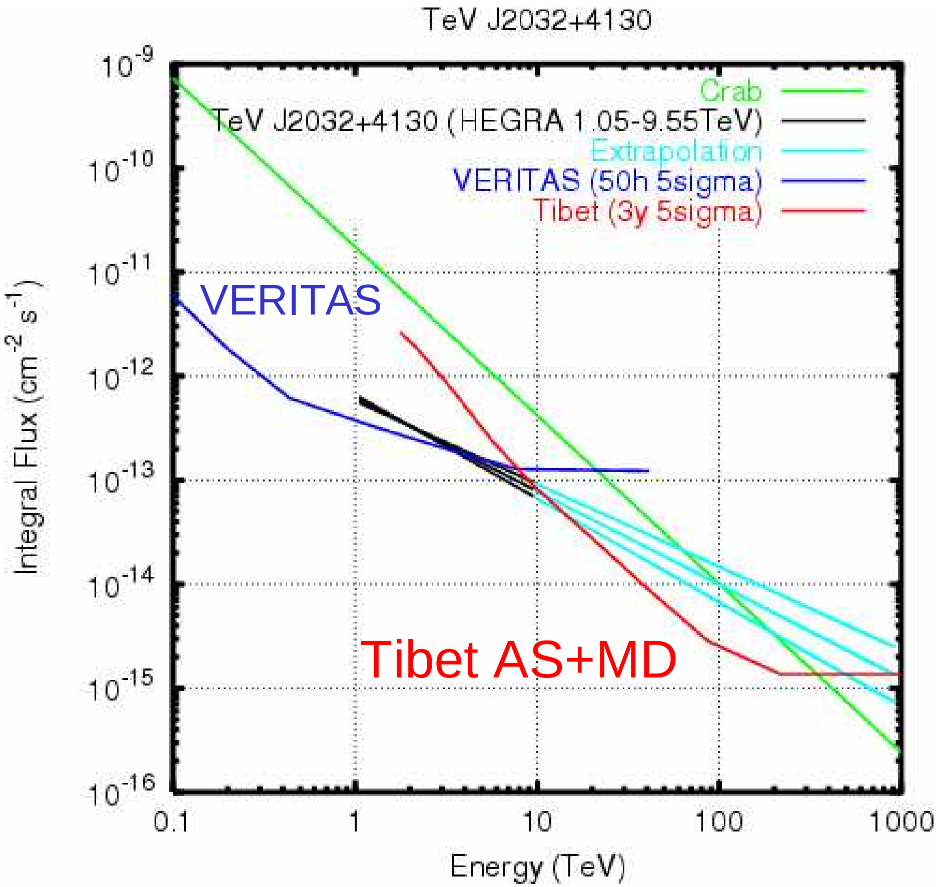

Cas A

Brightest shell-type SNR in radio
Distance ~3.4 kpc
Age 1680 years
HEGRA live time ~232 hours
Flux ~3.3% Crabs
IC+bremsstrahlung? π^0 decay?

Aharonian et al, A&A, 370, 112 (2001)

TeV J2032+4130

Unidentified TeV source
Located near Cyg X-3 in Cyg OB2
HEGRA live time ~158 hours
Extended source ~6.2 ′
π^0 decay?

Aharonian et al, A&A, 431, 197 (2005)

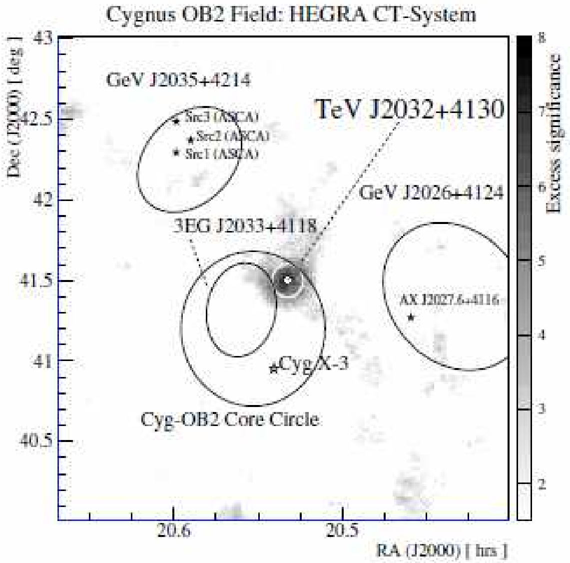

Fig. 2. Skymap of correlated event excess significance (σ) from all HEGRA IACT-System data (3.0° × 3.0° FoV) centred on TeV J2032+4 Nearby objects are indicated (EGRET sources with 95% contours). The TeV source centre of gravity (CoG) with statistical errors, and intr size (std. dev. of a 2D Gaussian, σ_{src}) are indicated by the white cross and white circle, respectively.

Aharonian et al, A&A, 370, 112 (2001)

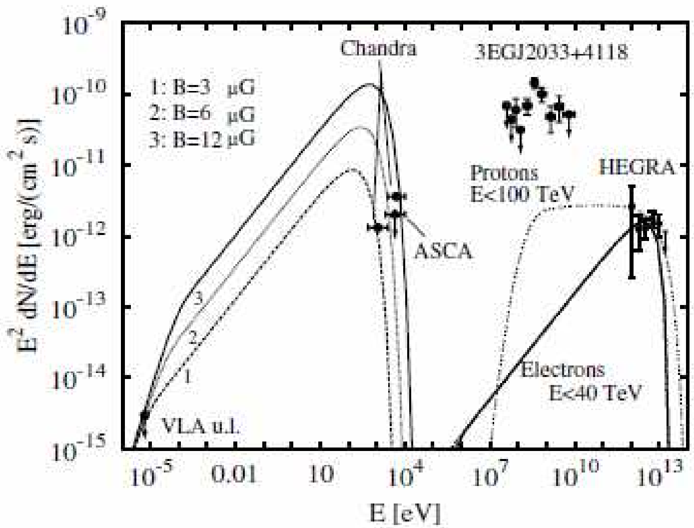

Fig. 3. Spectrum of TeV J2032+4130 (this work – HEGRA) compared with purely hadronic (Protons $E < 100$ TeV) and leptonic (Electrons $E < 40$ TeV) models. Upper limits, constraining the synchrotron emission (leptonic models), are from the VLA and *Chandra* (Butt et al. 2003) and ASCA (Aharonian et al. 2002). In the model a minimum electron energy $\gamma_{min} \sim 10^4$ is chosen to meet the VLA upper limit. EGRET data points are from the 3rd EGRET catalogue (Hartman et al. 1999).

Lang et al. Astrophys.&Space Sci., 297, 345 (2005)

A NEW TeV SOURCE CONFIRMED IN WHIPPLE ARCHIVAL DATA: TeV J2032+41

Abstract. A re-analysis of data near Cygnus X-3 in 1989–1990 using the Whipple Observatory atmospheric Cherenkov imaging telescope confirms the existence of the TeV J2032 + 4130 source first reported at a conference by the Crimean Astrophysical Observatory and confirmed independently by the HEGRA Collaboration in a referred publication. The significance of the Whipple observations at the a priori HEGRA position is 3.3σ. The peak signal was found at RA = 20 h 32 m, Dec = +41°33′. This is 0.6° north of Cygnus X-3. The flux level (12% of the level of the Crab Nebula) is intermediate between that reported by the Crimean (100%) and HEGRA (3%) groups.

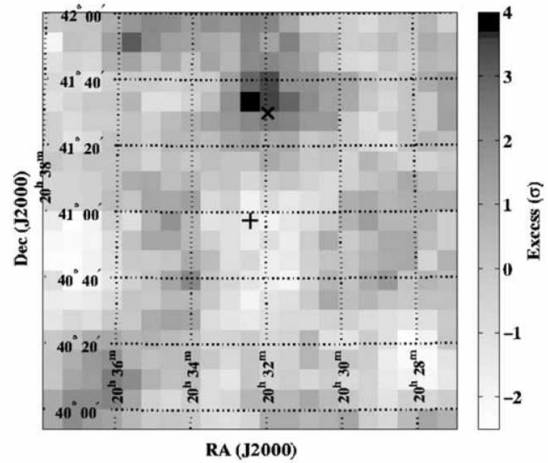

Figure 1. Sky map of the excess significance (σ) in a 2° × 2° region centred on Cygnus X-3 (marked with a +). The HEGRA position for TeV J2032 + 4130 is marked with an ×.

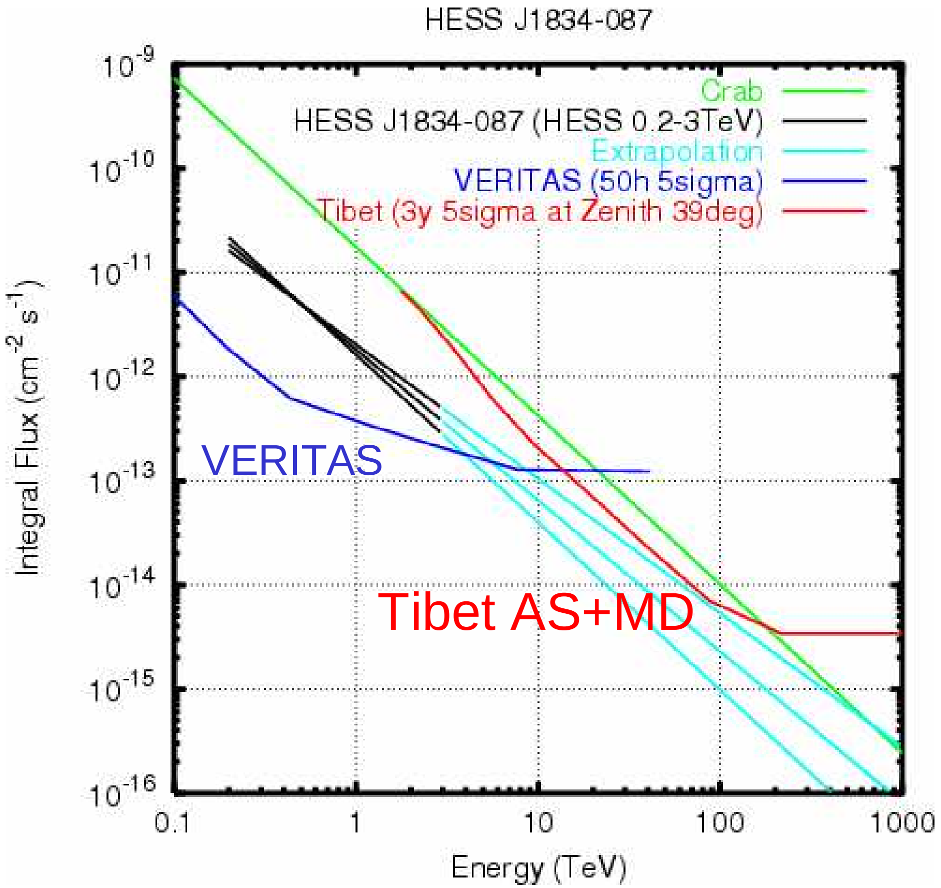

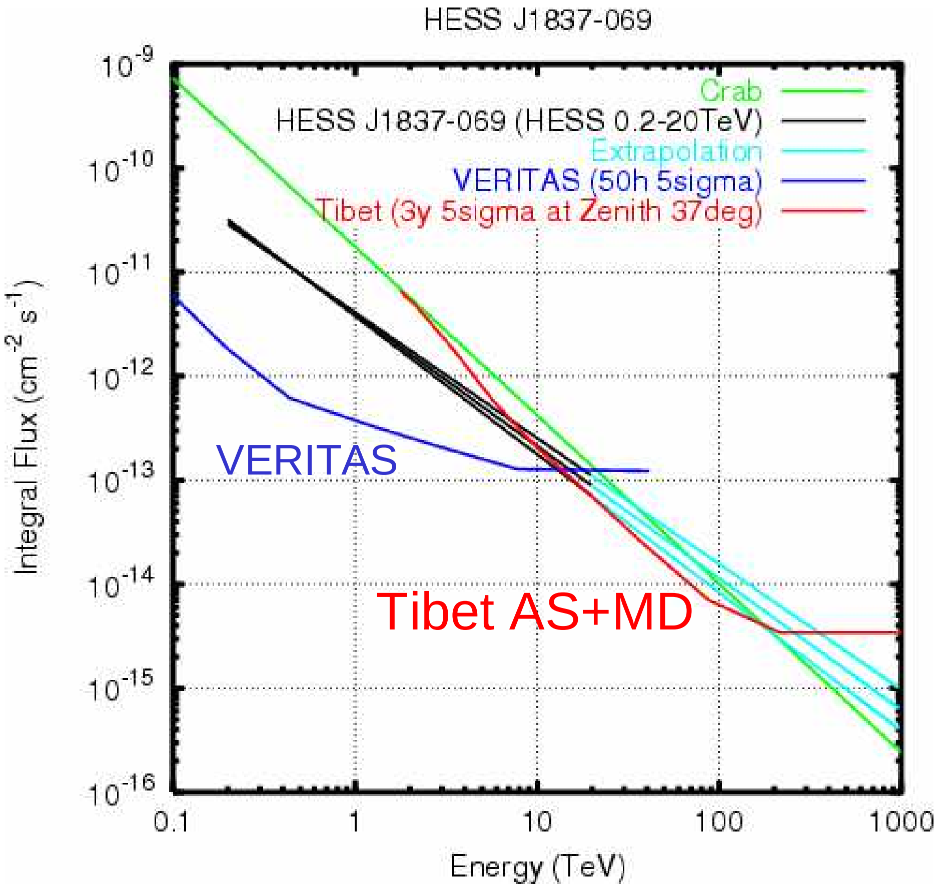

HESS J1834-087

Counterpart G23.3-0.3
Shell-type SNR
Distance ~4.8 kpc

Zenith at Tibet ~39 °

Aharonian et al, ApJ, 636, 777 (2006)

HESS J1837-069

Counterpart AX J1838 ? (UID)
G25.5+0.0? (SNR)

Zenith at Tibet ~ 37 °

Aharonian et al, ApJ, 636, 777 (2006)

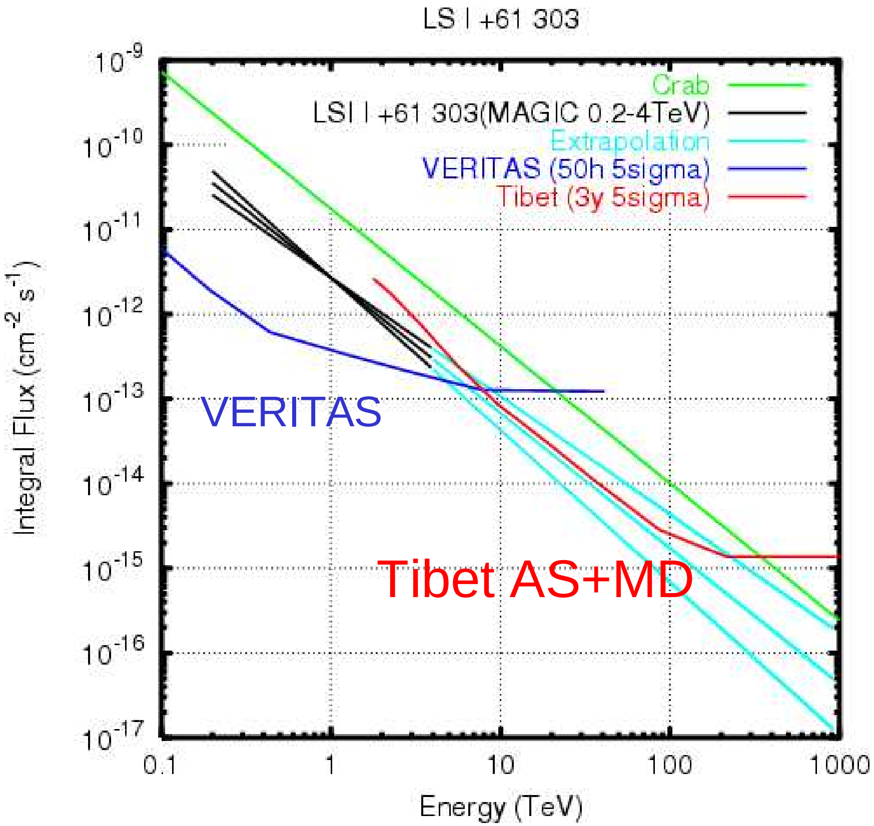

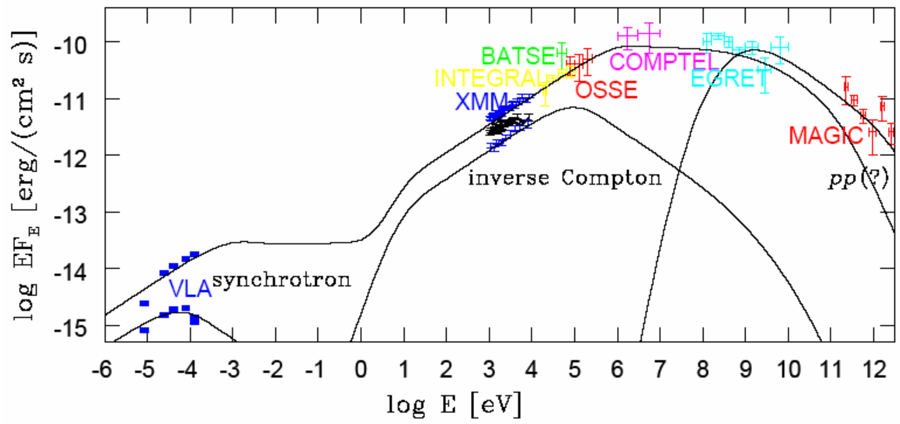

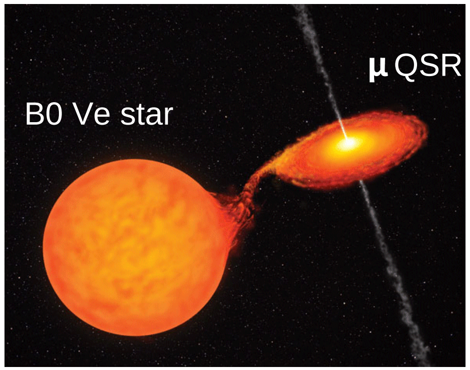

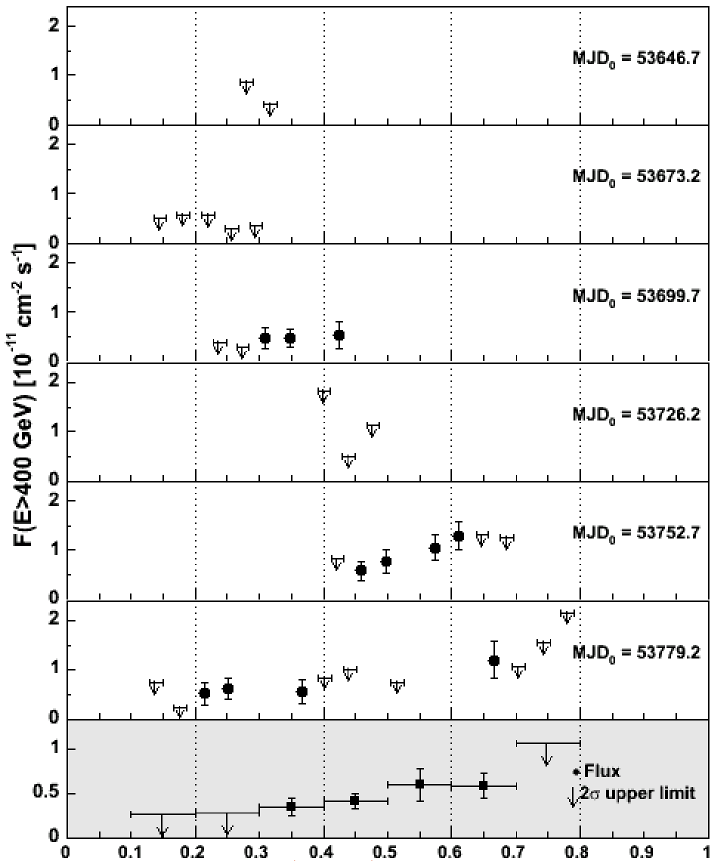

Albert et al, Science, 312, 1771 (2006)

LS I +61 303

High Mass XRB

Orbital period 26.5 days

Distance ~2 kpc

π^0 decay?

Zenith at Tibet ~31 °

Large Zenith Angle - Efficiency
(Normalized to Dec 20 deg Efficiency)

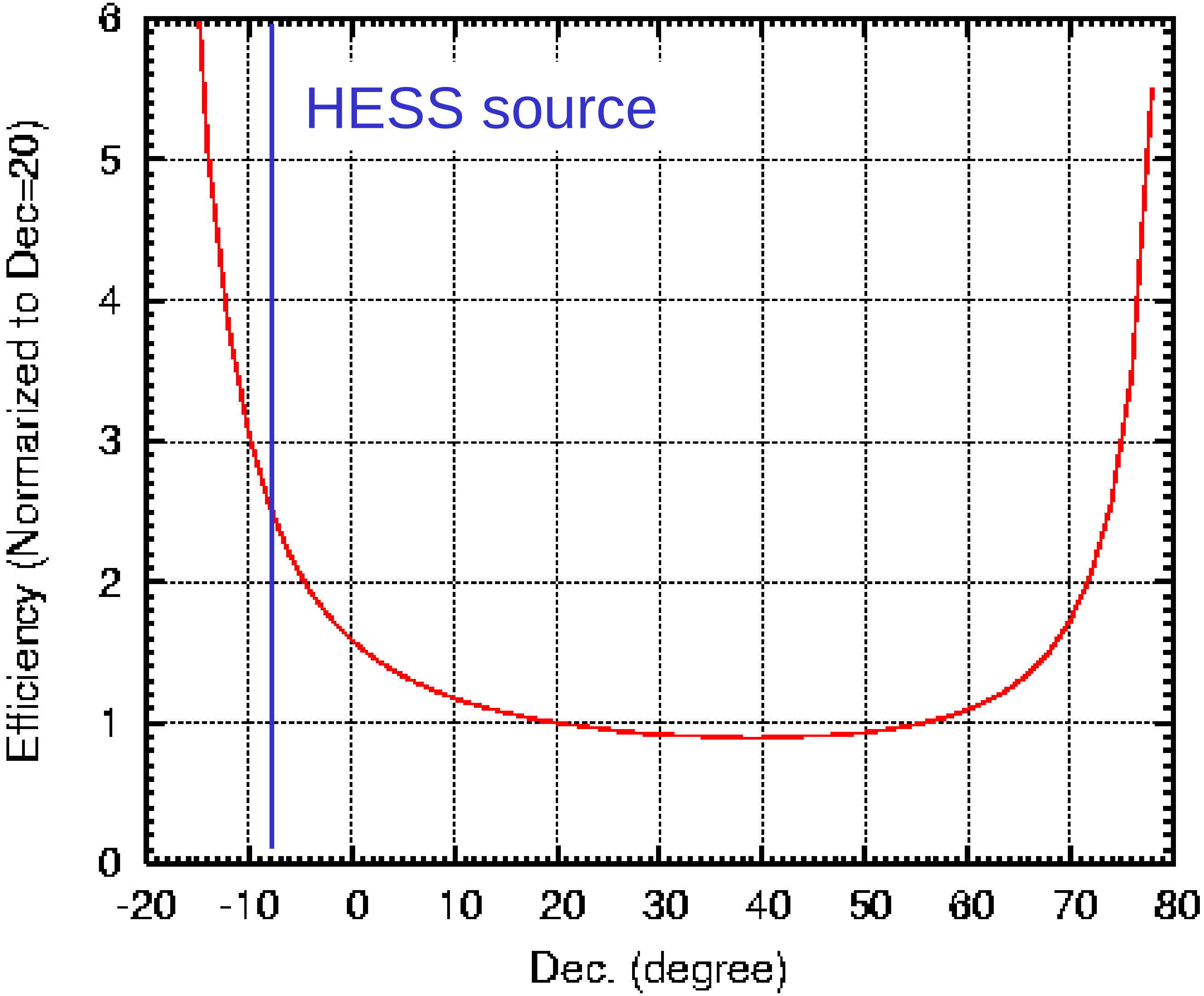

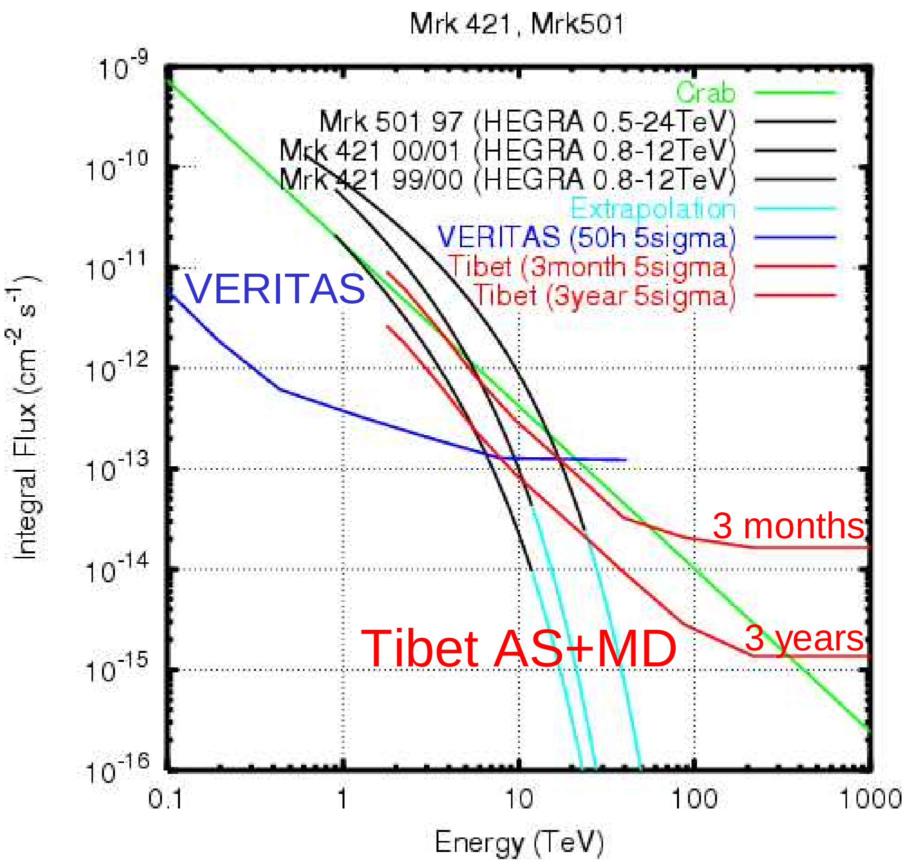

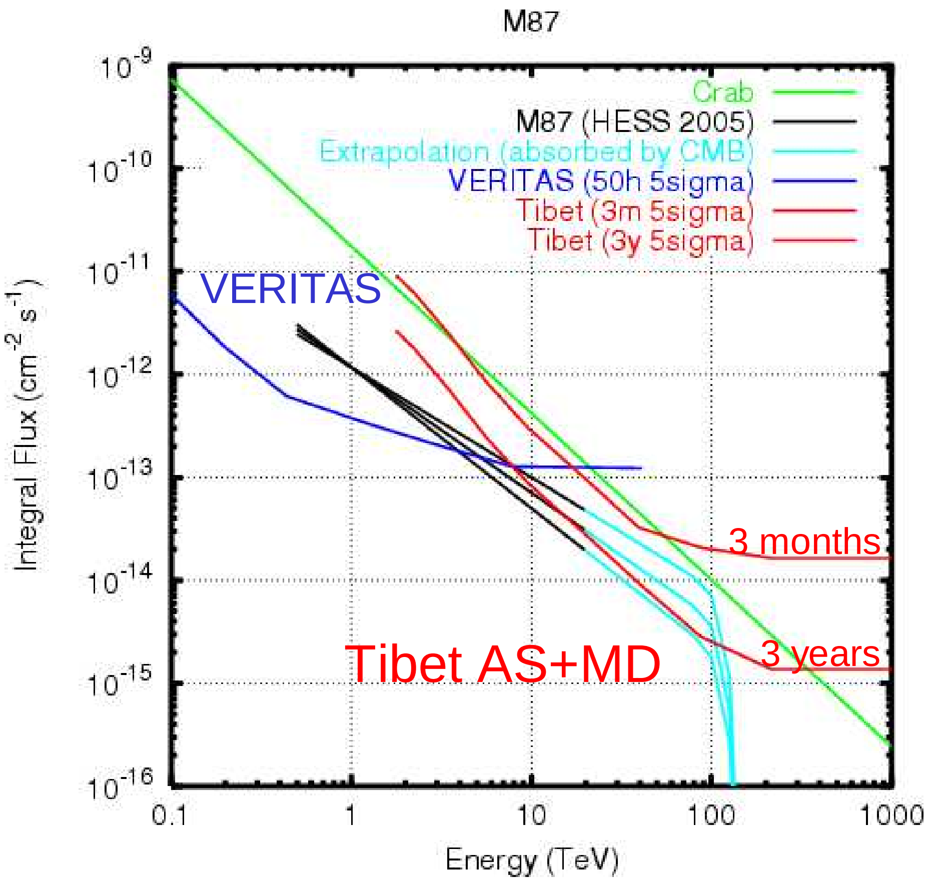

Mrk421 Mrk501

Averaged spectrum for a few month

AGN (BL Lac)

z=0.031 (Mrk 421)

z=0.034 (Mrk 501)

SSC or ERC or PIC model

Aharonian et al, A&A, 349, 11 (1999)

M87

AGN (FR-I)

z=0.00436 ~16 Mpc

l = 122.4, b = -50.5

Zenith at Tibet ~18 °

Beilicke et al, New Astro. Rev., 48, 407 (2004)

The HEGRA survey of the Galactic plane

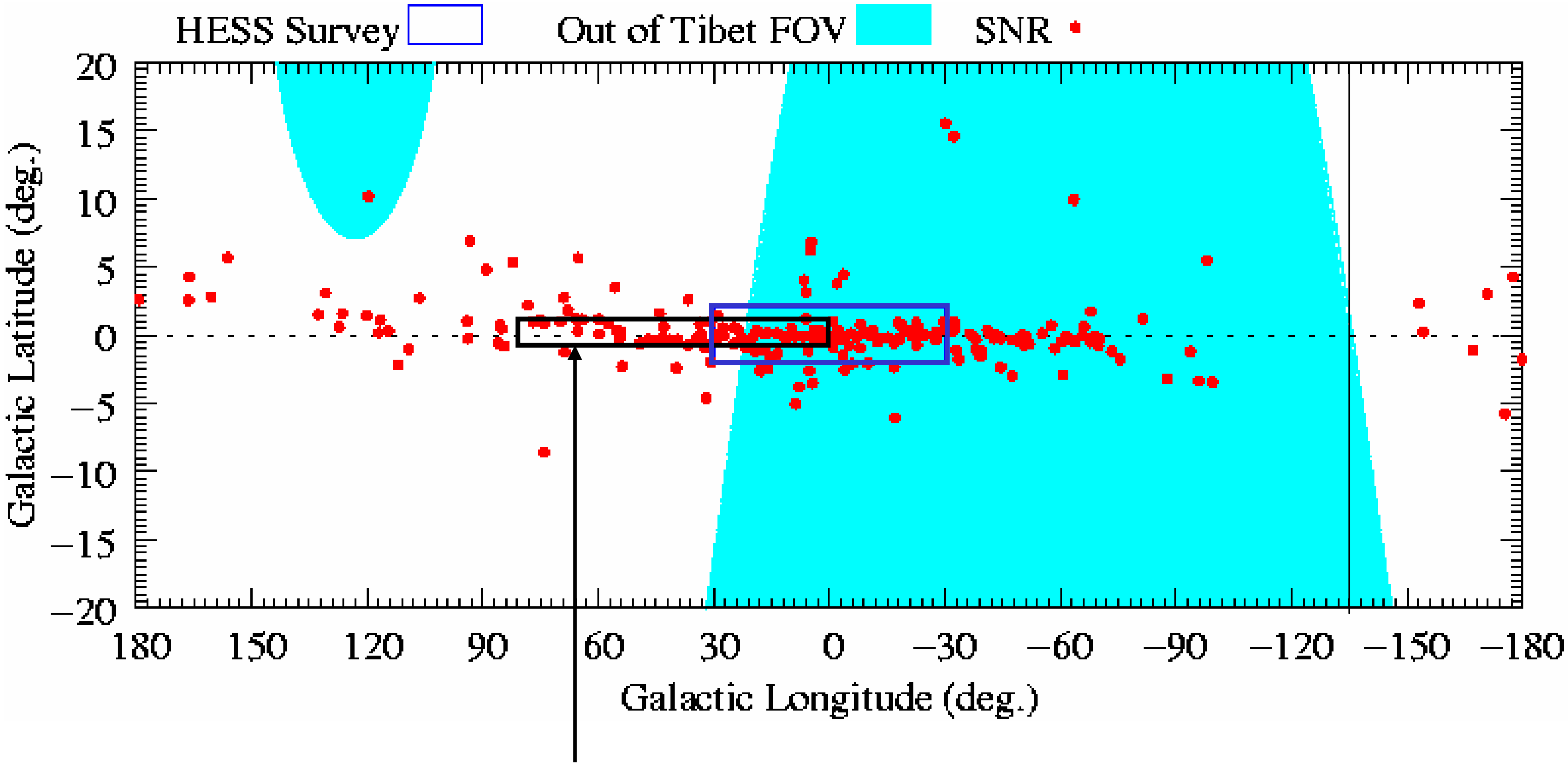

Other sources in the Northern sky?

HEGRA survey gave upper limits 0.1-several Crabs

Aharonian et al, A&A, 395, 803 (2002)

Not as sensitive as HESS survey

The H.E.S.S. survey of the Inner Galaxy

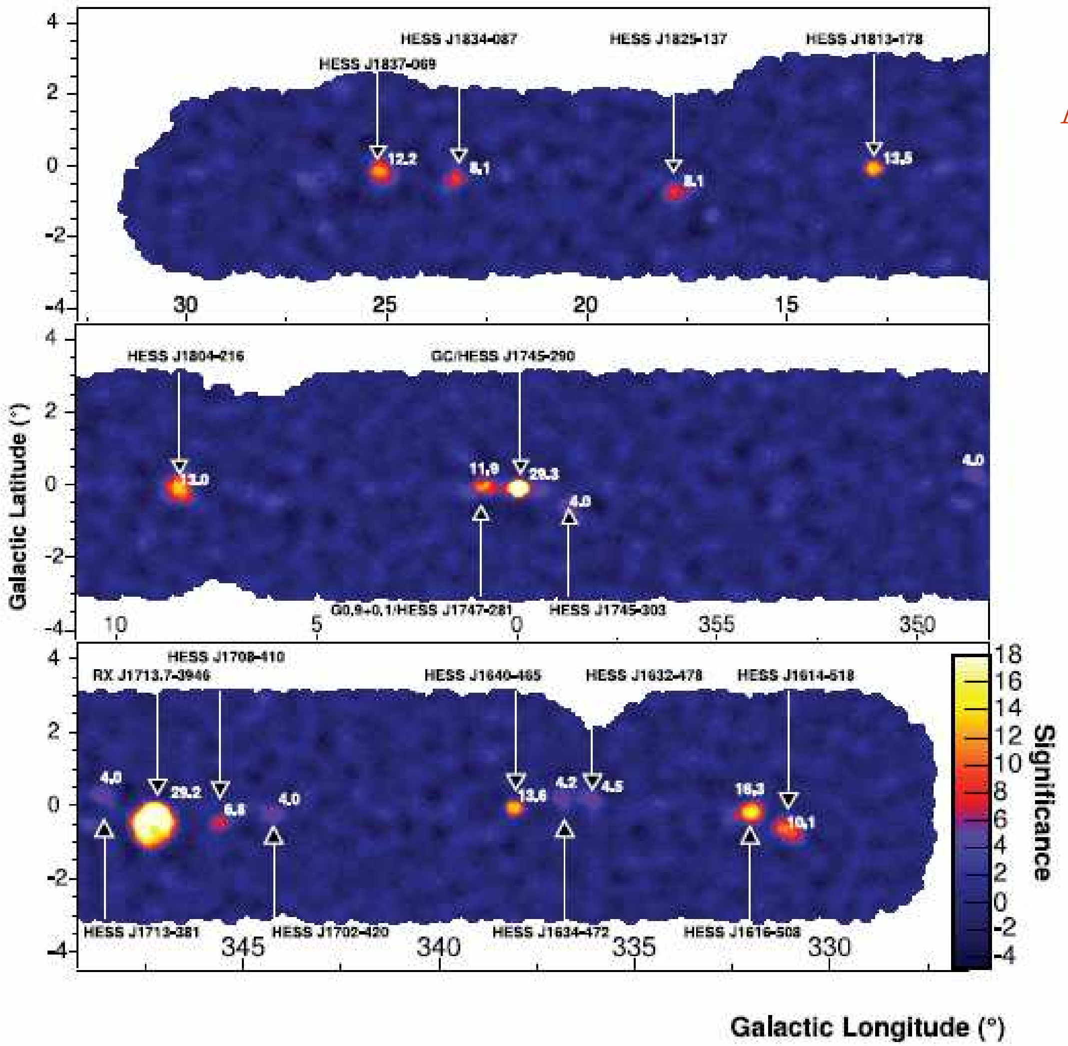

Fig. 6.—Significance map of the H.E.S.S. Galactic plane survey in 2004, including data from reobservations of source candidates detected in the original scan and observations of the known gamma-ray emitter RX J1713.7−3946 and the Galactic center region. The typical energy threshold for this map is 250 GeV. The on-source counts for each grid point are integrated in a circle of radius $\theta = 0.22°$. The background for each grid point has been derived using a ring of mean radius 0.6° and an area 7 times that of the on-source circle. The labels indicate the gamma-ray sources described in this work, along with the known gamma-ray sources RX J1713.7−3946 (HESS J1713−397), G0.9+0.1 (HESS J1747−281), and the Galactic center (HESS J1745−290). The numbers in the map give the post-trial significances of the gamma-ray sources. The significance scale is truncated at 18 σ; the signals from the Galactic center and RX J1713.7−3946 exceed this level.

Aharonian et al, ApJ, 636, 777 (2006)

|l | < ~30 °
|b| < ~2 °
~2% Crabs survey

17 sources were found
(14 new sources)

Angular Resolution
HESS → ~0.1 ° (>100GeV)
Tibet → ~0.2 ° (>100TeV)

The H.E.S.S. survey of the Inner Galaxy

Aharonian et al, ApJ, 636, 777 (2006)

Source (HESS J)	Flux (C.U.)	Index ($E^{-\Gamma}$)	Size (arcmin)	Counterpart / other names
1614-518	25%	2.46	12	--
1616-508	19%	2.35	8	PSR J1617-5055 ? (PWN)
1632-478	12%	2.12	8	IGR J16320-4751, AX J163252-4746 ? (XRB/UID)
1634-472	6%	2.38	7	G337.2+0.1 ?,IGR J16358-4726 (SNR/XRB)
1640-465	9%	2.42	2	G338.3-0.0 ? 3EG J1639-4702 ? (SNR/UID)
1702-420	7%	2.31	5	--
1708-410	4%	2.34	3	--
1713-381	2%	2.27	4	G348.7+0.3 ? (SNR)
1713-397	66%	2.19	15	RX J1713.7-3946, G347.3-0.5 (SNR)
1745-290	5%	2.20	<3	Sgr A* / Sgr A East ? (SNR/BH)
1745-303	5%	1.82	9	3EG J1744-3011 ? (UID)
1747-281	2%	2.40	<1.3	G0.9+0.1 (PWN)
1804-216	25%	2.72	12	G8.7-0.1, PSR J1803-2137 ? (SNR/PWN)
1813-178	6%	2.09	2	G12.82-0.02, AX J1813-178 ? (SNR)
1825-137	17%	2.46	10	PSR J1826-1334 / 3EG J1826-1302 ? (PWN/UID)
1834-087	8%	2.45	5	G23.3-0.3 / W41 ? (SNR)
1837-069	13%	2.27	5	G25.5+0.0 ?, AX J1838-0655 ? (SNR/UID)

SNR ~8 PWN ~3 XRB ~2 UID ~1 Unknown ~3

Energy Spectrum of HESS sources

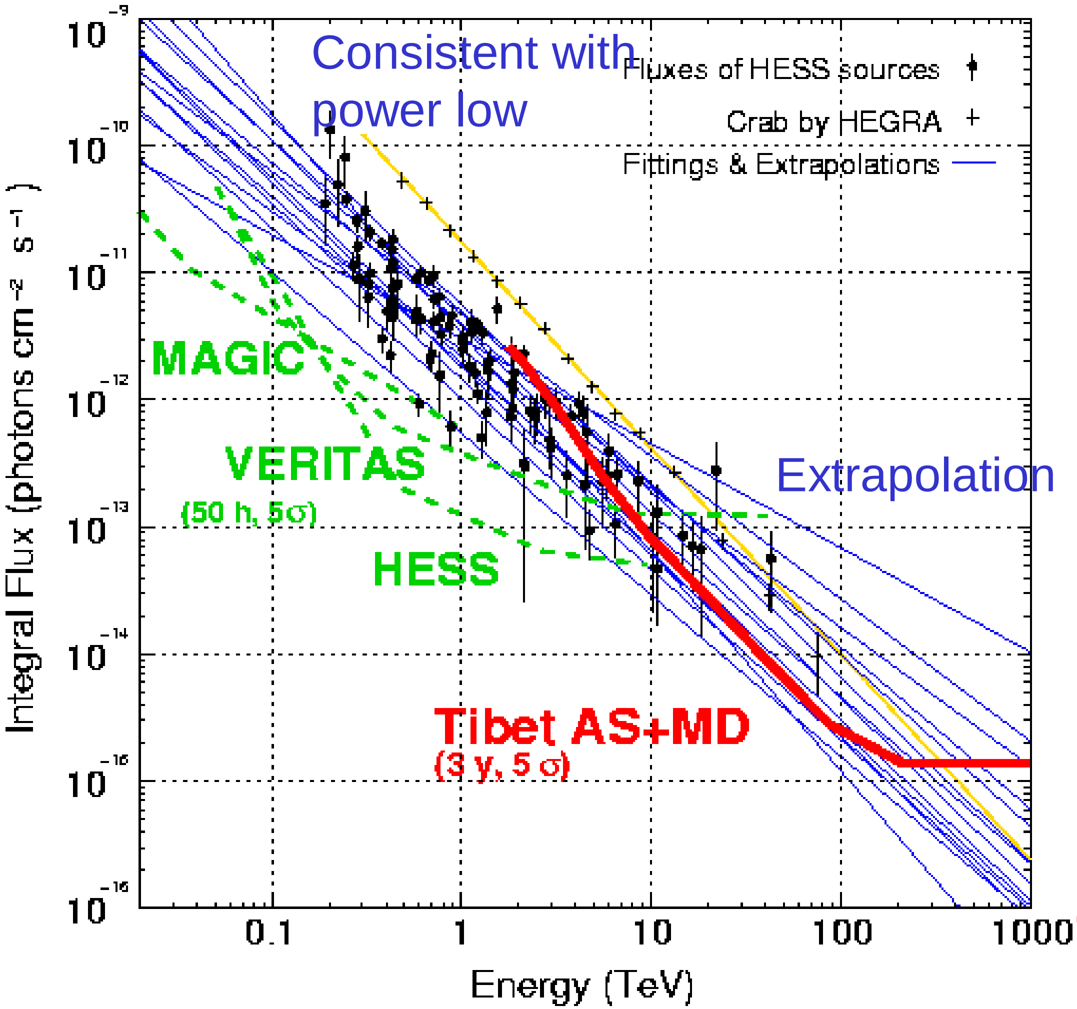

Aharonian et al, ApJ, 636, 777 (2006)

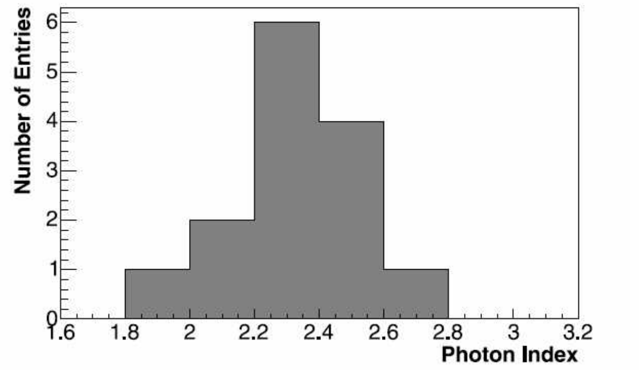

FIG. 8.—Distributions of the photon index of the new sources. The mean photon index is 2.32 with an rms of 0.2.

Indices are harder

(If it constructed
in the southern hemisphere,)

Most of HESS sources
detectable by Tibet AS+MD!

Expectation of the Number of SNRs in the Northern Sky

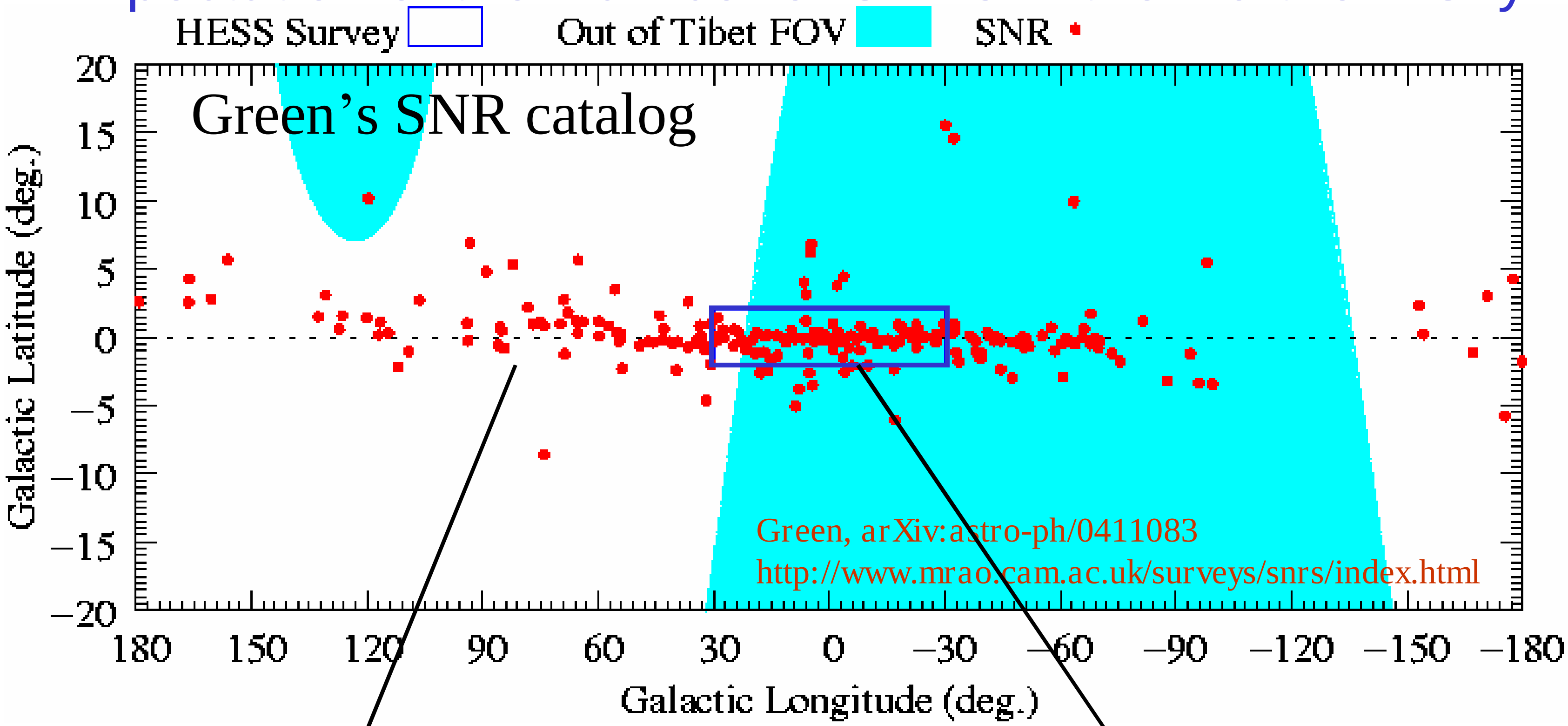

Tibet F.O.V. region
86 SNRs

Expected >10 new sources!?
in 100 TeV region

HESS survey region
82 SNRs

detected 14 new sources
in TeV region (faint in X-ray, etc)

Aharonian et al, ApJ, 636, 777 (2006)

Extragalactic Background Radiation (EBR)

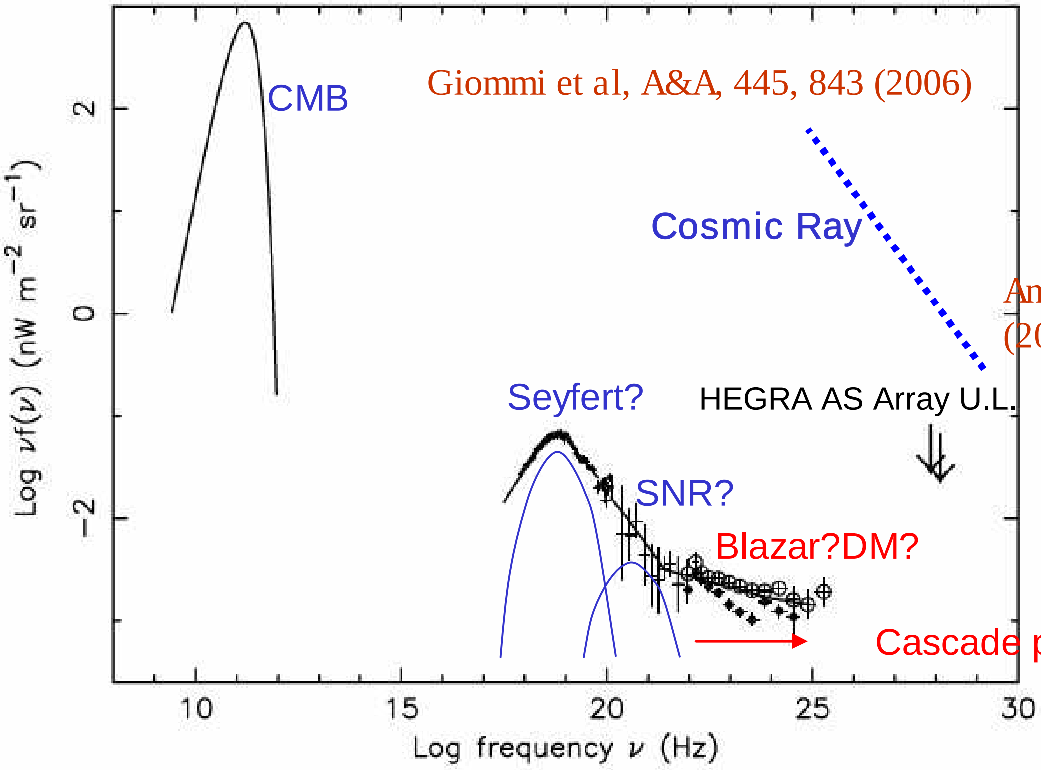

Ando & Komatsu Phys. Rev. D **73**, 023521 (2006)

Aharonian et al, Astro. Phys., 17, 459 (2002)

Wagner Mem. Soc. Astron. Ital., 73, 76 (2002)

The et al, ApJ, 403, 32 (1993)

Cascade photons by X-particle?

Fig. 5. The extragalactic Cosmic Background Energy distribution at microwave, X-ray and γ-ray energies.

EBRs ~10^5 events

CRs ~10^8 events

/ 3 years / 1 sr (>100TeV)

Need B.G. rejection ～10^{-3}

ABSTRACT

We present a new assessment of the contribution of the blazar population to the extragalactic background radiation across the electromagnetic spectrum. Our calculations rely on deep blazar radio counts that we have derived by combining several radio and multi-frequency surveys. We show that blazar emission integrated over cosmic time gives rise to a considerable broad-band non-thermal cosmic background that in some parts of the electromagnetic spectrum dominates the extragalactic brightness.

We confirm that blazars are the main discrete contributors to the Cosmic Microwave Background (CMB), where we estimate that their integrated emission causes an apparent temperature increase of 5−50 μK in the frequency range 50−250 GHz. The CMB primordial fluctuation spectrum is contaminated starting at multipole $l \approx$ 300−600, in the case of a completely random source distribution, or at lower l values if spatial clustering is present. We estimate that well over one hundred-thousand blazars will produce a significant signal in the maps of the upcoming Planck CMB anisotropy mission. Because of a tight correlation between the microwave and the X-ray flux, these sources are expected to be X-ray emitters with flux larger than a few 10^{-15} erg cm^{-2} s^{-1} in the soft X-ray band. A large fraction of the foreground sources in current and near-future CMB anisotropy maps could therefore be identified and removed using a multi-frequency approach, provided that a sufficiently deep all-sky X-ray survey will become available in the near future.

We show further that blazars are a major constituent of all high energy extragalactic backgrounds. Their contribution is expected to be 11−12% at X-ray frequencies and possibly 100% in the ~0.5−50 MeV band. At higher energies (E > 100 MeV) the estimated blazar collective emission, obtained by extrapolating their integrated micro-wave flux to the γ-ray band using the SED of EGRET detected sources, overestimates the extragalactic background by a large factor, thus implying that not only blazars dominate the γ-ray sky but also that their average duty cycle at these frequencies must be rather low. Finally, we find that blazars of the HBL type may produce a significant amount of flux at TeV energies.

Galaxy Cluster

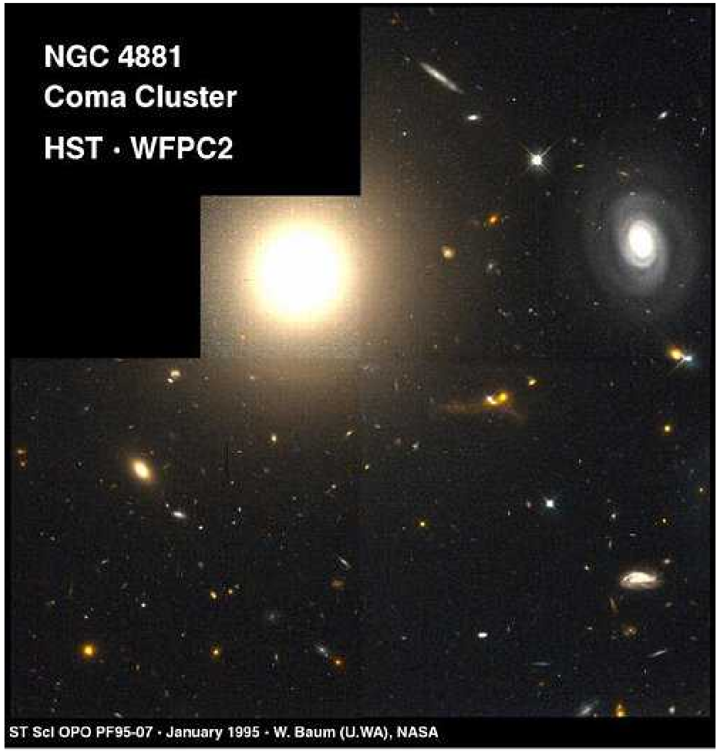

ABSTRACT

All sufficiently massive clusters of galaxies are expected to be surrounded by strong accretion shocks, where protons can be accelerated to $\sim 10^{18}$–10^{19} eV under plausible conditions. Such protons interact with the cosmic microwave background and efficiently produce very high energy electron-positron pairs, which then radiate synchrotron and inverse Compton emission, peaking respectively at hard X-ray and TeV gamma-ray energies. Characterized by hard spectra (photon indices ~ 1.5) and spatial distributions tracing the accretion shock, these can dominate over other nonthermal components depending on the shock magnetic field. HESS and other Cerenkov telescopes may detect the TeV emission from nearby clusters, notwithstanding its extended nature. The hard X-rays may be observable by future imaging facilities such as *NeXT* and possibly also by the *Astro-E2* Hard X-Ray Detector. Such detections will provide not only a clear signature of ultra–high-energy proton acceleration, but also an important probe of the accretion shock itself, as well as magnetic fields in the outermost regions of clusters.

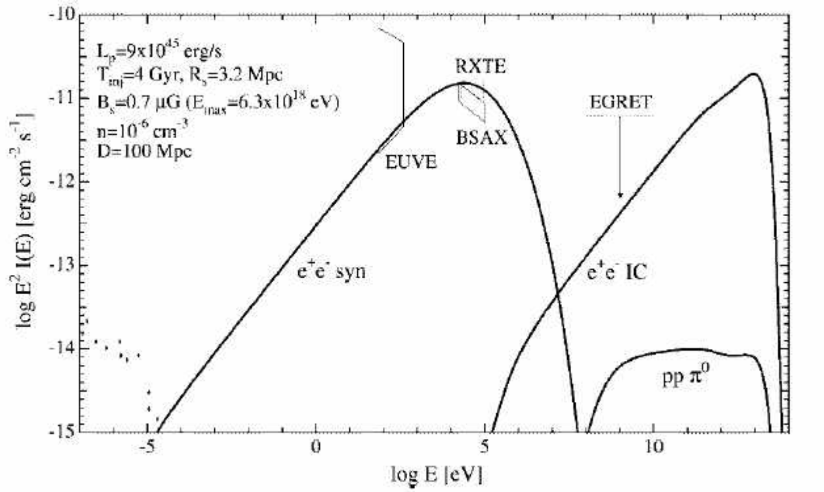

FIG. 2.—Spectra of proton-induced emission for the model parameters labeled in the figure (see also text), compared with observational data for the Coma Cluster from the *Extreme Ultraviolet Explorer*, *BeppoSax*, *Rossi X-Ray Timing Explorer*, and EGRET compiled by Reimer et al. (2004). [*See the electronic edition of the Journal for a color version of this figure.*]

Inoue, Aharonian & Sugiyama, ApJ, 628, L9 (2005)

Name	Coma Cluster (Abell 1656)
R.A.	13h 00m (Rough position)
Dec.	+28 ° (Rough position)
Apparent Size	~120'
Red Shift	0.0232

Summary (Tibet AS + MD)

10-1000 TeV candidates in the northern sky:

Promising sources: Crab, TeV J2032+4130,
Diffuse **γ** from Milagro region
HESS J1837-069, Mrk 421

Interesting: Cas A, M87, HESS J1834-089, Mrk 501
LS I +61 303

Expected # of new sources from HESS data: >~10 !?

+Some others?

2. Next phase of Tibet hybrid exp. YAC

Yangbajing Air shower Core detector

- Measure the energy spectrum of the main component at the knee.
- Detector：Low threshold BD grid ＋AS array。
- Observe energy flow of AS core within several x 10m from the axis.

YAC array

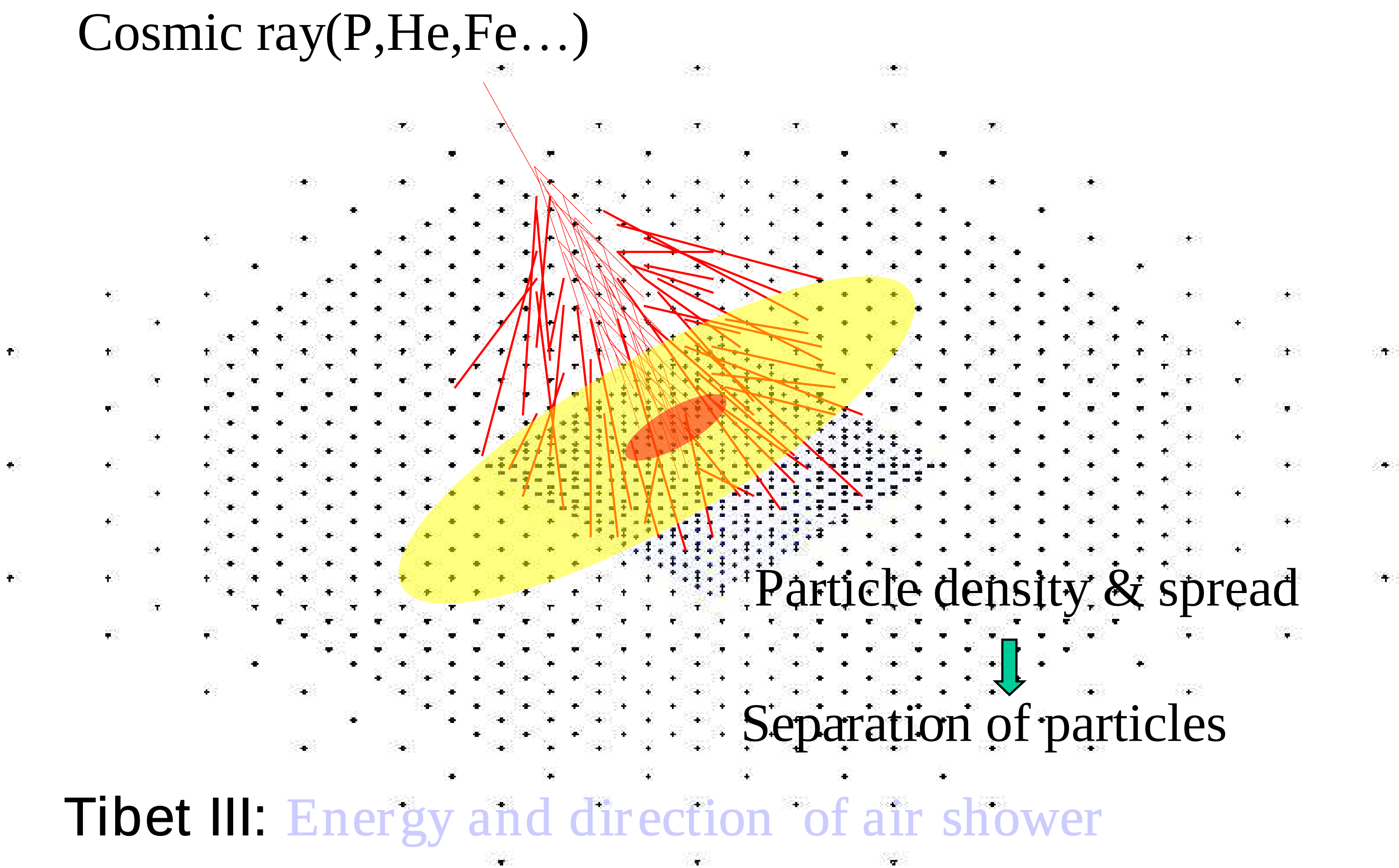

Tibet III: Energy and direction of air shower

Design of YAC

40cm x 50cm, 20x20 channels

$S=5000m^2$

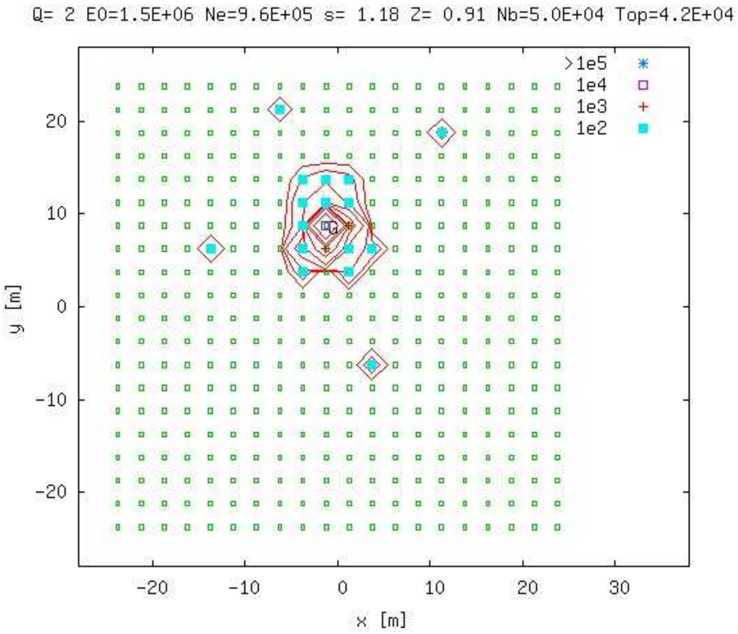

3.75m spacing 400ch

N_b>100, any 5

(>30GeV)

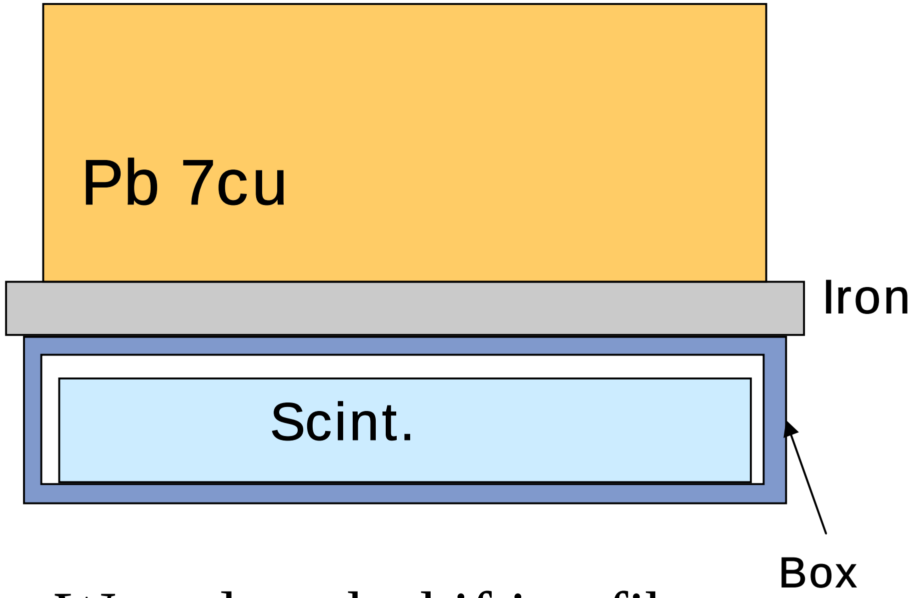

Wave length shifting fiber
+ 2 PMTs
(Low gain & High gain)
$10^2 < N_b < 10^6$

MC Event Map

Proton

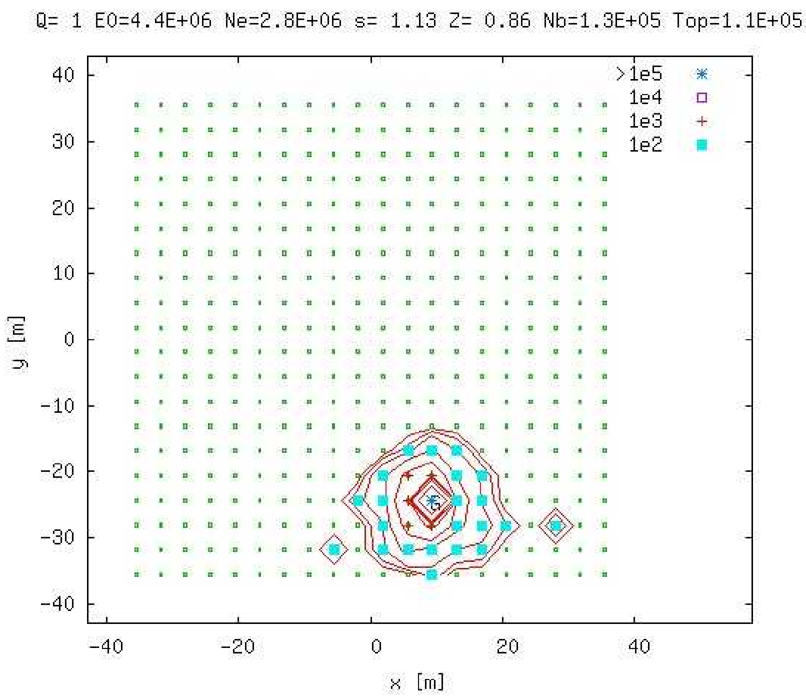

Fe

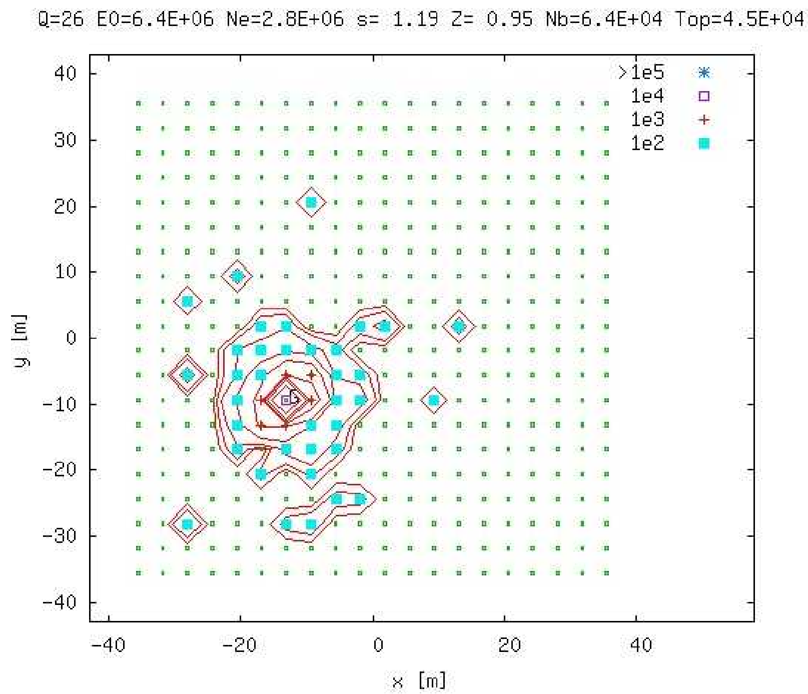

Separation of Fe by YAC (use ANN)

Iron and others

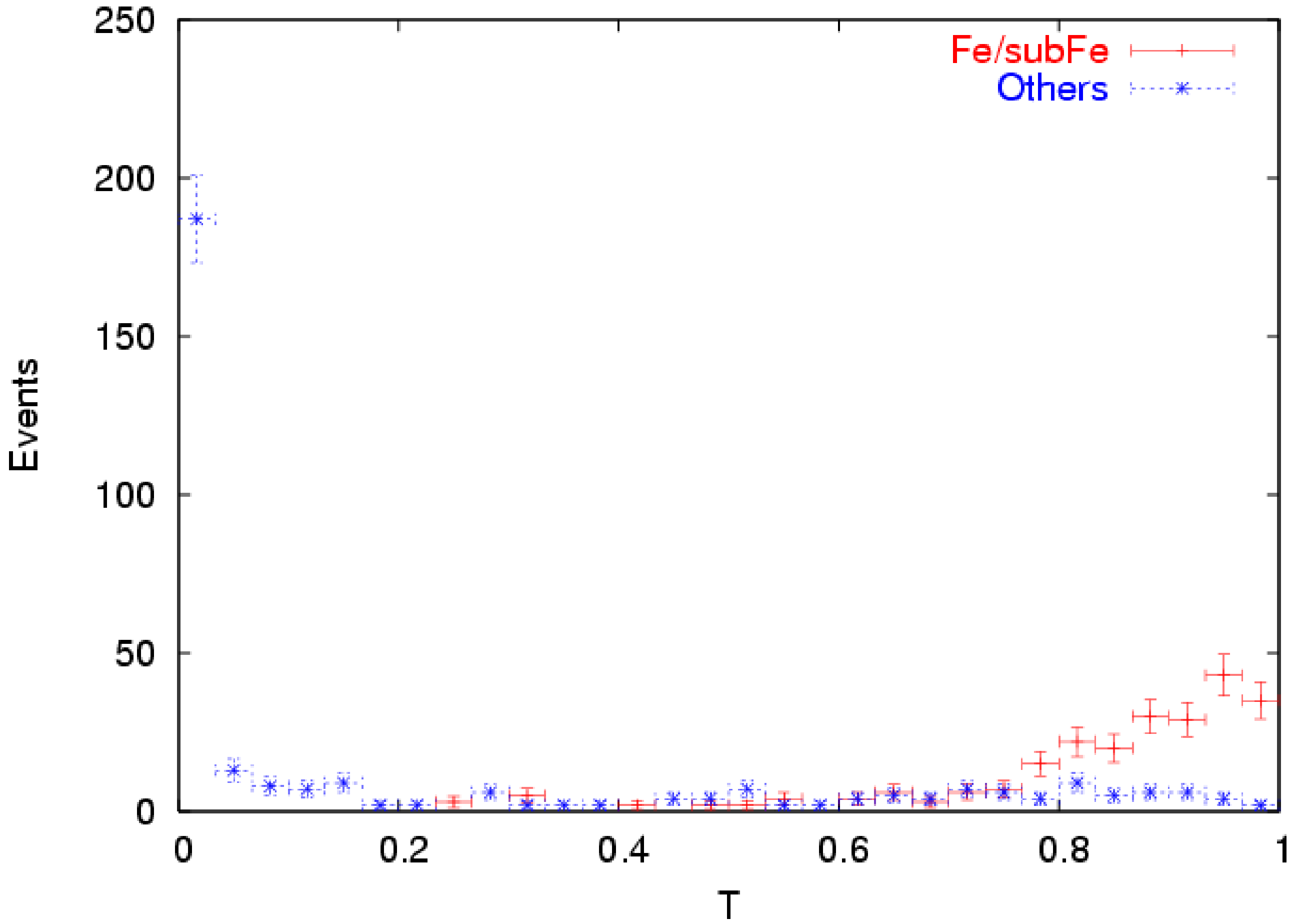

Detection efficiency of YAC

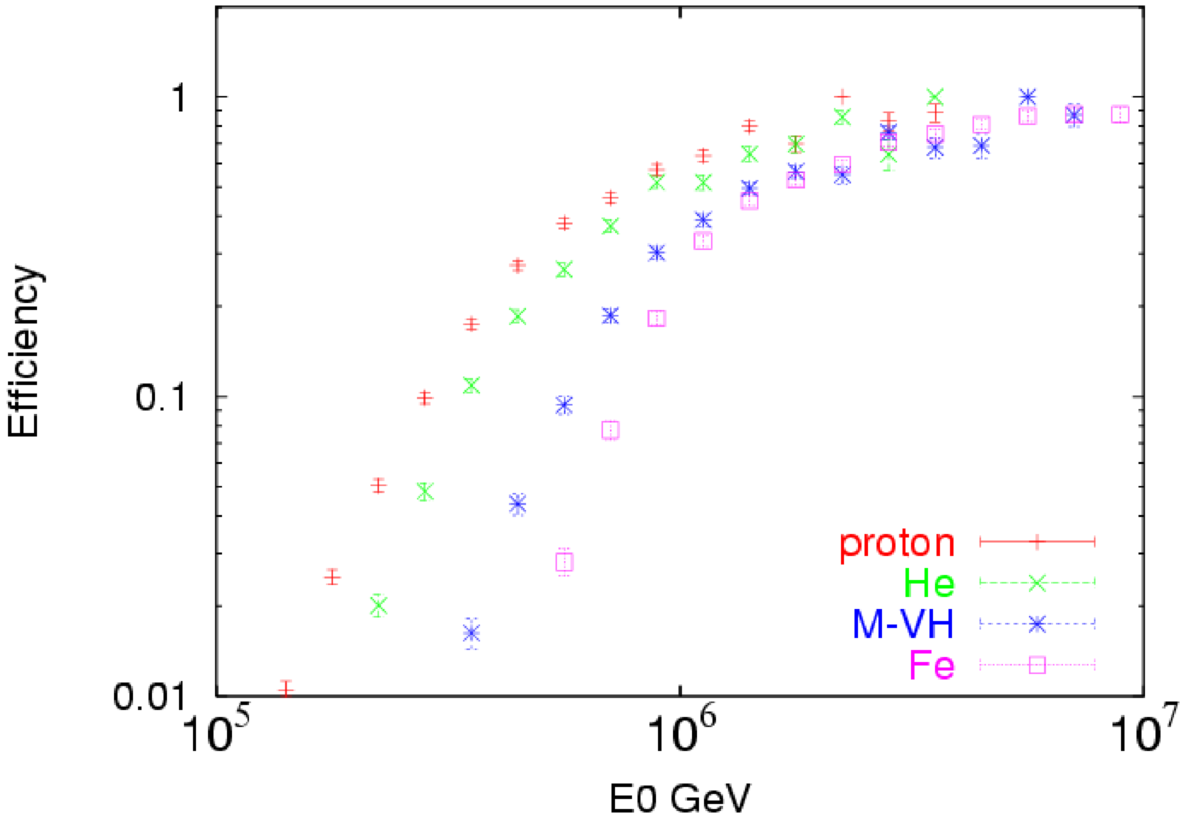

Expected results by YAC